ADVANCED OXIDATION PROCESSES: ASSESSMENT OF NATURAL ORGANIC MATTER REMOVAL AND INTEGRATION WITH MEMBRANE PROCESSES

by

Rupa Lamsal

Submitted in partial fulfilment of the requirements
for the degree of Doctor of Philosophy

at

Dalhousie University
Halifax, Nova Scotia
July 2012

DALHOUSIE UNIVERSITY

DEPARTMENT OF CIVIL AND RESOURCE ENGINEERING

The undersigned hereby certify that they have read and recommend to the Faculty of Graduate Studies for acceptance a thesis entitled "**ADVANCED OXIDATION PROCESSES: ASSESSMENT OF NATURAL ORGANIC MATTER REMOVAL AND INTEGRATION WITH MEMBRANE PROCESSES**" by Rupa Lamsal in partial fulfillment of the requirements for the degree of Doctor of Philosophy.

Dated: July 4, 2012

External Examiner: ___________________________________

Research Supervisors: ___________________________________

____

Examining Committee: ___________________________________

____

Departmental Representative: _____________________________

DALHOUSIE UNIVERSITY

DATE: July 4, 2012

AUTHOR: Rupa Lamsal

TITLE: **ADVANCED OXIDATION PROCESSES: ASSESSMENT OF NATURAL ORGANIC MATTER REMOVAL AND INTEGRATION WITH MEMBRANE PROCESSES**

DEPARTMENT OR SCHOOL: Department of Civil and Resource Engineering

DEGREE: PhD CONVOCATION: October YEAR: 2012

Signature of Author

DEDICATION

This thesis is dedicated to my late father Krishna P. Devkota, who taught me the value of hard work and to my husband, Lok, and my son, Rajul, who have been my inspiration and strength.

TABLE OF CONTENTS

LIST OF TABLES

LIST OF FIGURES

ABSTRACT

Stringent water quality regulations and general aesthetic issues have urged drinking water industry to apply advanced water treatment technologies that can meet multiple treatment objectives. Removal of significant amount of natural organic matter (NOM), including colour causing organics, to meet stringent disinfection by product (DBP) regulations from source water with low alkalinity and low turbidity is very challenging with conventional water treatment processes. Membrane filtration processes are effective in removing significant amount of NOM thus minimizing the formation of carcinogenic DBPs. However, fouling of membrane is a major problem affecting system performance. Improved pretreatment of feed water helps reduce or eliminate membrane fouling.

This study characterized source water, examined fouling in nanofiltration (NF) membranes and explored various pretreatment options to reduce NF fouling. Resin fractionation was performed to characterize NOM and to identify the major fractions responsible for DBP formation in natural source water of the Tatamagouche water treatment plant (WTP) in Nova Scotia. The source water primarily comprised of hydrophilic neutrals (HIN) and hydrophobic acid (HOA) compounds, with the latter being a major contributor to the DBP formation. Fouling behaviour of the NF membranes was examined at bench- and full-scale levels to understand the impact of source water quality on membrane fouling in the Tatamagouche and Collins Park WTPs. Bench- and full-scale results revealed higher fouling in the Collins Park WTP which together supported ongoing membrane cleaning practices in the plant. Surface enhanced Raman spectroscopy (SERS), demonstrated here as a novel technique, suggested that carbohydrates and proteins are the main foulants in the source water. Bench-scale experiments conducted to evaluate the performance of ozone (O_3), ultraviolet (UV), hydrogen peroxide plus ozone (H_2O_2/O_3), H_2O_2 plus UV (H_2O_2/UV) and O_3 plus UV (O_3/UV) for reducing NOM and DBP precursors suggested that the O_3/UV AOP offers the optimum reduction of NOM. Integrating AOP pretreatments with NF membrane resulted in an improved permeate flux but not permeate quality of the NF membrane.

LIST OF ABBREVIATIONS AND SYMBOLS USED

AFM	Atomic force microscopy
AOC	Assimilable organic carbon
AOPs	Advanced oxidation processes
ATR-FTIR	Attenuated total reflectance fourier transform infrared spectroscopy
BCAA	Bromochloroacetic acid
BCDM	Bromodichoromethane
BDCAA	Bromodichloroacetic acid
BDOC	Biodegradable organic carbon
Ca	Calcium
$CaCO_3$	Calcium carbonate
CDBAA	Chlorodibromoacetic acid
Cl^-	Chloride
CO_2	Carbondioxide
cm	Centimeter
Da	Daltons
DBAA	Dibromoacetic acid
DBCM	Dibromochloromethane
DBP	Disinfection by product
DBPFP	Disinfection by products formation potential

DCAA	Dichloroacetic acid
DOM	Dissolved organic matter
DOC	Dissolved organic carbon
Fe	Iron
FTIR	Fourier-transform infrared
GC ECD	Gas chromatography electron capture detector
hr	hour
HAA	Haloacetic acid
HAAFP	Haloacetic acid formation potential
H_2O_2	Hydrogen peroxide
H_2O_2/O_3	Hydrogen peroxide – ozone
H_2O_2/UV	Hydrogen peroxide – ultraviolet
HIA	Hydrophilic acid
HIB	Hydrophilic base
HIN	Hydrophilic neutral
HOA	Hydrophobic acid
HOB	Hydrophobic base
HON	Hydrophilic neutral
HPC	Heterotrophic plate count
HPI	Hydrophilic
HPO	Hydrophobic
HPSEC	High performance size exclusion chromatography
HPM	High pressure membrane

IMS	Integrated membrane system
$K_3Fe(C_2O_4)_3.3H_2O)$	Potassium ferrioxalate
Lmh	Liter per meter square per hour
L/min	Liter per minute
LPM	Low pressure membrane
MBAA	Monobromoacetic acid
MF	Microfiltration
µm	Micrometer
µL	Microliter
µg/L	Micrograms per liter
MCAA	Monochloroacetic acid
MTBE	Methyl *tert*-butyl ether
mV	Millivolt
MW	Molecular weight
MWCO	Molecular weight cut-off
NF	Nanofiltration
NMR	Nuclear magnetic resonance
NOM	Natural organic matter
NTU	Nephelometric turbidity units
O_3	Ozone
O_3/UV	Ozone - UV
PAC	Powered activated carbon
psi	Pounds per square inch

rpm	Revolutions per minute
RO	Reverse Osmosis
SEC	Scanning electron microscopy
SERS	Surface enhanced Raman spectroscopy
SOC	Synthetic organic chemical
SUVA	Specific ultraviolet absorbance
TBAA	Tribromoacetic acid
TCAA	Trichloroacetic acid
TEM	Transmission electron microscope
TFC	Temperature correction factor
THM	Trihalomethane
THMFP	Trihalomethane formation potential
TiO_2	Titanium dioxide
TMP	Transmembrane pressure
TOC	Total organic carbon
UF	Ultrafiltration
UFC	Uniform formation condition
USgpm	US gallon per meter
UV	Ultraviolet radiation
UV_{254}	Ultraviolet absorbance at 254 nm
WTP	Water Treatment plant

ACKNOWLEDGEMENTS

I sincerely thank my supervisor, Dr. Graham Gagnon, for providing me an opportunity to conduct this interesting research project and sharing his enthusiasm for drinking water treatment processes. Your support, guidance, and continued encouragement have been instrumental in getting me to this point. I would like to thank to my co-supervisor, Dr. Margaret Walsh, for her guidance and encouragement. I appreciate your energy in reviewing each manuscript several times and providing valuable comments that immensely improved the manuscripts. It has been an honour to work with both of you for the past four years at Dalhousie University.

I would like to thank Dr. Craig Lake and Dr. Christa Brosseau for not only being available as supervisory committee but also providing several suggestions in research works over the course of this dissertation. Dr. Robert Guy provided inputs to improve PhD proposal. Thanks are due to Dr. Madjid Mohseni for agreeing to be my external examiner.

Funding from the Natural Sciences and Engineering Research Council of Canada (NSERC) and faculty of graduate scholarship are gratefully acknowledged.

Staffs of Tatamagouche and Collins Park water treatment plants allowed access to plants for water sampling and to full-scale plant data. Special thanks to Mike Chaulk from CBCL Ltd. for providing both full-scale plant information and membrane fouling data. I wish to express my debt to Dr. Christa Brosseau and her students, Scott Harroun and Joel Bergman from St. Mary's university for helping me analysing Raman spectroscopy.

I would like to acknowledge the contributions of technical support from members of the water quality laboratory. In particular, I would like to thank Heather Daurie for ordering laboratory supplies and helping me handling analytical instruments. Many thanks are due to Emily Zevenhuizen, Krysta Montreuil, Jonathan Nash, and Peter for providing technical guidance in laboratory experiments. Thanks to many friends, Sarah Jane Payne, Yamuna Vadasarukkai, Ryan Brookman, Krysta R. Montreuil, Meghan Woszczynski, Lena Faust, John Bergese, Wendy Krkosek and many others, with whom I enjoyed a number of fun and intellectual exchanges during my stay in Halifax.

Thanks to my parents for their constant love and support. Last but not least, I would like to express my deepest thanks to my husband, Lok, and son, Rajul. Without your support, love and constant encouragement throughout this whole process, I would not be in this position. I am unable to express the amount of love and appreciation I have for you.

CHAPTER 1 INTRODUCTION

Stringent water quality regulations of the Disinfectant and Disinfection By-Products Rule (D/DBPR) (USEPA, 2006b) and the long term 2 enhanced surface water treatment rule (LT2ESWTR) (USEPA, 2006a) in the drinking water industry have urged application of advanced water treatment technologies which can meet multiple treatment objectives. Nova Scotia, like several other provinces in Canada, has challenging source water quality due to low level of turbidity and alkalinity. In addition, the water quality of many of the surface source waters are highly varied with season, with elevated levels of organics and colour in spring and fall due to periods of high precipitation. Removal of significant amount of natural organic matter (NOM) to meet stringent disinfection by-product (DBPs) regulations and pathogen control from these source waters can be challenging with conventional water treatment processes.

Membrane technology has several advantages compared to conventional water treatment processes as it can provide physical removal of NOM including the dissolved organic carbon (DOC) fraction, while reducing the reliance upon chemical disinfection, thus minimizing carcinogenic DBPs (Siddiqui et al., 2000). For small systems, membrane plant design capital costs are competitive with conventional processes (Pressdee et al., 2006). Production of high water quality with no sludge production and small footprint requirement compared to conventional treatment processes have resulted in water utilities considering membrane technology. Another important reason for growing application of membrane treatment is its ability to produce consistently high quality finished water regardless of feed water characteristics (Anselme et al., 1993). Low pressure microfiltration (MF) and ultrafiltration (UF) membranes are primarily used for the removal of particulate matter whereas high pressure nanofiltration (NF) and reverse osmosis (RO) membranes are used for the removal of organic matter, multivalent ions and micro pollutants. Integrated membrane system (IMS), using low pressure (MF/UF) membranes followed by high pressure (NF/RO) membranes, have been used as a multi-barrier approach in drinking water treatment.

The major challenge associated with membrane processes is the decrease in the permeate flux and permeate quality due to membrane fouling (Seidel and Elimelech, 2002). A well-known operational consequence of membrane fouling is an increase in the frequency of hydraulic backwashing and chemical cleaning, which results in increased operating costs. Therefore, an improved understanding of fouling causing materials is important to ensure membrane processes remain an effective tool in order to meet regulatory requirements and improve membrane sustainability (Carroll et al., 2000; Cho et al., 2000; Cho et al., 1998a).

Natural organic matter (NOM) commonly found in source water is a complex heterogeneous mixture of organic compounds with different molecular weights that has been considered as a major contributor to membrane fouling in water treatment (Her et al., 2008a; Hong and Elimelech, 1997a; Nilson and DiGiano, 1996). In addition, NOM possesses various challenges to drinking water quality and its treatment processes. It forms disinfection by-products (DBPs) upon reaction with chlorine (Edzwald et al., 1985), and causes negative effect on aesthetic properties and promotes biological growth in water distribution systems (Rittmann and Snoeylink, 1984). The effectiveness of a treatment process is dependent on characteristics and concentrations of NOM present in the source water. Specific knowledge of the NOM characteristics of the source water is crucial to improve and optimize treatment processes, to predict DBP formation potentials (Amy et al., 1987a) and to understand the role of specific NOM components that are responsible for membrane fouling.

Advanced oxidation process (AOP) is an emerging technology in the drinking water industry that have been proven to be a powerful and efficient treatment method for removal of NOM and DBPs (Chin and Bérubé, 2005; Toor and Mohseni, 2007; Wang et al., 2006). AOPs are the processes in which oxidation of organic compounds occurs primarily through reactions with hydroxyl radicals (HO•). Ozone and UV based AOPs are the most common AOPs in drinking water treatment. In addition, ozone and UV based AOPs such as $H_2O_2/O_3$and O_3/UV are efficient for the removal of colour and odour.

The application of AOPs prior to membrane filtration could mitigate membrane fouling caused by NOM. The combination of these processes would serve as robust multiplebarriers for providing protection against broad ranges of chemicals and microorganisms. Ozone oxidation prior to membrane filtration has shown to effectively reduce membrane fouling (Karnik et al., 2005a; Karnik et al., 2005b; Kim et al., 2008). There are very limited studies that have investigated the effect of AOPs on membrane fouling. The mechanisms by which fouling is reduced and NOM are removed in combined AOPs have not been extensively investigated. In addition, limited data investigating the effects of different AOPs on combined AOPs and membrane filtration on membrane fouling and finished water quality exist.

1.1 Research objectives

The two main objectives of this research are as follows:

- To characterize natural organic matter (NOM) removal by integrated membrane filtration and to evaluate the NF fouling behaviour in two full-scale IMS surface water plants.

- To evaluate advanced oxidation processes (AOPs) to reduce NOM and investigate AOPs as pretreatment alternative to control NF fouling. This research aimed to establish effect of these pretreatment processes on permeates flux and permeate quality of NF membrane.

Research was conducted at bench- and full-scale to address the following specific objectives.

1) Conduct advanced characterization of NOM in surface water sources and determine NOM removal efficiency of UF-NF integrated membrane system design.
2) Evaluate the fouling behaviour of NF membranes both in bench- and full-scale studies of two surface source waters.
3) Compare the effectiveness of different oxidation and advanced oxidation processes for the removal of NOM and DBP precursors from drinking water sources.
4) Evaluate normal Raman and Surface Enhanced Raman Spectroscopy for studying fouling on NF membrane.
5) Evaluate AOPs as a pretreatment for NF membranes and to determine the effect on permeate flux decline and permeate water quality.

To achieve these specific objectives, experiments were conducted in five different phases.

Phase 1 characterized the NOM in raw and UF treated water at a full-scale integrated membrane plant.

Phase 2 examined the effect of water quality on fouling behaviour of NF membranes at bench-scale level using two surface source waters and compared these research findings with data collected on NF fouling from two full-scale IMS plants.

Phase 3 compared ozone, UV and AOPs including H_2O_2/O_3, H_2O_2/UV, O_3/UV for the removal of NOM and DBP precursors from a surface source water.

Phase 4 evaluated normal Raman and Surface Enhanced Raman Spectroscopy (SERS) as a new technique for studying fouling on NF membrane.

Phase 5 examined H_2O_2/O_3, H_2O_2/UV, and O_3/UV AOPs as a pretreatment for NF membrane and to determine the effect of permeate flux and permeate water quality.

1.2 Organization of thesis

The main chapters of this thesis are organized in the style of a refereed journal paper. Therefore, each chapter contains an abstract, introduction, materials and methods, results and discussion, and conclusion section.

Chapter 2 provides an overview of the relevant published information related to this research topic. As such, an overview of NOM characterization, membrane filtration and factors impacting membrane fouling are presented. This section also provides a review of published literature on ozone and UV-based AOPs for NOM removal. The effect of oxidation and AOP pretreatment on permeate flux and permeate quality of high pressure membranes are reviewed and discussed.

Chapter 3 provides an overview of the two small-scale IMS drinking water treatment plants in Nova Scotia from which water samples were procured in this research. This chapter also provides an explanation of the materials and methods that are common to the experimental work presented in Chapters 4, 5, 6, 7 and 8. The chapter specific materials and methods are described in those chapters.

Chapter 4 presents the results of Phase 1 of this research, which involved advanced study on the characterization and removal of NOM in raw and UF treated water at a full-scale IMS plant. NOM fractionation experiment performed in this chapter was conducted by Krysta Montreuil (Master's student in Dr. Gagnon's laboratory). This work is currently in press in Journal of *Desalination*.

Chapter 5 presents the findings from Phase 2 of this research, which examined the fouling behaviour in NF membranes at bench-scale using two surface source waters and compared with NF fouling data collected from two full-scale IMS plants. The potential significance of feed water properties and/or membrane properties on fouling behaviour was investigated. This work is currently in press in Journal of *Water Supply: Research and Technology – AQUA*.

Chapter 6 presents the findings from Phase 3 of this research, which compared five different oxidation and AOPs for the removal of NOM from surface source water. This work has been published in Journal of *Water Research*.

Chapter 7 proposed the use of surface enhanced Raman spectroscopy (SERS) as a novel method for analyzing NF membrane fouling caused by natural source waters. This work has been published in Journal of *Separation and Purification Technology*.

Chapter 8 presents results from Phase 6 of this research which investigated H_2O_2/O_3, H_2O_2/UV, O_3/UV AOPs as a pretreatment for NF membrane and evaluated the impact of these AOPs on permeate flux and permeate quality.

Chapter 9 provides a summary and conclusion of the research work conducted in this thesis.

Chapter 10 provides recommendations for alternative advanced treatment technology in terms of reduction of NOM and membrane fouling. Recommendations for future research are also presented based on the findings in this study.

CHAPTER 2 LITERATURE REVIEW

2.1 Natural Organic Matter Characterization

Natural Organic Matter (NOM) is a complex heterogeneous mixture composed of humic acids, fulvic acids, low molecular weight (MW) organic acids, carbohydrates, proteins, and other compound classes (Nyström et al., 1996; Yuan and Zydney, 2000). It is ubiquitously present in surface waters and poses various challenges to drinking water treatment and finished water quality. These problems include: (i) negative effect on water quality due to colour, taste, and odour, (ii) increased disinfectant dose requirement, which in turn results in carcinogenic DBP production (Singer, 1999), (iii) promoted biological growth in distribution systems (Rittmann and Snoeylink, 1984) and (iv) increased levels of complex heavy metals and adsorbed organic pollutants (Ravichandran et al., 1998; Schmitt et al., 2002). Due to these adverse water quality problems and stricter regulations in drinking water quality, improved treatment methods are needed. In water treatment facilities, the effectiveness of a treatment process is highly dependent on the characteristics and concentrations of the NOM present in source water. Specific knowledge of NOM characteristics is crucial for predicting the DBP formation potentials (Amy et al., 1987a).

Several methods are available for NOM characterization. Matilainen et al. (2011) provides a comprehensive review of most of the available methods used to characterize

NOM present in drinking water sources. The nonspecific parameters are UV absorbance at 254 nm (UV_{254}), total organic carbon (TOC) and colour. Specific UV absorbance (SUVA), which is the ratio of UV_{254} to DOC, can provide insights into the aromaticity or hydrophobicity of NOM. SUVA and hydrophobic/hydrophilic distribution provide a means for selecting potential treatment strategies. For example, hydrophobic or humic acid fractions can be readily removed by coagulation, activated carbon and membrane filtration processes (Owen et al., 1995b). Those macromolecules can be transformed by oxidation processes into less hydrophobic and lower MW organics that may be less problematic for membrane fouling (Song et al., 2004). Humic substances with higher aromatic carbon content and a higher SUVA than non-humic substances produce more DBPs (Singer, 1999). Specifically, polysaccharides and proteins have been shown to be major foulants in NF membrane systems (Cho et al., 1998a; Speth et al., 1998).

High performance size-exclusion chromatography (HPSEC) is a technique frequently used to characterize NOM utilizing its apparent molecular weight (MW) (Chin et al., 1994; Her et al., 2002). Chin et al. (1994) used the HPSEC technique with a UVA detector to analyze the MW distribution of a water sample and to calculate weight-averaged MW (M_w), number-averaged MW (M_n), and polydispersivity (M_w/M_n), which is an index of NOM homogeneity. Her et al (2002) optimized the HPSEC technique by coupling UV absorbance with an online DOC detector. The main advantage of using HPSEC with sequential UVA and DOC detectors is that it can detect virtually all of the organic carbon present in a sample unlike UVA that detects only double bond organic compounds.

Resin fractionation of NOM is a common technique used to isolate different constituents of NOM present in natural water (Leenheer, 1981; Leenheer and P.Croue, 2003). This method fractionates NOM into hydrophobic (HPO) and hydrophilic (HPI) components. Many researchers have used the XAD-8 and XAD-4 resin fractionation techniques (Croue et al., 2004; Wei et al., 2008; Sharp et al., 2006). The XAD-8 resin favours the isolation of hydrophobic NOM (NOM containing high MW matter with aromatic character). The hydrophilic fraction is not adsorbed onto both of the resins. The XAD-4 resin adsorbs weakly the hydrophobic acid fractions, which are commonly defined as the transphilic NOM.

Leenheer (1981) developed a comprehensive fractionation procedure in which hydrophobic and hydrophilic organics can be further separated by charge into acid, base and neutral fractions. Although this procedure has been applied to natural water systems, it is not recommended for samples with dissolved organic matter (DOM) less than 5mg/L typically found in water treatment plants. Marhaba et al. (2003b) developed a fractionation procedure intended specifically to characterize source waters containing low DOC (< 5mg/L).

The DOC concentration of each organic fraction varies depending on the NOM source. The compositions of NOM in different source waters are compared in Table 2.1. Overall, hydrophobic acid and hydrophilic neutral fractions have been found to be the most abundant in source waters (Kanokkantapong et al., 2005; Marhaba and Van, 2000; Panyapinyopol et al., 2005; Swietlik and Sikorska, 2005).

Table 2.1 Percentages of NOM Fractions in Various Source Waters

	Sources of NOM			
Organic Fractions	(Marhaba and Van, 2000)	(Swietlik and Sikorska, 2005)	(Panyapinyopol et al., 2005)	(Kanokkantapong et al., 2005)
Hydrophobic acid (HOA)	8-12%	73%	34%	31 -34%
Hydrophobic base (HOB)	0-6%	>1%	3%	0.8 -5.7%
Hydrophobic neutral (HON)	13- 22%	12%	6%	5.7 -12%
Hydrophilic acid (HIA)	44 -55%	7%	18%	8 -18%
Hydrophilic base (HIB)	4 -5%	5%	3%	3.3 -5.5%
Hydrophilic neutral (HIN)	9 -25%	3%	45%	25 -44%

The composition of six organic fractions, their ability to form disinfection by-products formation potential (DBPFP) in drinking water is summarized in Table 2.2.

Table 2.2 Composition of Organic Fractions and Their Impact on Disinfection By-products Formation Potential (DBPFP)

Organic fractions	**Organic carbon class**	**DBP FP**
Hydrophobic acid (HOA)	Humic substances, fulvic acids, C5-C9 aliphatic carboxylic acids, aromatic carboxylic acids	High
Hydrophobic base (HOB)	aromatic amines protein, amino acids, amino sugars	Moderate
Hydrophobic neutrals (HON)	Hydrocarbons, amides, esters, ketones, aldehydes, long chain (> C_9) aliphatic carboxylic acids and amines, 3-ring aromatic carboxylic acids	Moderate
Hydrophilic acids (HIA)	Low MW carboxylic acids, sugar acids, fatty acids, mixtures of various hydroxyl acids	NA
Hydrophilic base (HIB)	Polysaccharides, aromatic amines, amphoteric proteinaceous materials containing aliphatic amino acids, amino sugars	Moderate
Hydrophilic neutrals (HIN)	Short chain aliphatic amines, alcohols, neutral aldehydes; esters; carbohydrates; cylic amides, polysaccharides, low MW alkyl alcohols	NA
References	(Aiken et al., 1992; Barber et al., 2001a; Leenheer, 1981; Marhaba et al., 2003b; Peuravuori et al., 1997)	

Hydrophobic acid (HOA) was observed as a main contributor for DBPFP (Croue et al., 2000; Lin and Wang, 2011). Other studies have shown that hydrophilic acid, neutral or base fractions can have greater trihalomethane formation potential (THMFP) than hydrophobic acids (Dotson et al., 2009; Hwang et al., 2001). Liang and Singer (2003) have observed hydrophilic neutral as an important precursor to DBPs in waters with low colour. Therefore, a detailed understanding on the type and concentration of the organic fractions in source water is important in optimising NOM removal for the mitigation of DBPs.

2.2 Overview of Membrane Processes

Membranes are classified into four categories based on their pore size or molecular weight cut-off (MWCO). The ability of each membrane to remove particles, organic and inorganic compounds, and pathogens on the basis of pore size is presented in Table 2.3.

Table 2.3 Membrane Pore Sizes and Removal Capacity (MWH, 2005)

Types	**Pore sizes (µm)**	**Water pollutants**
MF	0.1	Particles, sediment, algae, protozoa, bacteria
UF	0.01	Small colloids, virus,
NF	0.001	DOC, divalent ions (Ca^{2+}, Mg^{2+})
RO	Non porous	Monovalent ions (Na^{+}, Cl^{-})

Microfiltration (MF) and ultrafiltration (UF) membranes have shown to be effective for the removal of particles, colloids, protozoa, and viruses (USEPA, 2001). NF membranes are able to remove DOC and divalent ions. Reverse osmosis (RO) is a non-porous membrane capable to remove monovalent ions.

Membranes are further categorized into low and high pressure membranes. Low pressure membrane (LPM) includes MF and UF and high pressure membrane (HPM) includes NF and RO. The typical configuration of LPMs are hollow-fiber and tubular membranes. Hollow-fiber membranes operate in an inside-out or outside-in mode. The operational mode of the LPM is cross-flow and dead-end filtration mode as is illustrated in Figure 2.1. In cross-flow configuration, the flow stream is tangential to the membrane surface while in dead-end configuration, the feed stream passes through the membrane. MF and UF membranes commonly operate in a dead-end filtration mode. Back flushing is possible with this configuration for controlling the hydraulically reversible fouling caused by particulate and colloidal materials on the membrane surface. Chemical cleaning is performed at regular intervals to control irreversible fouling.

The most common configuration of HPM is spiral wound element in which feed stream flows in cross-flow mode. In cross-flow configuration, the formation of a cake (foulant) layer is reduced due to the shear forces on the membrane surface. Moreover, membranes with cross-flow configuration can be operated in higher flux and for longer periods of time since most of the solids are carried away from the membrane surface in the concentrate flow (USEPA, 2003). Unlike in dead end mode, back-flushing is not possible in HPM. Chemical cleaning is a common practice to control membrane fouling in cross-flow configuration.

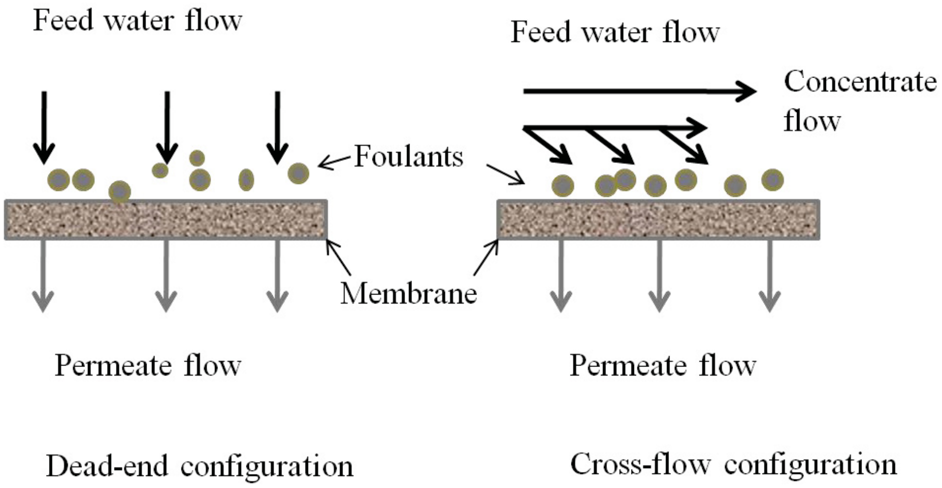

Figure 2.1 Membrane Flow Configurations.

2.3 Factors Affecting Membrane Fouling

Membrane fouling caused by the deposition of suspended or dissolved substances on the surface or within the pores of the membrane results in the loss of membrane performance and deterioration of water quality. Common fouling causing substances (foulants) in the source water are inorganic (e.g. calcium carbonate, calcium sulphate, magnesium sulphate, and iron hydroxide), organic (colloidal or dissolved NOM), colloids (e.g. biological debris, clay), and biological (i.e. bacteria) materials (Her et al., 2007; Kimura et al., 2004; Schäfer et al., 1998). A decrease in permeate flux or an increase in transmembrane pressure (TMP) indicates membrane fouling. At the bench scale, pressure is usually kept constant and the reduction in performance of the membrane (or fouling) is measured by a reduction in permeate flux. In full scale level, however, the permeate flux is kept constant and membrane fouling is measured by an increase of feed pressure or TMP.

There are five factors that affect membrane fouling and NOM removal: i) Water quality matrix such as NOM concentrations, ionic strength, concentration of monovalent and divalent ions, and pH (Braghetta, 1995; Childress and Elimelech, 1996; Hong and Elimelech, 1997b; Seidel and Elimelech, 2002), ii) NOM properties including molecular weight, hydrophobicity/hydrophilicity, and charge density (Jarusutthirak et al., 2007; Seidel and Elimelech, 2002), iii) membrane characteristics such as surface roughness, MWCO, charge density, and hydrophobicity/hydrophilicity (Boussu et al., 2008; Hobbs et al., 2006; Lee and Lee, 2007; Tang et al., 2009), and iv) hydrodynamic and operating conditions such as, permeate flux, pressure, and concentration polarization (Tang et al., 2007a). How each of these parameters affects membrane fouling and NOM rejection are discussed in the following sections.

2.3.1 Water Quality Matrix

Low pH, high ionic strength, and high concentrations of divalent ions (e.g. calcium ions) result in high permeate flux decline and low NOM rejection. For source waters with low pH, protonation of organic acid constituents of NOM and membrane causes a decrease in their charge density (Braghetta, 1995; Braghetta et al., 1998; Hong and Elimelech, 1997a). High ionic strength (conductivity) of source water results in a decrease in the charge density of NOM and the membrane due to double layer compression (Braghetta, 1995; Braghetta et al., 1998; Hong and Elimelech, 1997a; Jones and O'Melia, 2000). Because of low repulsion forces, adsorption of NOM onto the membrane surface is promoted. At higher calcium concentrations, charge density of NOM and charged membrane decreases due to their complexation with calcium ions, which results in more NOM adsorption (Hong and Elimelech, 1997a; Jucker and Clark, 1994; Schäfer et al., 2001).

The apparent molecular size of NOM molecules decreases at low pH, high ionic strength, and high calcium concentrations due to their compact and coiled configurations, resulting in low NOM rejection (Braghetta et al., 1997; Hong and Elimelech, 1997a). However, Braghetta et al. (1997) observed increased rejection of uncharged solutes at high ionic strength possibly caused by double layer compression that lowers the MWCO of the membrane. The reduction of charge density of NOM and membrane at high ionic strength, low pH, and high calcium concentration enhances adsorption of NOM onto the membrane surface (Braghetta et al., 1997; Hong and Elimelech, 1997a; Jucker and Clark, 1994).

2.3.2 NOM Properties

NOM properties including molecular weight, hydrophobicity/hydrophilicity, and charge density are important factors for membrane fouling and NOM rejection. The fouling potential of NOM is enhanced by chemical and physical interactions between the NOM and the membrane surface. These include hydrophobic interactions, hydrogen bridges, and electrostatic interactions. Hydrophobic interaction between NOM and the membrane surface is an influential factor on adsorptive membrane fouling by NOM (Jucker and Clark, 1994; Nilson and DiGiano, 1996). Nilson and DiGiano (1996) observed that hydrophobic NOM fraction resulted in more flux decline than hydrophilic NOM during the NF process. However, Braghetta et al., (1998) have shown that the hydrophilic fraction of NOM exhibits more fouling potential than the hydrophobic fraction of NOM. High fouling potential of hydrophilic fraction such as polysaccharides and proteins has also been reported (Cho et al., 1998a; Seidel and Elimelech, 2002; Speth et al., 1998). Fan et al. (2001) have found that the order of fouling potential of NOM fractions in low pressure membranes is hydrophilic neutral > hydrophobic acids > transphilic acids > hydrophobic charged. Hydrophilic neutrals foul more than hydrophobic acids due to bulky macromolecular shape and neutral character of polysaccharides that make it prone to foul and adsorb on membrane surfaces (Speth et al., 1998). Lin et al. (2000) found that large-sized molecules of hydrophilic and hydrophobic NOM components cause the largest flux decline. Jarusutthirak et al. (2002) studied the effect of effluent organic matter on UF and NF membranes and found that the high molecular weight of hydrophilic components was the main contributor of NOM fouling. It follows that low

UV absorbing compounds and high molecular weight hydrophilic components that occur through adsorption mechanisms cause NOM fouling.

Charge density (zeta potential) of NOM also plays a role on flux decline and NOM rejection. The negative charges of NOM develop as a result of deionization of acidic functional groups (e.g. R-COO^-, R-NH^-) hindering their adsorption onto negatively charged membranes thereby resulting in high NOM rejection (Braghetta et al., 1997; Cho et al., 1999; Cho et al., 2000).

2.3.3 Membrane Characteristics

Molecular weight cut-off (MWCO), roughness, and hydrophobicity/hydrophilicity are the membrane surface characteristics that influence flux decline and NOM rejection. Table 2.4 summarizes the techniques available for membrane surface characterization. Atomic force microscopy (AFM) has been used for the determination of the MWCO of membranes by measuring the membrane surface pore radius (Bowen and Doneva, 2000; Bowen et al., 1997; Calvo et al., 1997; Richard Bowen et al., 1996). Bowen et al. (2000) used AFM to quantify the mean surface pore diameters of five different UF membranes with the MWCO in the range 1,000 -10,000 Da and observed pore diameters in the range of 1.93- 3.14 nm. Yuan and Zydney (2000) observed increased flux decline with the UF membrane with higher MWCO due to deposition of humic acid on the membrane surface which caused higher hydraulic resistance. Water quality parameters could change apparent pore sizes of charged NF membranes due to double layer compression.

Surface charge or charge density of a membrane plays a significant role in membrane flux decline and NOM rejection. The charge density of a membrane is measured by using streaming potential analyzer or a zeta-meter. Water quality parameters (pH, ionic strength) and NOM adsorption can significantly affect membrane surface charge. NOM adsorption onto a negatively charged membrane reduces the negative charge of the membrane surface (Cho et al., 1998a; Jucker and Clark, 1994). Other studies reported an increase in the negative charges of the membrane surface due to adsorption of humic acid onto the membrane surface (Childress and Deshmukh, 1998; Hong and Elimelech, 1997a). Zeta potential was become less negative for the NF270 membrane and more negative for other membrane types (HL, SR2, NF90) after filtration of source water from the French River (Tatamagouche, Nova Scotia) and the Grand River (Kitchner -Waterloo, Ontario) (Makdissy et al., 2010). Membrane hydrophobicity/hydrophilicity affects adsorptive fouling by NOM. Membrane hydrophobicity has been quantified by contact angle measurements (G.Crozes et al., 1993; Harrison et al., 2007; Jucker and Clark, 1994). Crozes et al (1993) reported that a hydrophobic polyamide membrane caused more permeate flux decline compared to a hydrophilic cellulose acetate membrane. Membrane hydrophobicity may be influenced by characteristics of adsorbed solute or foulants onto the membrane.

Surface roughness of membranes affects flux decline and solute rejection. An increase in surface roughness of the membrane results in an increase in the membrane fouling rate (Hobbs et al., 2006; Li et al., 2007; Vrijenhoek et al., 2001). Hobbs et al. (2006) examined the effect of surface roughness on fouling of the RO and NF membranes with a high organic surficial groundwater. Those studiesobserved enhanced membrane fouling with an increase in surface roughness. Tang et al. (2007) found that membrane flux was independent of virgin NF membrane properties but was dependent on hydrodynamic conditions.

2.3.4 Hydrodynamic and Operating Conditions

Membrane operating conditions, such as cross-flow velocity (CFV) and initial flux, affect membrane fouling and NOM removal (Cho et al., 2002; Crozes et al., 1997; Tang et al., 2007a). High initial flux resulted in severe flux reduction. Tang et al. (2007a) observed severe permeate flux reduction at high initial flux, low pH and high calcium concentration. Cho et al. (2002) have provided details on the effect of *f/k* ratio (ratio of permeation flux and the back diffusional mass transfer coefficient) on NF and UF membranes fouling. A higher *f/k* ratio indicates higher potential for NOM accumulation at the membrane surface and a higher fouling potential.

2.4 Characterization of Membrane Surface and Foulant Layer

The characterization of virgin and fouled membranes is essential for detailed understanding of the membrane fouling mechanisms and nature of foulant. Various techniques have been developed to characterize the membrane surface and foulant layer. Details on these techniques and membrane characteristics are summarized in Table 2.4. Surface charge, hydrophobicity, and roughness of the membrane surface and the foulant layers can be evaluated using a zeta-meter or streaming potential analyzer, contact angle, and AFM, respectively as described in Section 2.3. Scanning electron microscopy (SEM) and transmission electron microscopy (TEM) are used for analyzing shape, size, and morphology of foulant layers deposited onto the membrane surface (Braghetta et al., 1998; Harrison et al., 2007; Makdissy et al., 2010; Tang et al., 2007a).

The functional groups of foulants deposited on membrane surface are identified using ATR-FTIR technique (Cho et al., 1998b; Her et al., 2008a; Her et al., 2004). Cho et al.(1998a) observed polysaccharides (hydrophilic neutrals) as the main foulant after filtering NOM containing source water. Jarusutthirak and Amy (2006) found polysaccharides, proteins, and/or amino sugar like compounds in RO, NF and tight UF membranes fouled with soluble microbial products and effluent organic matter.

Table 2.4 Instruments/Techniques Used for Membrane Surface and Foulant Characterization

Instrument	**Characteristics**	**References**
Zeta-meter or streaming potential analyzer	Surface charges	(Hobbs et al., 2006)
		(Hong and Elimelech, 1997b)
Contact angle	Hydrophobicity/hydrophilicity	(Xu et al., 2006), (Jucker and Clark, 1994), (Cho et al., 1998a)
AFM[a]	Membrane surface roughness	(Lee et al., 2004)
	Topographical information	(Zhu and Elimelech, 1997)
		(Bowen et al., 1997)
SEM[b]	Shape, size, and morphology	(Harrison et al., 2007)
		(Mosqueda-Jimenez and Huck, 2006)
		(Gwon et al., 2003), (Her et al., 2007)
		(Braghetta et al., 1998)
TEM[c]	Shape, size, and morphology	(Tang et al., 2007a) (Makdissy et al., 2010)
ATR-FTIR[d]	Functional groups or molecular structure	(Her et al., 2008a; Her et al., 2004; Her et al., 2007)
Raman Spectroscopy	Functional groups or molecular structure	(Khulbe et al., 1996; Khulbe and Matsuura, 2000; Khulbe et al., 1997)
SERS[e]	Protein foulants	(Cui et al., 2011)

[a] Atomic Force Microscopy

[b] Scanning Electron Microscopy

[c] Transmission Electron Microscopy

[d] Attenuated Total Reflection-Fourier Transform Infrared Spectroscopy

[e] Surface Enhanced Raman Spectroscopy

Raman spectroscopy, a complementary technique to infrared spectroscopy, is an alternative technique for molecular identification. It has been used for characterization of membrane morphology (Khulbe et al., 1996; Khulbe and Matsuura, 2000; Khulbe et al., 1997). The Raman spectra are narrower and cleaner than the infrared spectra and the Raman technique requires no special preparation. Nevertheless, the Raman spectroscopy has not gained significant attraction for identification of organic compounds due to inherently weak signals and interference from fluorescence.

Surface enhanced Raman Spectroscopy (SERS) is an extension of normal Raman spectroscopy that provides enhanced Raman signal and quenching of fluorescence through the use of noble metal substances (e.g. silver, gold). It has been used for the identification and quantification of organic contaminants (Brosseau et al., 2009b; Brosseau et al., 2009a), inorganic contaminants (Alvarez-Puebla et al., 2007; Baker and Moore, 2005), and pathogens (Rule and Vikesland, 2009; Sengupta et al., 2006) in environmental samples. Recently, Cui et al. (2011) have used SERS to study protein fouling on the polyvinlylidene fluoride (PVDF) UF membrane. The fouling propensity of different types of proteins was evaluated, and fouled area of the membrane was evaluated by the silver staining and Raman mapping. In this thesis, SERS is used to examine fouling caused by naturally occurring organic compounds on the NF membrane, which is used in drinking water treatment.

2.5 Advanced Oxidation Processes for NOM Removal

The application of AOPs has gained significant interest in the drinking water industry for the removal of various types of organic compounds. Their application to water treatment includes the removal of NOM or DBP precursors (Amirsardari et al., 2001; Chin and Bérubé, 2005), colour and odour causing compounds (Karimi et al., 1997; Koch et al., 1992), and trace organic contaminants present in the water sources (Dickenson et al., 2009; Wert et al., 2009). Ozone and UV AOPs are recognized to effectively inactivate coliform indicators and more resistant pathogenic microorganisms such as *Giardia* and *Cryptospridium* in water treatment. In particular, ozone and UV-based technologies are well established in commercial water treatment application.

AOPs result in either complete oxidation or transformation of NOM into lower molecular weight organics. Under strong oxidation conditions, NOM is mineralized and forms carbon dioxide, water, and the corresponding salts. In commercial water treatment applications, low or moderate advanced conditions are applied due to economical feasibility. Under these conditions, NOM is partially oxidized and higher molecular weight NOM is transformed into smaller and more biodegradable compounds such as aldehydes and carboxylic acids (Backlund, 1994; Edwards and Benjamin, 1992; Lamsal et al., 2011; Sarathy and Mohseni, 2007). Such changes in the chemical characteristic of NOM also result in reducing TOC concentrations and/or alter the characteristics of the DBP precursor material potentially reducing its reactivity with chlorine. However, partial oxidation could result in increased DBPFP during VUV (Bond et al., 2009), TiO_2/UV

(Liu et al., 2002), and H_2O_2/UV treatments (Toor and Mohseni, 2007). During VUV and H_2O_2/UV processes, the DBP speciation has been found to shift to more brominated DBPs (Wang et al., 2006).

Several studies have reported a decrease in DOC concentration and DBPFP of the source water by AOPs (Amirsardari et al., 2001; Chin and Bérubé, 2005; Sierka and Amy, 1985). Between UV_{254} and DOC, the two surrogate parameters of NOM, UV_{254} suggests larger removal of NOM than DOC as observed in various AOPs studies: H_2O_2/UV (Goslan et al., 2006; Lamsal et al., 2011; Sarathy and Mohseni, 2007), H_2O_2/O_3 (Kleiser and Frimmel, 2000; Lamsal et al., 2011), O_3/UV (Amirsardari et al., 2001; Chin and Bérubé, 2005). The increased reduction of UV_{254} values suggest that the higher MW NOM are rapidly broken down into lower MW by-products with no UV absorbance. These low MW by-products are less susceptible to attacks by HO• radicals and therefore are not mineralized completely (Sanly et al., 2007). Degradation of hydrophobic acids can lead to an increase in the hydrophilic fractions (Liu et al., 2010; Sanly et al., 2007).

2.6 Effects of AOPs on Membrane Permeate Flux and Quality

A detailed understanding and characterization of the hydroxyl radical-induced transformation of NOM is necessary for the application of AOPs as a pretreatment to membrane filtration. The humic substances, the predominant form of NOM, are high in aromatic carbon and have a negative charge. This charge is primarily contributed by three main functional groups of NOM, namely carboxylic acids, methoxyl carbonyls, and phenolic groups (Thurman, 1985). Several studies have reported the changes in NOM properties during ozonation (Edwards and Benjamin, 1992; Owen et al., 1995b; Westerhoff et al., 1999). Changes in NOM properties in preozonated water and the impact of NOM fractions on permeate flux and permeate quality of membrane are presented in Table 2.5. Similar changes in NOM properties are assumed in ozone based AOPs (i.e. H_2O_2/O_3 and O_3/UV) and H_2O_2/UV AOP.

As presented in Table 2.5, AOP induced changes affect either favourably or unfavourably membrane filtration processes with regard to permeate flux and permeate quality. An increase in membrane permeate flux is related to the transformation of humic, hydrophobic, or aromatic fractions of NOM into less humic, hydrophilic, less aromatic or aliphatic forms, and lower MW organic molecules during AOPs pretreatment (Fan et al., 2001; Nilson and DiGiano, 1996; Schäfer et al., 1998). Substantial structural changes of NOM during ozonation lead to a significant decrease in membrane fouling and an increase in permeate flux (Van Geluwe et al., 2011). There exists an efficient removal of aromatic rings that decreases the adsorption of NOM by hydrophobic interactions and a significant increase of the number of carboxylic functions, which are repelled by the negative membrane surface.

Table 2.5 Ozone Induced Changes in NOM Properties and Their Impact on Membrane Permeate Flux and Permeate Quality

NOM properties	**Effects on NOM**	**References**	**Impact on permeate flux and permeate quality**	**References**
Humic content, molecular weights, aromaticity, hydrophobicity	Decrease	(Owen et al., 1995a) (Westerhoff et al., 1999)	Decrease the adsorption of NOM by hydrophobic interactions	(Jucker and Clark, 1994)
			May decrease the steric rejection of NOM due to transformation of macromolecules into lower MW organics.	(Cho et al., 2000; Fan et al., 2001; Nilson and DiGiano, 1996)
Binding capacity with multivalent cations	Increase except during excessive oxidation		NOM with higher binding capacity with Ca^{2+} or Mg^{2+} exhibits higher membrane fouling potential	(Fan et al., 2001; Jucker and Clark, 1994; Nilson and DiGiano, 1996)
Carboxylic functions	Increase	(Owen et al., 1995a; Westerhoff et al., 1999)	May increase permeate flux	(Van Geluwe et al., 2011)
Charge density (zeta potential)	Decrease except in absence of Ca		More amenable to adsorption with negatively charged NF membrane, therefore, increase adsorptive fouling.	(Braghetta et al., 1997; Cho et al., 2000; Yuan and Zydney, 2000)
Biodegradable organic carbon	Increase	(Owen et al., 1995a)	Promote biofouling	
Polarity	Increase	(Van der Bruggen et al., 1999; Owen et al., 1995a; Westerhoff et al., 1999)	Organic with high dipole moment have lower retention	(Van der Bruggen et al., 1999)

The negative impact of AOP induced changes is related to an increase in BDOC during ozone based AOPs, which promote biofouling. Ozone preferentially reacts with the humic fraction of NOM whereas the non-humic substances, such as polysaccharides, may accumulate in the preoxidized water resulting in organic fouling (Speth et al 1999). Nevertheless, AOPs are more effective at decreasing all fractions of NOM compared to ozonation (Chin and Bérubé, 2005; Lamsal et al., 2011). It is therefore assumed that AOPs are less problematic compared to ozone oxidation with reference to accumulation of non-humic substances.

Song et al. (2004) provided a detailed description of chemical interactions between NOM molecules and NF membrane surfaces. The structure of the DK-NF membrane used here consists of polyamide moiety with carboxylic and amide groups as in the NF70 membrane. These carboxylic and amide groups of the membrane can form covalent bonds with carboxylic and phenolic groups of NOM molecules which can cause severe membrane fouling. After oxidation, aromatic moieties in humic acid transform into quinone and carbonyl groups (Wang et al., 2001). These quinone and carbonyl groups have lower propensity for covalent bonding with the carboxyl and amide groups of the membrane, but can form hydrogen bonds. Since the hydrogen bonds have lower dissociation energy as compared to covalent bonds, the membrane fouling after oxidation is reversible and less severe. Therefore, AOPs pretreatment can potentially reduce NF fouling.

Preoxidation may decrease the membrane's ability to reject NOM due to the transformation of macromolecules into lower MW organics. An increase in intramolecular Ca^{2+} and Mg^{2+} binding due to oxidation results in charge reduction of NOM and may decrease electrostatic rejection by a charged membrane. Such effect would not apply to Ca^{2+} and Mg^{2+} free water. Van der Bruggen et al. (1999) observed low rejection of organic molecules with higher dipole moments (i.e. polar molecules) compared to molecules with little or no dipole moment due to electrostatic attraction between membrane and polar molecules. These polar molecules are directed towards the membrane surface and readily pass through the pore.

As discussed above, oxidation as a pretreatment may favourably and unfavourably influence membrane fouling. The application of ozone oxidation of feed water prior to membrane filtration resulted in a significant decrease in membrane fouling (Geluwe et al., 2011). A previous study with the TiO_2/UV pretreatment process observed an improved permeate flux of the UF membrane due to changes in NOM molecular characteristics (i.e. transformation into less adsorbable organic materials) (Huang et al. 2008). Song et al. (2004) observed an increase in permeate flux of the NF membrane with the H_2O_2/UV pretreatment for surface water. In this thesis, three different AOPs (H_2O_2/O_3, H_2O_2/UV, and O_3/UV) pretreatment for the NF membrane are compared, and the effect of those AOPs on membrane permeate flux and permeate quality are evaluated.

CHAPTER 3 MATERIALS AND METHODS

This chapter provides raw source water characteristics, and analytical methods that are common to experimental sections presented in Chapter 4, 5, 6, 7, and 8. Materials and methods that are chapter specific are described in the particular chapter.

3.1 French River Raw Water

The main source of sample water during this research was collected from French River, Tatamagouche, Nova Scotia, Canada. Table 3.1 presents the general water quality parameters of the French River.

Table 3.1 French River Water Characteristics

Parameters	**Units**	**Range**	**Average values**
pH		6.6 - 7.1	6.85
Turbidity	NTU	1.1 - 5.6	3.4
Colour	Pt-Co	19 - 45	32
Alkalinity	mg/L as $CaCO_3$	4 - 27	15.5
UV_{254}	cm^{-1}	0.064 - 0.416	0.24
TOC	mg/L	3.1 - 5.65	4.4
DOC	mg/L	2.8 - 5.3	4.05
SUVA	$(Lmg^{-1}m^{-1})$	1.8 - 3.2	2.5

The French River is a shallow river that flows through the surrounding agricultural and natural land-use areas. The water quality of the river is degraded during periods of high precipitation and seasonal changes occur during spring and fall due to run-off. The typical water quality is characterized as low alkalinity, low turbidity and moderate TOC.

3.2 Tatamagouche Water Treatment Plant

The Tatamagouche WTP is a new surface WTP that serves drinking water for the Tatamagouche village, Nova Scotia, Canada. The water treatment facility includes an IMS designed with UF membranes preceding NF membrane (Figure 3.1) which has beenin operation since January 2008. The raw water is pumped through a pretreatment strainer and redundant UF skids, each containing 18 ZeeWeed® 1000 UF modules, which have a nominal pore size of 0.02 microns. The units operate in parallel and each is designed to produce a continuous output of 533 L/min with a net raw water flow of 561 L/min at 95% recovery. Each UF module has a membrane area of 41.8 m^2. Under design (max) operating conditions the net operating flux is 21.3 $Lm^{-2}hr^{-1}$. The UF permeate is directed to an intermediate transfer tank which provides storage and feed water to the NF units. Each NF unit (GE Osmonics PRO-100NF) is equipped with 1.0 micron cartridge pre-filtration for membrane protection prior to a 4-2 membrane array consisting of 6 pressure vessels, each containing 4 x 200 diameter NF modules (OSMO PRO RO365). Each membrane element has an area of 33.9 m^2 which provides a total area of 813.6 m^2 per skid. The overall treatment system is designed at 71% recovery. The NF permeate is chlorinated in chlorine contact chamber to ensure pathogen reduction and is then stored in a clear-water tank for pumping into the distribution system. The NF concentrate is combined with the UF reject and discharged to the river. The entire plant operation is automated and the plant starts production of drinking water with a demand signal from the water tower located in the village.

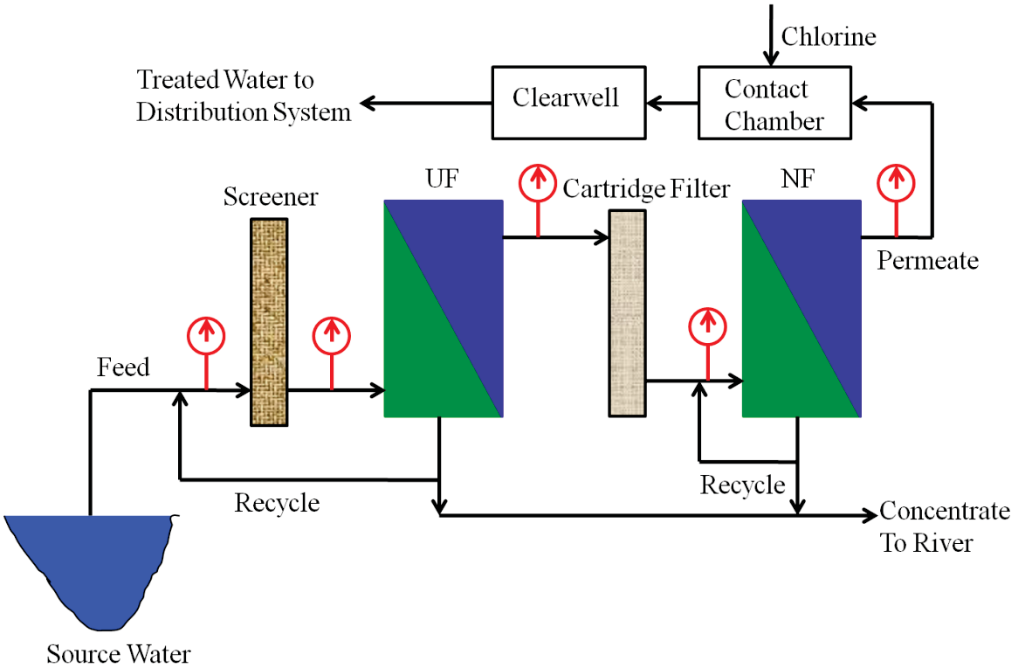

Figure 3.1 Schematic of the Tatamagouche WTP.

3.3 Fletcher Lake Raw Water

Fletcher Lake raw water was used to provide comparative studies of NF fouling in bench scale and full scale level, which provides source water to IMS in the Collin Park WTP located in the communities of Wellington, Nova Scotia, Canada. The Lake is a part of the Shubenacadie watershed, one of the largest and most developed watersheds in Nova Scotia. Fletcher Lake is used for many recreation purposes and is largely developed along the eastern and south western edges with residential properties and light commercial businesses. There are two municipal wastewater treatment plants located along the southern lakefront which discharge treated effluent into the lake. Storm water flows from properties, highways, and the surrounding catchment area also discharge to the lake. As source water for municipal drinking water the general water chemistry is typical of that found in many similar surface supplies. The average water characteristics provided from August 2009 to August 2010 are given in Table 3.2.

Table 3.2 Average Water Quality Characteristics of the Fletcher Lake Raw Water

Parameters	**Units**	**Average**	**Standard deviation**
pH		6.92	0.29
Turbidity	NTU	1.3	1.2
Conductivity	µS/cm	177	25
UV_{254}	cm^{-1}	0.164	0.001
TOC	mg/L	4.1	0.6
Calcium	mg/L	6.8	0.5
Iron	mg/L	0.26	0.21
Nitrate and nitrite	mg/L	0.21	0.10

3.4 Collins Park Water Treatment Plant

Figure 3.2 shows a schematic diagram of the Collins Park WTP. The treatment plant includes an integrated UF/NF membrane system with redundant UF trains and a single NF train. Raw water is pumped from the lake through 50 micron self-cleaning strainers and into parallel UF module racks. Each rack contains 4 HYDRAcap UF modules (Nitto Denko /Hydranautics Corporation, Oceanside, USA) having an active membrane area of 46.5 m^2 per module. The modules operate in a dead-end filtration mode at a design flow rate of 191.2 L/min per rack at a flux of 93 L/m^2.hr and recovery of 95.7%. Permeate from the UF modules is stored in an intermediate transfer tank to be used as NF feed water.

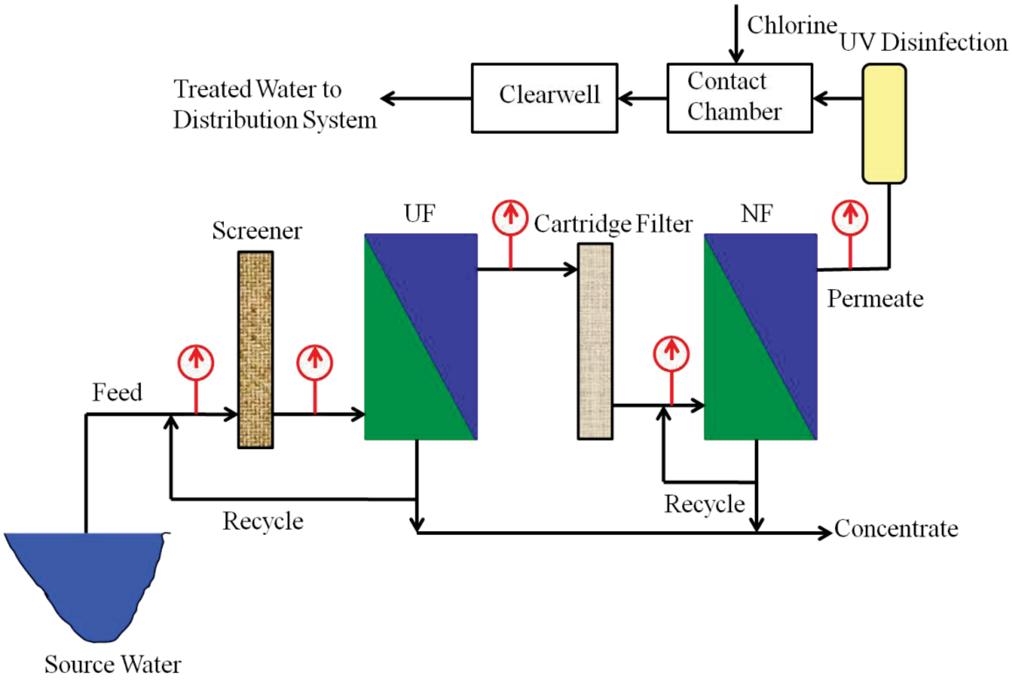

Figure 3.2 Schematic Diagram of the Collins Park WTP.

The NF system consists of pre-filtration through a 5 micron cartridge filter and a 1-1 membrane array of two FRP pressure vessels, each containing 4 × 200 NF modules (Hydranautics ESPA4). Each NF module has an area of 37.1 m^2 providing a total of NF membrane area of 296.8 m^2. The permeate production rate from the system is 110 L/min at a recovery of 80% and average per module flux of 22.1 L/m^2.hr. UV radiation is used as primary disinfectant after NF membrane to kill chlorine resistant organisms such as Cryptosporidium and Giardia. The UV treated water is finally disinfected with chlorine and stored in the clear well before pumping into distribution system.

3.5 Bench-Scale AOPs Studies

3.5.1 Ozone Water Treatment

A bench scale experimental set-up for the ozone experiments is shown in Figure 3.3. It consists of a compressed air system, ozone generator (VMUS-4), a contactor (reactor), and an off-gas collection system. The reactor was a glass tank with a working volume of 10 L (0.305 m diameter × 0.41 m height). The inflow and outflow of the ozone gas line in the reactor was fitted with a laboratory stopper (Fisher scientific # 14141R) at the top of the reactor and the sample was taken from the bottom of the reactor. Compressed air with a flow rate of 2 L/min was passed into the ozone generator (VMUS-4), where high voltage corona discharge causes break down of oxygen molecules into radicals that combine with oxygen molecules to form ozone. Ozone gas was bubbled into the base of the reactor using a fine bubble diffuser at a flow rate of 2 L/min and pressure of 15 psi. A potassium iodide solution (20 gm potassium iodide in 1 L milli-Q water) was used to collect the residual ozone gas in the off-gas from the reactor. Ozonation was done in a semi-batch mode by continuously passing O_3 gas at room temperature (23±1 ^{o}C) for 5, 15, 30, 45 and 60 min times. The optimum ozone dose for the sample water was identified as that which reduced UV_{254} and TOC to the greatest degree and those results were compared with other AOPs.

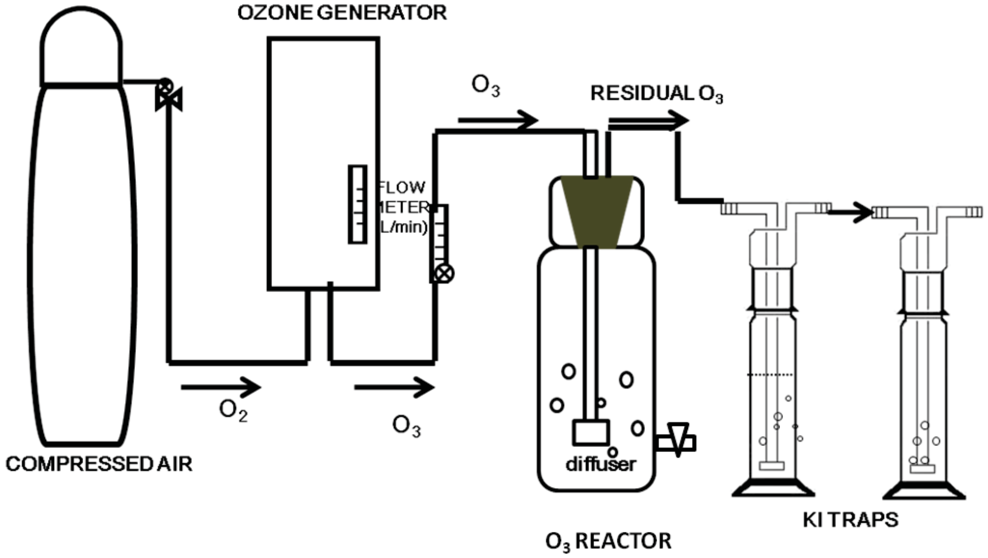

Figure 3.3 Schematic of Laboratory Set-up for the Ozone Experiment.

Ozone consumption during treatment was calculated based on the mass of ozone produced, the mass of the ozone remaining in the contactor and the mass of the ozone collected in the KI traps following Chin and Bérubé (2005):

$$\frac{M_{consumed}}{V_{sample}} = \frac{M_{produced} - M_{aqueous} - M_{gaseous}}{V_{sample}}, \qquad (3.1)$$

where $M_{produced}$ is the total mass of O_3 produced which was determined by multiplying the ozone production rate of ozone generator by the duration of experiment. The ozone production rate of the generator was 1.6 ± 0.11 mg/min as measured by method 2350E (APHA, 1995). $M_{aqueous}$ is the residual aqueous ozone concentration and was measured by Indigo colorimetric method 4500-O_3B (APHA, 1995) immediately after completion of the experiment. $M_{gaseous}$ represents the mass of excess O_3 collected in off-gas system (in the KI traps) and was measured by method 2350E (APHA, 1995), and V_{sample} is the working volume of the sample (3L).

3.5.2 UV Treatment

A low pressure ultraviolet lamp (Trojan UV Max.) with 43 Watt power was used for the UV experiment. The dimension of the chamber assembly was 0.495 m × 0.09 m, and the length of the lamp (i.e., sleeve length) was 0.405 m. The UV reactor is a glass tube with a working volume of approximately 2 L. Raw water was pumped into the reactor at a flowrate of 167 mL/min using a masterflex pump to achieve the maximum UV dose (>1000 mJ/cm^2) delivered by the lamp. The delivered UV dose in the UV and UV based AOP experiments was 1140 mJ/cm^2, which was determined by using potassium ferrioxalate $K_3Fe(C_2O_4)_3.3H_2O$) actinometer as described by Jagger (1967). In brief, 6 mM of potassium ferrioxalate was added to 4 L of distilled water in an amber bottle and the bottle was capped with a rubber stopper before application to the UV lamp to limit exposure to light. The solution was pumped through the UV lamp at a flowrate of 167 mL/min. Samples before and after the UV irradiation were collected and measured as described by Jagger (1967). The delivered UV fluence was calculated with the following equation as described by Jagger (1967) and reported by Harris et al. (1987):

$$\text{Fluence}\left(\frac{\text{mJ}}{\text{cm}^3}\right) = \frac{[\text{Fe}^{2+}]_a - [\text{Fe}^{2+}]_b}{\varphi} \times \frac{4.719\times10^8\ \text{mW}\times\text{S}}{\text{Einstein}} \times \frac{\text{L}}{10^3\ \text{cm}^3}\,. \qquad (3.2)$$

Here φ = 1.26 moles Fe^{2+} /Einstein; $[Fe^{2+}]_a$= sample concentration of Fe^{2+} after irradiation (mol/L); and $[Fe^{2+}]_b$= sample concentration of Fe^{2+} before irradiation (mol/L). Since UV dose is normally expressed in per area term (e.g., mJ/cm^2), volumetric dose was converted into irradiated surface area, by multiplying the observed value from Equation (3.2) with mean irradiated depth (which was estimated to be the ratio of the irradiated volume to the approximate irradiated surface area. This approximation assumes that average UV intensity is constant over the entire irradiated surface area.

3.5.3 H_2O_2/UV AOP Treatment

For the H_2O_2/UV AOP experiments, different concentrations of H_2O_2 (5, 10, 15, 23, 34, 68, 102, 136 and 170 mg/L) (50% Fisher Scientific) were first mixed with 3 L of the raw water for about 5 minutes. The mixture was then pumped through the UV reactor at the flow rate of 167 mL/min as in the UV experiments. The optimum H_2O_2 concentration for the sample water was identified as that which reduced UV_{254} and TOC to the greatest degree and those results were compared with other AOPs.

3.5.4 H_2O_2/O_3 AOP Treatment

H_2O_2/O_3 AOP was conducted in the same reactor used for ozone experiment. 23 mg/L of H_2O_2 (50% Fisher Scientific) was mixed with the raw water approximately 5 min and the mixture was ozonated at different times (5, 15, 30, 45 and 60 min). The ozonation was performed in the same conditions as that during in the ozone experiments.

3.5.5 O_3/UV AOP Treatment

The laboratory set-up for O_3/UV experiment is shown in Figure 3.4. It consisted of an ozone generator, an ozone reactor, a UV reactor, a recycling loop and an off-gas collection system. Ozone was bubbled through the base of the ozone reactor same as that during ozone experiment. A masterflex pump and nylon soft tubing was used to recycle water from lower outlet of the ozone reactor to the UV reactor at the flow rate of 167 mL/min. Two glass bottles (0.5 L) in series were used to trap residual ozone from the reactor.

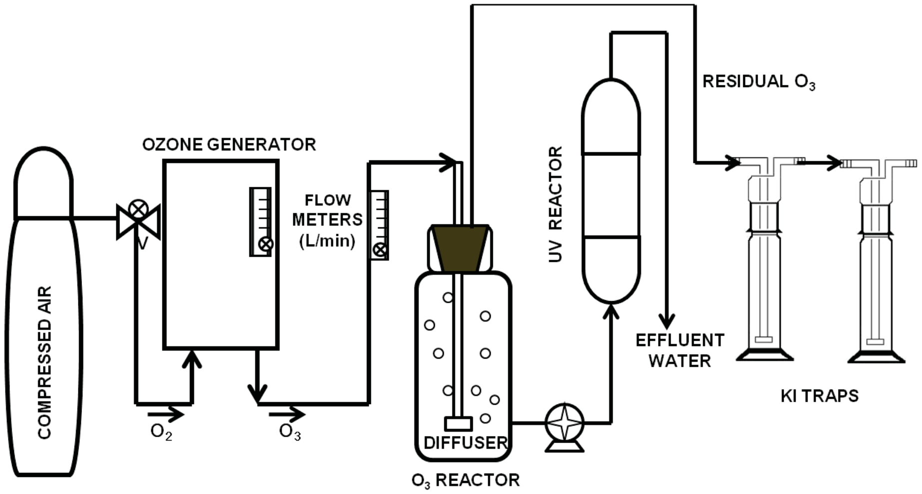

Figure 3.4 Schematic of Laboratory Set-up for O_3/UV Experiment.

3.6 Bench-Scale Membrane Filtration Systems

3.6.1 Nanofiltration Membrane Set-up and Operating Conditions

Bench-scale commercially available DK-NF membrane test sheets (GE Osmonics, Minnetonka, CA) were used in this study. The properties of the membrane are presented in Table 3.3. The DK-NF membrane is a thin-film composite membrane having a three-layered structure with a porous polysulfone support and an active polyamide layer. The membranes were received as flat sheet and pre-cut form (14.6 cm × 9.5 cm). The experimental membrane area of a coupon was 140 cm^2. The MWCO of the membrane was 400 Da (Li et al., 2008).

Table 3.3 Properties of the DK-NF Test Membrane

Properties	**Value**
Skin layer material	Cross-linked aromatic polyamide
Typical flux/psi	22GFD@100psi[a]
pH range	2-11[a]
Salt rejection	98% $MgSO_4$[a]
Molecular weight cut-off	400 Da[b]
Contact angle	40.6 ± 5.2 °[c]
Root mean square roughness	16.4 ± 3.1 nm[c]
Zeta potential at pH 9	-18.5 mV[c]

[a] Nominal value reported by manufacturer

[b] Li et al. (2008)

[c] Tang et al., (2009)

A bench-scale cross flow filtration unit (SEPA II, GE-Osmonics, Minnetonka, MN, USA) used in the NF fouling experiments are shown in Figures 3.5 and 3.6. The membrane cells were fitted with feed and permeate spacers in an attempt to simulate the hydrodynamics of spiral-wound membrane elements. Specifically, the thickness of the feed spacer was set at 0.2 mm (65 mil). Virgin test membrane sheets were soaked in milli-Q water for 24 hours prior to loading into the bench-scale NF module. The milli-Q water was refreshed four times during pre-soak procedure.

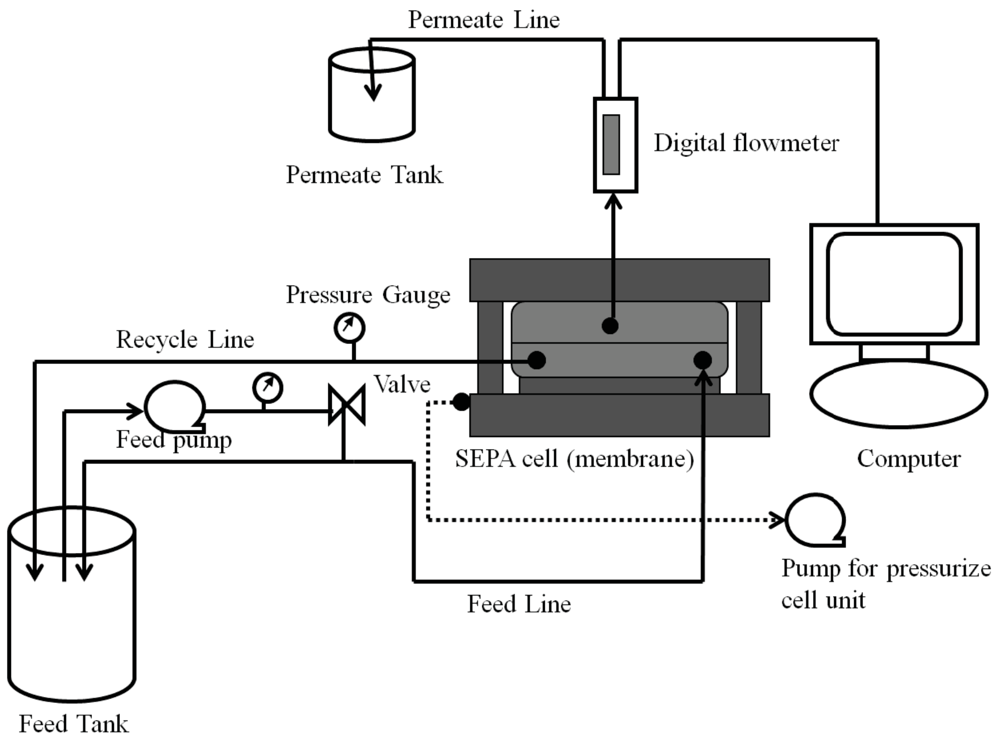

Figure 3.5 Schematic of the Nanofiltration Experimental Set up.

The membrane test sheets were then pre-compacted with milli-Q water overnight in the test-unit prior to commencing the fouling experiments. Feed waters were pumped at a flow rate of 800 mL/ min (cross-flow velocity = 0.09 m/s) into the membrane cell body with a constant flow diaphragm pump (Hydracell, Wanner Engineering, Inc., Minneapolis, MN) equipped with variable speed motor and variable frequency drive (Baldor Electric Co., Forth Smith, AR). The bench-scale membrane test unit was operated at constant pressure, variable flux mode, and a TMP of 72 psi.

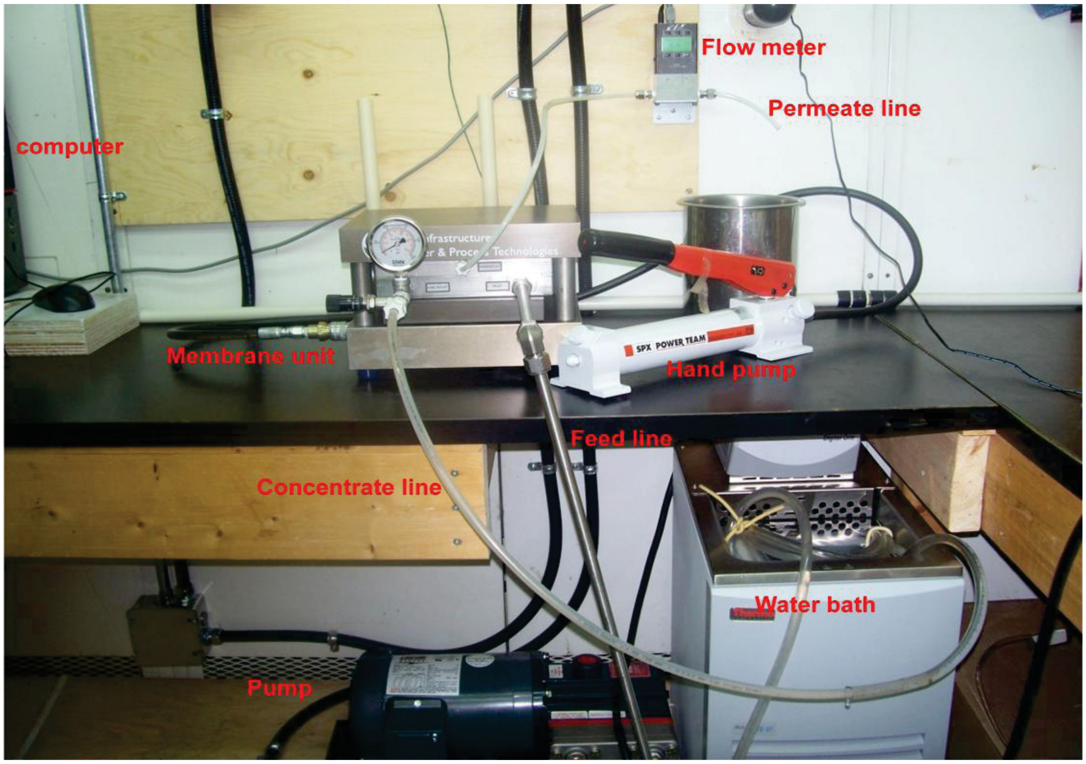

Figure 3.6 View of the Bench Scale Nanofiltration Experimental Set up.

The bench-scale NF apparatus was operated in recycle mode, in which concentrate and permeate were returned to the feed water tank. To maintain constant temperature (24 ± 2^{o}C) of the feed water, the concentrate line was passed through a refrigerated bath (Thermo Scientific NESLAB RTE Series, P/N U00694) before recycling into the feed tank. The membrane fouling experiments were conducted for 4 days (96 hours). The permeate flow rate was monitored regularly by measuring the volume of water collected in each hour in a graduated cylinder.

The source waters were pre-filtered through a mixed cellulose ester 0.45µm membrane (GN-6 Metricel, Pall, East Hills, NY, USA) to remove larger particles prior to the NF treatment. Different types of feed waters were subjected to NF process. These include (i) Fletcher Lake raw water, (ii) French River raw water, (iii) UF permeate from and (iv) preoxidized waters with H_2O_2/O_3, H_2O_2/UV, and O_3/UV AOPs from the French River as illustrated in Figure 3.7.

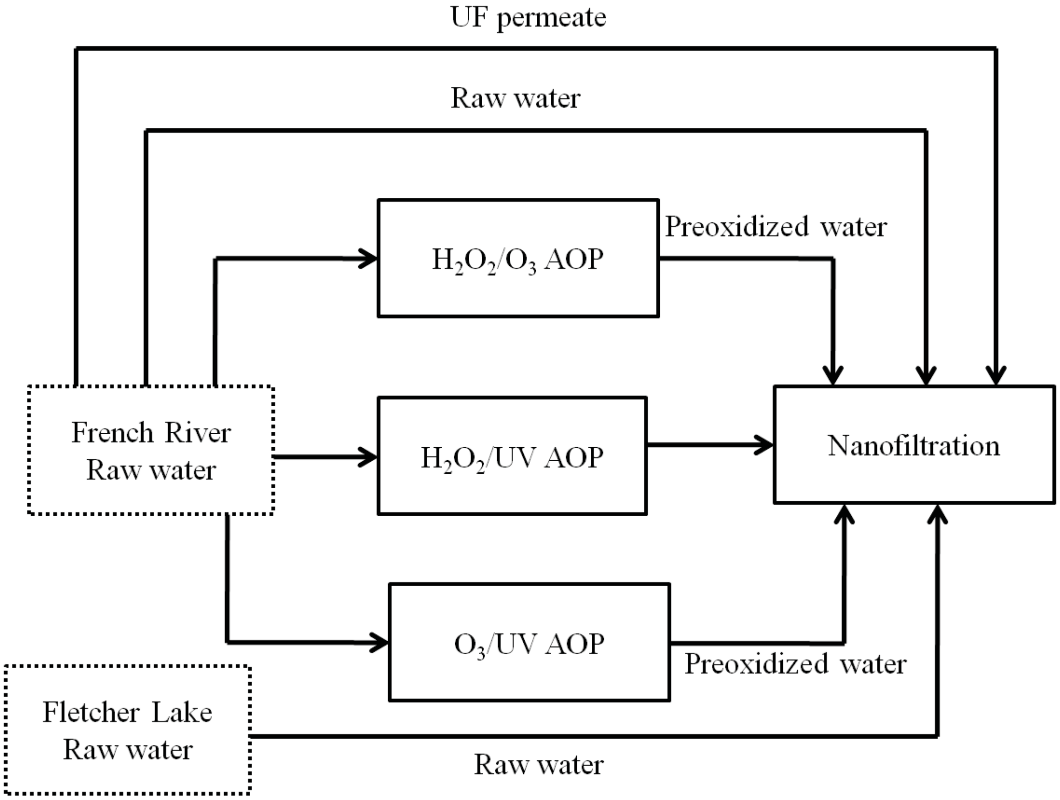

Figure 3.7 Process Diagram of Experimental Work of Nanofiltration with Different Feed Waters.

3.7 Analytical Methods

3.7.1 General Water Quality Parameters

Conductivity, pH and temperature were measured using a combination of pH/mV/Temperature/DO/ISE and conductivity meters (Accumet Excel XL50). Conductivity and pH probes were calibrated daily using standard buffer solutions from Fisher Scientific. The pH meter was calibrated with pH 4, 7 and 10 standard buffers. The alkalinity was determined following the potentiometric titration method 2320 (APHA, 1995). A spectrophotometer (HACH DR/4000, HACH Co., Loveland, CO) was used for analyzing UV_{254} and colour. Before measuring UV_{254}, samples were filtered through 0.45 μm pore size membrane (Cole-Parmer® Nylon Membranes) and measured following the method 5910B (APHA, 1995).

3.7.2 Total and Dissolved Organic Carbon

TOC and DOC were measured following method 5310C (APHA, 1995). Samples were first transformed into 40 mL vials, headspace free, and acidified with phosphoric acid to reduce pH to 2.0. Measurements were performed with a TOC-V CHP analyzer (Shimadzu Corporation, Kyoto, Japan). The detection limit of the TOC instrument is 40 ppb (0.04 mg/L). DOC was measured following the same method as TOC, but after filtering the sample through 0.45 μm polysulfone membrane filter (Cole-Parmer® Nylon Membranes) that had been pre-ringed with 500 mL of milli-Q water. For the TOC and DOC analyses, the operating conditions for the TOC analyzer were as follows: TOC standard platinum catalyst, injection volume 50 µl, oven temperature 680°C, carrier gas flow 150 mL/min potassium phthalate standards 0 to 10 mg/L, and correlation > 0.99.

Specific UV absorbance (SUVA) which can be used as a surrogate parameter to monitor the changes in aromatic nature of NOM in water was calculated from UV_{254} and DOC as outlined by Edzwald et al. (1985).

$$SUVA\ \left(m^{-1} \times \frac{L}{mg}\right) = \frac{UV_{254}(cm^{-1})}{DOC\left(\frac{mg}{L}\right)} \times 100\ \frac{cm}{m} \qquad 3.2$$

3.7.3 Molecular Weight Distribution Analysis by HPSEC

High performance size exclusion chromatography (HPSEC) (Perklin Elmer, Series 200) with UV/VIS detector was used to determine the molecular weight distribution of NOM present in sample water. A TSK–GELG3000SW (30 cm × 7.5 mm) column which contains silica-based, hydrophilic bonded phase packing materials that minimize interaction with compounds present in the sample. Sodium acetate at a flow rate of 0.7 mL/min was used as a mobile phase (eluent). The sample injection volume was 20 µL and analysis time was 30 min for each sample. The column was calibrated with sodium polystyrene sulphonate (PSS Polymer) standards with different molecular weights (14900, 7540, 5180, 1530 Da). All PSS standards and samples were detected at 254 nm wavelength. Before analysis each sample was filtered through 0.45 µm filter and preserved for maximum of seven days without addition of buffer. The reproducibility of the measurement was assured by running samples in duplicates.

3.7.4 Disinfection By-products Formation Potential

Raw water, oxidized water, the UF and NF permeates were chlorinated according to the uniform formation condition (UFC) protocol (Standard methods 5710) proposed by Summers et al. (1996) to determine the DBP formation potentials (DBPFP). For the H_2O_2/UV and H_2O_2/O_3 processes, residual H_2O_2 after the treatment processes reacted with chlorine so that higher chlorine doses are needed to meet the desired free chlorine residual in the UFC test. Following Liu et al. (2003), bovine liver catalase (Filtered aqueous solution, Code: CTR without thymol, ≥40,000 units per mg protein, Worthington, Biochemical Corporation) with 0.2 mg/L concentration was used to quench the residual hydrogen peroxide in the treated samples prior to conducting the UFC test. A stock solution of 1500 mg/L sodium hypochlorite (NaOCl) solution was added to the samples and incubated at room temperature for 24 hours to obtain a free chlorine residual of 1.0 ± 0.4 mg/L for the UFC test. Both the H_2O_2 quenching and UFC tests were performed in 130 mL amber bottles with Teflon liners inside the caps. The THM samples were collected headspace free in 20 mL glass vials and preserved with 50 g/L ammonium chloride (1 drop of NH_4Cl), 8 g/L sodium thiosulphate (2 drops of $Na_2S_2O_3.5H_2O$) , and 0.1 N hydrochloric acid (3 drops of HCl) .

The THM analysis was performed following the method 551.1 (USEPA, 1995a) employing liquid-liquid extraction with the pentane and gas chromatography electron capture detector (GC-ECD) measurement. Gas chromatography analyses of THMs were carried out using a Hewlett Packard 5890 Series II-Plus GC, equipped with a DB-5 column for primary analysis, and a DB-1701 column for confirmation. A Fisons mass spectrometer (Trio 1000) was periodically used for compound identification. THMs quantified in the described analysis were chloroform, bromodichloromethane (BDCM), dibromochlormethane (DBCM) and bromoform.

The HAA samples were collected headspace free in 20 mL pre-cleaned glass vials and preserved with ammonium chloride. The samples were prepared by liquid-liquid extraction with methyl *tert*-butyl ether (MTBE) following the method 552.2 (USEPA, 1995b). Samples were analyzed in GC-ECD using a Hewlett Packard 5890 Series II-Plus GC, equipped with a DB-5 column for primary analysis, and a DB-1701 column for confirmation. Samples were monitored for 9 HAAs: chloroacetic acid (CAA), bromoacetic acid (BAA), dichloroacetic acid (DCAA), trichloroacetic acid (TCAA), bromochloroacetic acid (BCAA), dibromoacetic acid (DBAA), bromodichloroacetic acid (BDCAA), chlorodibromoacetic acid (CDBAA) and tribromoacetic acid (TBAA).

CHAPTER 4 CHARACTERIZATION AND REMOVAL OF NATURAL ORGANIC MATTER BY AN INTEGRATED MEMBRANE SYSTEM[1]

4.1 Abstract

NOM fractionation of French River water (Nova Scotia, Canada) was performed at an integrated membrane system (IMS) employing UF and NF for water treatment. An attempt was made to evaluate this surface water and the effect of UF treatment on DBP precursor removal. Each NOM fraction was assessed in terms of THM and HAA formation potential. The NOM fractionation was performed by separating DOC into six fractions: hydrophobic acid (HOA), base (HOB) and neutral (HON) and hydrophilic acid (HIA) base (HIB) and neutral (HIN). The raw water was found to be mostly comprised of HIN (approximately 50%) and HOA (approximately 35%). Upon treatment with UF, 66% of the DOC was removed. The key finding of this work was that the HOA fraction was the main contributor to DBP formation potential. Removal of 93% of the HOA components through UF treatment resulted in a reduction of THM and HAA formation potential of 54 and 30%, respectively, despite the fact that HOA comprised 35% of the DOC in the raw water. The results showed that the UF component of the IMS contributes to the overall DBP precursor removal at this full-scale plant.

---

[1] Note: This work is currently in press in Journal of *Desalination*.

4.2 Introduction

NOM present in drinking water sources is problematic as it produces DBPs during chlorination which can potentially cause long-term adverse health effects (Komulainen, 2004). The adverse effects related to the formation of chlorinated organic compounds have driven water utilities to consider advanced NOM removal treatment processes. In recent years, there have been a number of research projects conducted to evaluate IMS such as UF followed by NF membrane in terms of treatment efficacy (Lee and Lee, 2006). UF membrane pretreatment is efficient in reducing turbidity, particles and suspended solids (Jacangelo et al., 1995) and is effective for the reduction of NF membrane fouling resulting from the accumulation of particles and suspended solids. However, UF membranes have been shown to not provide complete removal of NOM, especially dissolved organic matter (DOM) (Bonnèlye et al., 2008; Laine et al., 1990). The residual DOM present in the water can be removed by NF treatment processes. Owen et al., (1995b) proposed that NF with MWCO of 400 to 800 Da is effective in removing NOM and thereby controlling the formation of DBPs.

NOM present in water is considered as a major foulant for NF and RO membranes (Her et al., 2008a; Kaiya et al., 1996). In order to understand the role of specific NOM components responsible for NF fouling, it is necessary to thoroughly characterize NOM in feed water. Humic substances, a component of NOM, have been found to control the rate and extent of NF/RO fouling in some studies (Combe et al., 1999; Jones and O'Melia, 2000). Nilson and DiGiano (1996) observed that hydrophobic NOM fractions were responsible for the majority of permeate flux decline and were highly rejected by NF membranes compared with hydrophilic NOM. Other studies have revealed that the non-humic fraction of NOM (e.g., hydrophilic and neutrals) are responsible for determining the rate and extent of flux decline (Carroll et al., 2000; Lin et al., 2000). Fan et al., (2001) described the order of fouling potential of different NOM fractions as: hydrophilic neutral > hydrophobic acids > transphilic acids > charged hydrophilic. This finding was well supported by a study carried out by Lee et al (2004), who found that polysaccharides and proteins (hydrophilic neutrals) with lower HPSEC-DOC/UV response significantly foul low pressure membranes. Similar results were observed by Cho et al (1998a), and Speth et al.(1998) in NF membranes and Zhao et al. (2010) for RO membranes. Furthermore, many bench-scale studies with synthetic feed waters have demonstrated the high degree of fouling associated with proteins and polysaccharides (Ang and Elimelech, 2008; Lee et al., 2006; Lee and Lee, 2006). In summary, there has been a wealth of research on NOM fouling of both low and high pressure membranes.

In contrast, the objective of this research was to characterize NOM and assess DBP formation potential in raw and UF treated water at a full-scale plant. Although other studies have characterized NOM and its association with DBP formation, this study specifically assessed the ability of UF membranes to remove DBP precursors and identified the key components involved in removal. To accomplish this, raw water and UF permeate samples were fractionated, following a procedure developed by Leenheer (1981) and modified by Marhaba et al. (2003a), into six different NOM fractions.

Disinfection by-product formation was then assessed before and after UF treatment. Although NF water quality parameters are presented as well as some anecdotal data regarding NF fouling, the focus of this work is on the ability of the UF system to remove different components of DOC from the raw water.

4.3 Materials and methods

4.3.1 Water Quality Characteristics

Raw and UF permeate waters collected from the Tatamagouche drinking water treatment plant were used for bench-scale NOM fractionation and THM and HAA formation potential experiments. The detail description of the water treatment plant is presented in Section 3.1 of Chapter 3. The French River raw water quality characteristics during this study are shown in Table 4.1.

Table 4.1 Raw and Treated Water Characteristics. Values Represent the Average of Triplicate Measurements.

Water types	**pH**	**UV_{254} (cm^{-1})**	**Alkalinity (mg/L)**	**DOC (mg/L)**	**SUVA ($Lmg^{-1}m^{-1}$)**	**THMFP (µg/L)**	**HAAFP (µg/L)**
Raw	6.7	0.096	27.3	5.3	1.8	467.0	194.9
UF permeate	6.6	0.064	36.0	1.9	3.2	363.7	85.0
NF permeate	6.7	0.001	12.7	0.3	0.3	18.6	9.4

It is important to note that there is a high degree of seasonal variation in the source water quality, however, the results presented in this paper are representative of the water quality from this source outside of discrete events such as heavy rain falls. The French River, which flows through the surrounding agricultural and natural land-use areas, is vulnerable to degradation due to source run-off materials (e.g. soil, silt, organic matter) from agricultural fields. The major raw water quality characteristics include periodic elevation of colour and turbidity levels from natural occurring organic matter. The SUVA value for the UF permeate was observed higher than the raw water. The UF permeate has lower DOC values making SUVA higher than in the raw water.

4.3.2 NOM Fractionation

The dissolved organic matter from the raw and UF permeate was separated into six organic fractions: hydrophobic acid (HOA), base (HOB) and neutral (HON) and hydrophilic acid (HIA), base (HIB) and neutral (HIN). Resins were cleaned and packed into 2.5 cm × 120 cm Kontes Chromaflex chromatography columns following resin preparation procedures developed by Leenheer (1981). The hydrophobic fractions were absorbed onto DAX-8 resins (SUPELCO, Bellefonte, PA) by varying the influent pH to 7, 10 and 2 to extract the HON, HOB and HOA fractions respectively. The hydrophilic base fraction was absorbed onto AG-MP 50 (BIO-RAD, Hercules, CA) resins at a pH of 2 and extracted following the modifications proposed by Marhaba et al. (2003b). The hydrophilic acid fraction was subsequently absorbed onto WA 10 resins (SUPELCO) at a pH of 2 and the hydrophilic neutral fraction was that which remained after the sample

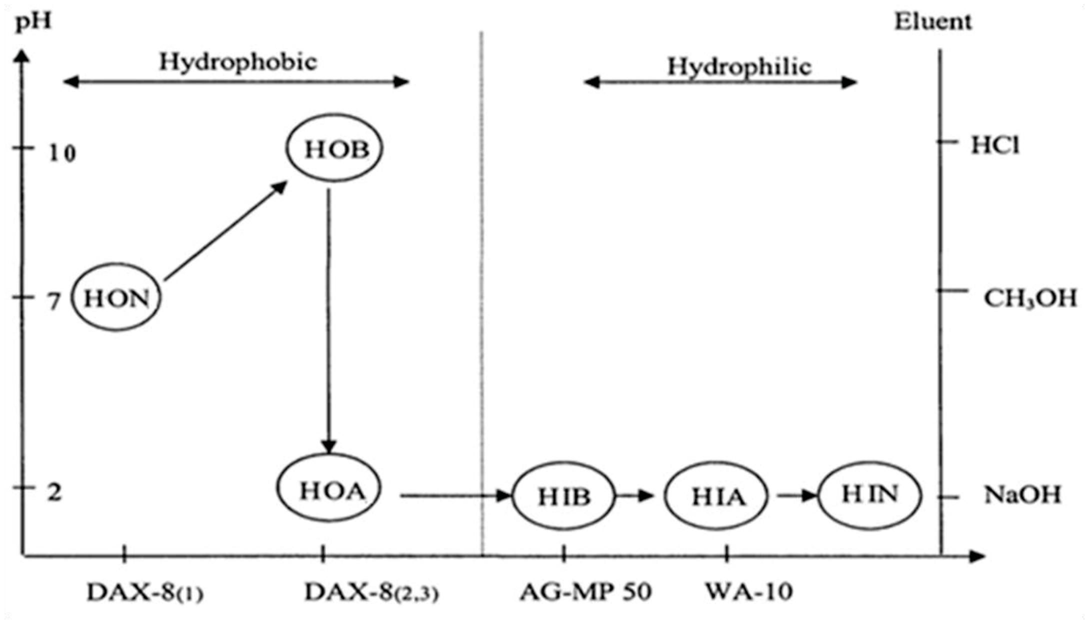

Figure 4.1 Schematic for the Resin Fraction Procedure (Adapted from Marhaba et al. 2003).

had passed through each of the five columns. Figure 4.1 describes the separation procedure used in this study. The left-hand axis shows the pH to which the samples were adjusted prior to passing through the columns. The right-hand axis shows the eluent used to desorbs the desired organic materials from the resins and the horizontal axis shows the order to which water samples were passed through each of the five columns.

4.3.3 Molecular Weight by HPSEC

High performance size exclusion chromatography (HPSEC) (Perklin Elmer, Series 200) with a UV/VIS detector was used to determine the molecular weight distribution of NOM present in water samples. The samples were brought to a pH between 3 and 7, passed through a 0.45 μm membrane filter and analyzed using a TSK G3000SW column (7.5 mm × 300 mm). The column contained silica-based, hydrophilic bonded phase packing materials that minimize interaction with compounds present in the sample. Sodium acetate with a flow rate of 0.7 mL/ min was used as a mobile phase (eluent). The sample injection volume was 20 μL and analysis time was 30 min for each sample. The column was calibrated with sodium polystyrene sulphonate (PSS) standards with different molecular weights (14900, 7540, 5180, 1530 Da). All PSS standards and samples were detected at a wavelength of 254 nm. The reproducibility of the measurements was assured by running duplicates.

4.3.4 Disinfection By-product Formation Potential

Six isolated organic fractions of raw and UF permeate waters were chlorinated according to the uniform formation condition (UFC) protocol (method 5710, APHA 1995) proposed by Summers et al. (1996) to determine THM and HAA formation potentials. The detailed DBP formation potential method is described elsewhere (Lamsal et al., 2011). In brief, a stock solution of 1500 mg/L sodium hypochlorite (NaOCl) solution was added to the samples and incubated at room temperature for 24 hours to obtain a free chlorine residual of 1.0 ± 0.4 mg/L for the test. The analysis of THM was performed according to USEPA Method 551.1 employing liquid-liquid extraction with pentane and gas chromatography electron capture detector (GC-ECD) measurement. For HAA, samples were prepared by liquid-liquid extraction with Methyl tert-butyl ether (MTBE) according to USEPA Method 552.2.

4.4 Results and Discussion

4.4.1 Dissolved Organic Carbon Analysis

The relative amount of DOC attributed to the six different organic fractions in the raw and full scale UF permeate waters are shown in Figure 4.2a and b, respectively. Fractionation of the NF permeate was not conducted since the DOC concentration was very low. The DOC of the raw water was 5.3 mg/L of which large percentage consisted of hydrophilic neutral (50.4%) and hydrophobic acid (35.3%). The hydrophilic acid and the hydrophobic neutral fractions accounted for 6.1 and 4.4% of the total DOC respectively, while the hydrophilic and hydrophobic basic organic fractions accounted for less than 2% each of the total DOC.

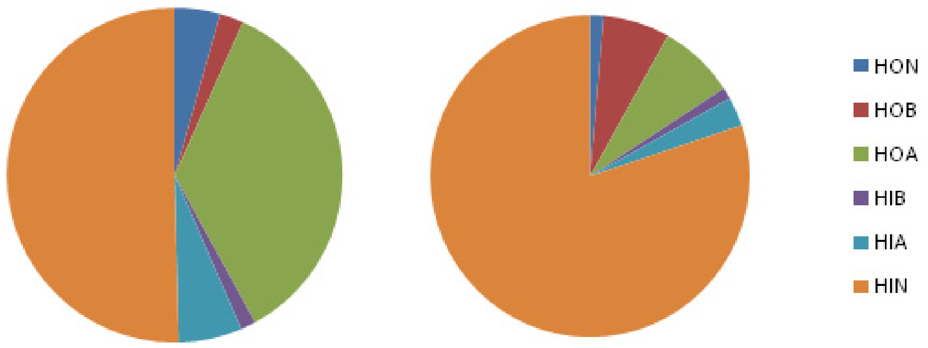

(a) Raw water (b) UF Permeate

Figure 4.2 Composition of Organic Matter in (a) Raw and (b) UF Permeate.

After treatment with UF, most of the remaining DOC (i.e. 2.0 mg/L) was found to be hydrophilic neutral in nature (80.1%). The overall removal of DOC by the UF membranes was quite high at 66%, although DOC removals by UF membrane has been found to vary considerably (Bonnèlye et al., 2008; Siddiqui et al., 2000). The high degree of variability is to be expected with UF due to the variability in size and characteristics of NOM in different water sources.

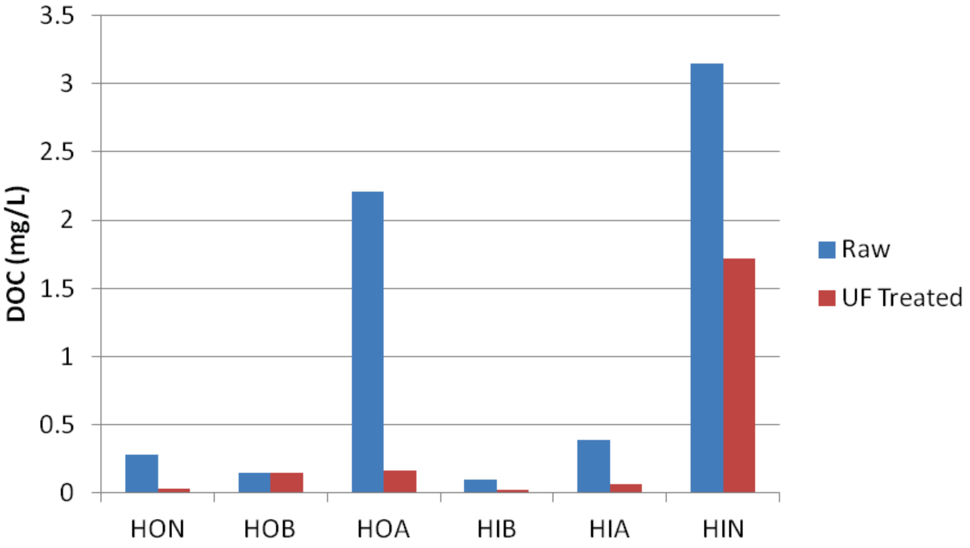

Figure 4.3 Concentration of NOM fractions in the Raw Water and UF permeate.

Figure 4.3 shows the actual concentrations of each of the NOM fractions in the raw water and UF permeate. The HIN fraction exhibited a relatively poor removal rate through the UF system (45%). This is a significant finding considering that more than half of the DOC of the raw water was characterized as HIN. The UF membrane showed a high degree removal of the HOA fraction (93%) which generally includes larger molecular weight organics (Sohn et al., 2007). The hydrophobic acid and base organic fractions accounted for 7.7 and 6.7% of the UF permeate, respectively, while the hydrophilic acid and base fractions each accounted for less than 3% of the total DOC in the UF permeate.

From the perspective of controlling NF fouling, the UF membrane was effective in the removal of key fouling contributors given the 66% removal of DOC. Given that UF membranes are designed to be efficient at particle removal, it was expected that the UF would provide a high level of pretreatment for the downstream NF process. The focus of this work was on the UF and its ability to reduce different organic fractions, however, anecdotal evidence was provided indicating that the UF pretreatment provided NF feed that led to very low fouling conditions (i.e. the NF membrane was cleaned only once in two years). The NF was able to remove most of the remaining DOC with excellent performance.

4.4.2 Molecular Weight Distribution Analysis

The size exclusion chromatograms for the raw, UF permeate and NF permeate waters are presented in Figure 4.4. The molecular weight ranges of each sample can also be identified. The molecular weight of the raw water ranged from 110 to 60,000 Da. The UF membrane showed a high degree of NOM removal, with organic matter in the source water having molecular weights in the range of 1,700 to approximately 60,000 Da (shown as Peaks 1 and 2) despite the fact that the MWCO of the membrane is

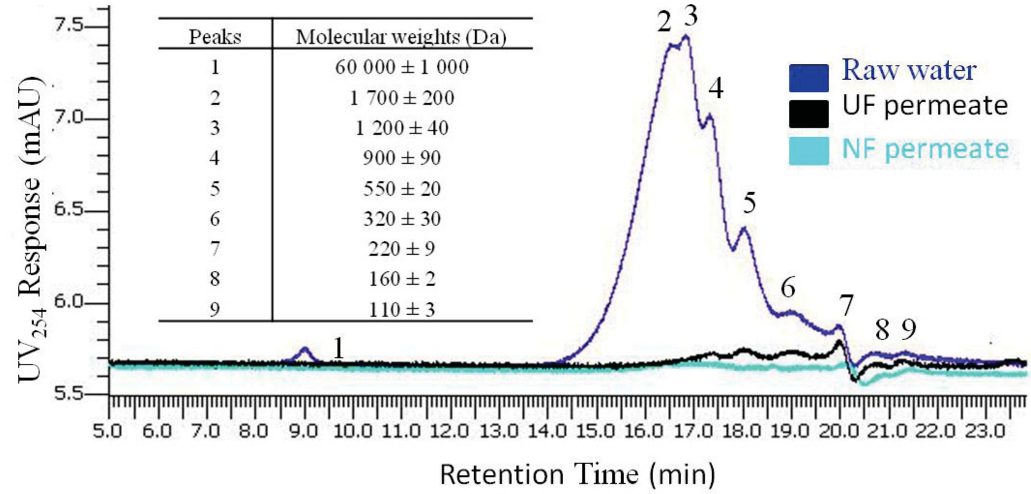

Peaks	Molecular weights (Da)
1	60 000 ± 1 000
2	1 700 ± 200
3	1 200 ± 40
4	900 ± 90
5	550 ± 20
6	320 ± 30
7	220 ± 9
8	160 ± 2
9	110 ± 3

Figure 4.4 Size Exclusion Chromatograms of Raw Water, UF Permeate and NF Permeate Elution Curves.

approximately 40,000 Da. The removal of NOM with a molecular weight lower than the MWCO of the UF membrane may have been due to the formation of a foulant layer on the UF membrane that caused a reduction of the effective pore size of the membrane. This phenomenon has been detected in previous research where pore blocking and/or cake layer formed in the UF and MF membranes caused increased removal of DOC (Schäfer et al., 2000). Furthermore, the concentration of organic matter with a molecular weight less than 1,700 Da was found to be well below the concentrations found in the raw water indicating removal in the UF system was achieved even for these small compounds. For particles of this size, the influence of electrostatic surface interactions may play a major role in NOM removal rates in addition to physical removal through size exclusion. The NF permeate showed no visual peaks in the chromatogram, suggesting that most of the UV absorbing organic material was removed which is in agreement with the DOC data (Table 4.1).

4.5 Disinfection By-Products Formation Analysis

The concentration of THMs formed under uniform formation conditions of the different fractions for the raw and UF permeate water is presented in Figure 4.5. The hydrophobic acid fraction of the French River source water was found to be the main contributor for THM formation potential. Lin and Wang (2011) also observed HOA as a main contributor for THM formation potential with similar quality source water (high DOC concentration and ~50% of DOC hydrophilic in nature). The HIN fraction was the second greatest contributor to THM formation (~60 µg/L) however it was much lower than the HOA fraction (~260 µg/L). Some studies have shown that hydrophilic acid, neutral or base fractions (i.e., less aromatic DOC fractions) can have greater THM yield than hydrophobic acids (Dotson et al., 2009; Hwang et al., 2001).

The higher degree of removal of the HOA fraction with UF treatment (e.g., 93%) resulted in a large reduction in overall THM formation potential (54%). The concentration of THMs due to the HIN fraction in the UF permeate was similar to that in the raw water. These data clearly show the benefit of HOA removal by the UF from a THM formation potential perspective.

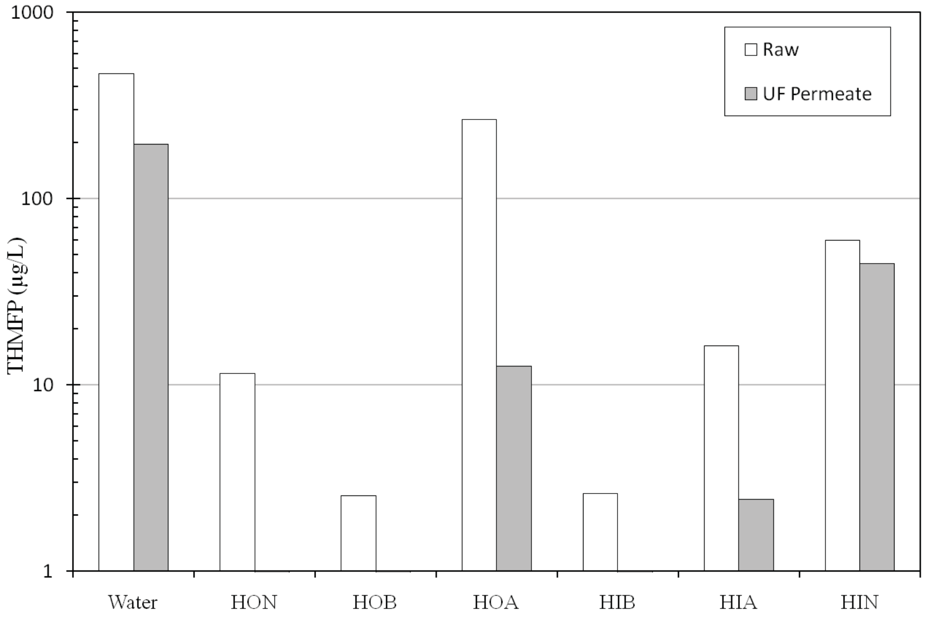

Figure 4.5 Total THMFP of Raw and UF Permeate Fractions.

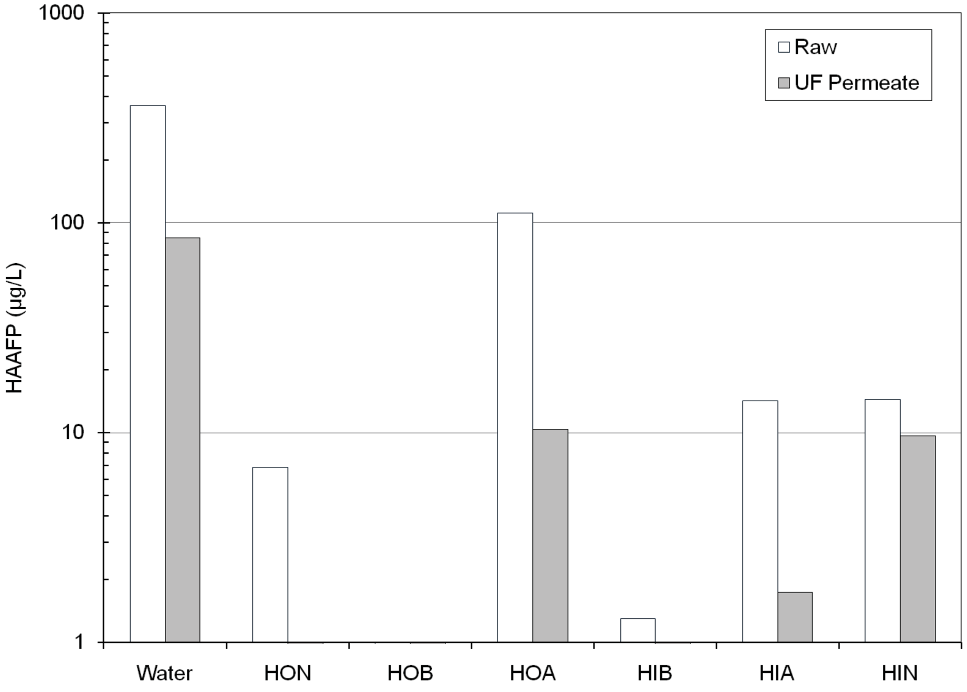

Figure 4.6 Total HAAFP of Raw and UF Permeate Fractions.

Figure 4.6 shows the concentrations of HAA formation potential for the different fractions present in the raw and the UF treated waters. The overall removal of HAA formation potential with UF treatment was 77%. The high degree of removal of the HOA fraction with UF treatment (93%) resulted in a large reduction in overall HAA formation potential (90%) associated with this fraction. The moderate removal of the HIN fraction (45%) resulted in a lower degree of removal of HAA (33%) formation potential associated with this fraction. Similar to that observed with the formation of THMs, HOA played a major role in the formation of HAAs in both the raw and UF permeate water samples. Figure 4.6 illustrates that both the HIN and HOA fractions contributed equally to the formation of HAAs for the UF permeate even though the HOA contribution to HAA formation was 10 times that of the HIN fraction in the raw water.

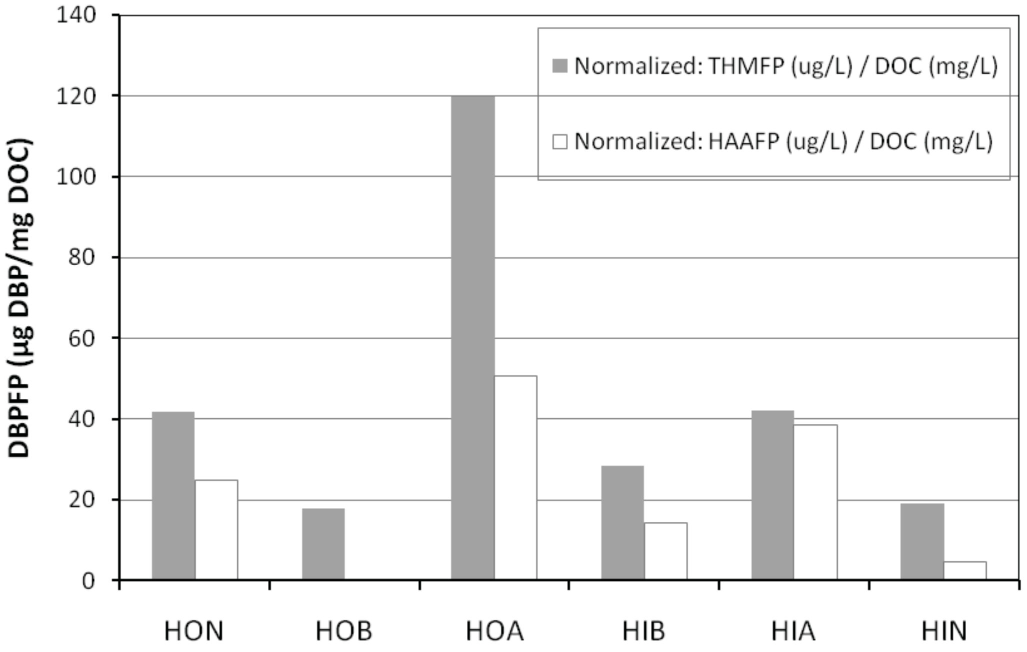

Figure 4.7 Normalized DBPFP from Different NOM Fractions.

Figure 4.7 shows the normalized THM and HAA formation potentials for each fraction in the raw water. The data presented in this figure illustrates the THM and HAA formation potentials per unit DOC, indicating the relative importance of removing these fractions from a DBP precursor removal standpoint. Clearly the HOA fraction is the most important fraction from a DBP formation perspective. For every milligram of HOA present, 120 μg of THM compounds are formed and 50 μg of HAA compounds are formed. Removal of the HIN fraction is much less important from a DBP formation perspective. For every milligram of HIN present, only 20 μg of THM and 5 μg of HAA compounds are formed. The high degree of removal of HOA compounds by the UF membrane demonstrates its effectiveness at achieving significant DBP precursor removal for the source water evaluated in this study.

4.6 Conclusions

The goal of this study was to characterize NOM from the French River through resin fractionation and evaluate the various fractions in terms of their DBP formation potential. The fractionation results showed that this source water is mainly composed of HIN and HOA organic fractions and with UF treatment, most of the HOA fraction was removed. The HOA fraction was found to be the primary DBP precursor and its removal led to large reductions in DBP formation potential in the UF permeate. A complete reduction of particles, significant reduction of the hydrophobic fractions and moderate reduction of the hydrophilic neutrals fraction of DOC was achieved by the UF membrane.

CHAPTER 5 FOULING BEHAVIOUR IN NANOFILTRATION MEMBRANES: BENCH- AND FULL SCALE STUDY OF TWO SURFACE WATERS[2]

5.1 Abstract

This study investigated the nanofiltration (NF) fouling behaviour by two surface waters that serve as source waters for full-scale IMS of the Tatamagouche and Collins Park drinking WTPs in Nova Scotia, Canada. Bench-scale NF fouling experiments conducted under controlled laboratory conditions showed a flux decline of 25% with the Collins Park source water compared to a flux decline of 15% with the Tatamagouche source water over 96 hours of operation. The higher rate of flux decline observed was related to the water quality parameters observed in the Collins Park source water. Membrane autopsy studies were performed on virgin and fouled membranes using different techniques to compare the fouling propensity of the two feed waters. SEM and AFM results showed considerable difference between the fouled membranes fed with two source waters. Analyses of full-scale NF fouling data from the two IMS plants reveal higher fouling in the Collins Park WTP. Full- and bench-scale NF fouling observations provide consistent results that together support ongoing membrane cleaning practices in the Collins Park WTP.

---

[2] Note: This work is currently in press in Journal of *Water Supply: Research and Technology- AQUA*.

5.2 Introduction

Membrane filtration technology has been gaining increased usage in the drinking water industry due to its superior removal of DBP precursors, minimal use of chemicals, reduction in sludge production and potential for use in a compact treatment train system while being economically feasible, particularly in small scale systems (Pressdee et al., 2006). Low pressure MF and UF membranes are mostly used for the removal of particulate matter and high pressure NF and RO membranes are used for the removal of organic substances, multivalent ions and micro pollutants. Integrated membrane system (IMS), using low pressure (MF/UF) membranes followed by high pressure (NF/RO) membranes, has been used as a multi-barrier approach in drinking water treatment. NF membrane is of particular interest in drinking water treatment applications because of capabilities for high rejection of dissolved organic compounds and multivalent ions and operations at much lower pressure than the RO membranes.

Despite of continued advancements in membrane filtration technologies, membrane fouling is the major expense in the operation of membrane processes in water treatment. In full-scale operations, NF/RO membranes are exposed to different water constituents such as inorganic ions, NOM and biological compounds such as microorganisms and soluble microbial product which can contribute to membrane fouling. Among these NOM present in the source water plays a vital role as primary foulant (Cho et al., 1999; Nilson and DiGiano, 1996; Schäfer et al., 2001).

The flux decline and NOM rejection in the NF membrane are mostly dependent on NOM properties including size (e.g., molecular weight), characterization (e.g., hydrophobic vs. hydrophilic), charge density (functional groups) (Her et al., 2008b; Mänttäri et al., 2000; Nilson and DiGiano, 1996; Tang et al., 2007a) and the chemistry of the feed water (i.e. ionic strength, pH and concentration of monovalent and divalent ions) (Braghetta, 1995; Childress and Elimelech, 1996; Hong and Elimelech, 1997a; Jarusutthirak et al., 2007; Seidel and Elimelech, 2002). The rate of NF/RO membrane fouling increases with an increase in electrolyte concentration, decrease in solution pH and addition of divalent cations (Hong and Elimelech, 1997a; Jarusutthirak et al., 2007).

Numerous previous studies have been conducted to understand the effect of feed water properties on NF membrane fouling using synthetic feed waters (Braghetta et al., 1997; Childress and Elimelech, 1996; Her et al., 2004; Hong and Elimelech, 1997a; Lee et al., 2005; Tang et al., 2007b). Of those studies utilizing real source waters, most have either used single source water or have conducted experiments only at bench-scale level (Her et al., 2008a; Jarusutthirak et al., 2007; Makdissy et al., 2010; Nilson and DiGiano, 1996). While bench-scale studies performed under controlled laboratory scale condition can provide insights into various aspects of membrane fouling, they may not represent the actual condition of full-scale membrane system. A combination of bench-and full-scale studies would help understand the effect of feed water properties on NF membrane fouling and to understand the actual conditions of NF membrane fouling.

There are few existing studies (Bellona et al., 2008; Bellona et al., 2010; Escobar et al., 2000; Escobar et al., 2002) that have compared or incorporated bench-scale results to full-scale results. However, the focus of these studies were specifically on the removal of assimilable organic carbon (AOC) and biodegradable organic carbon (BDOC) (Escobar et al., 2000; Escobar et al., 2002) and applicability of NF/RO membranes for water reuse (Bellona et al., 2008; Bellona et al., 2010). Therefore, further studies on effect of feed water properties on NF membrane fouling are needed both at bench- and full-scale level.

This study addresses fouling in commercial polyamide NF membrane by two surface source waters in Nova Scotia, Canada. The surface waters used in this study serve as source waters for two small-scale IMS drinking water treatment plants that utilize two different types of spiral wound NF membrane modules. Bench-scale NF fouling experiments were investigated under similar operating and NF membrane type conditions for the two source waters and results were compared. Membrane autopsies were conducted on virgin and fouled membranes using different techniques to characterize the properties of fouled membranes. In addition, full-scale NF fouling data collected from the two IMS plants were compared in order to understand the real NF fouling conditions in these water treatment plants.

5.3 Materials and Methods

5.3.1 Description of Small Systems and Raw Water Characteristics

This research was based in two small communities in Nova Scotia: (1) Tatamagouche, a village within the Municipality of the County of Colchester and (2) Collins Park, a subdivision within the Halifax Regional Municipality. Both communities are provided with municipal drinking water from public utilities. Both the Tatamagouche and Collins Park water treatment plants are based on integrated membrane systems that are designed to minimize chemical handling and ease operational duties to reflect operational challenges associated with small systems. The details about operating conditions in both plants are presented in Table 5.1.

The source water for the Tatamagouche WTP is the French River. The French River is a shallow river that flows through the surrounding agricultural and natural land-use areas. The water quality of the river is degraded during periods of high precipitation and seasonal changes during the spring and fall associated with run-off events. Two source water samples used in this study were collected in fall 2010 during a period when water quality was not deteriorated due to a heavy rainfall event. Each water quality parameters were measured in triplicate and standard deviations were reported. The water quality characteristics of the French River water are provided in Table 5.2.

Table 5.1 NF Membrane Type and Operating Conditions in Full Scale Plants

Membrane Design and Operating Conditions	**Tatamagouche WTP**	**Collins Park WTP**
NF Manufacturer and module	GE-Osmonics, OSMO-MUNI-NF 365	Hydranautics – ESPA4
Membrane Material	NA	Aromatic composite polyamide
Module area (m^2)	33.9	37.1
Number of Skids	2	1
Total Modules per skids	24	8
Total membrane area (m^2)	813.6	296.8
Array	4-2	1-1
Permeate Flow rates (L/min)	378.5	109.8
Recovery (%)	75	80
Inlet flowrate (L/min)	503.5	137.4
Total flowrate (L/min)	643.5	182.8
Average design flow per module (L/min)	15.78	13.74

Table 5.2 Feed Water Characteristics. Values are based on two samples and measured each parameter in triplicate.

Analyte	**Units**	**Tatamagouche WTP – French River**	**Collins Park WTP – Fletcher Lake**
pH		6.7 ± 0.04	6.6 ± 0.02
Turbidity	NTU	1.0± 0.15	1.3± 0.21
UV_{254}	cm^{-1}	0.064 ± 0.001	0.164 ± 0.001
Conductivity	µS/cm	74.7 ± 1.9	93.07 ± 5.0
DOC	mg/L	2.8 ± 0.04	4.5 ± 0.1
SUVA	L/mg.m	2.2 ± 0.04	3.6 ± 0.07
Na	mg/L	4.0 ± 0.01	17.5 ± 0.5
Ca	mg/L	4.7 ± 0.2	5.6
Mg	mg/L	0.7 ± 0.03	0.92 ± 0.03
NO_3^-	mg/L	0.38	0.81
PO_4^-	mg/L	2.0	8.40
Cl^-	mg/L	4.9	22.1

Both the UF and NF membrane filtration modules utilized in the Tatamagouche IMS plant design were manufactured by GE Water and Process Technologies. Raw water is pumped from the French River to redundant UF skids, each containing 18 ZeeWeed® 1000 UF modules. The units operate in parallel and each are designed to produce a continuous output of 533 L/min with a net raw water flow of 561 L/min at 95% recovery.

Each UF module has a membrane surface area of 41.8 m^2 or 1,505 m^2 total per skid. Under design operating conditions the net operating flux is 21.3 L/m^2.hr. The UF permeate is directed to an intermediate transfer tank which provides storage and feed water to redundant NF units operated in parallel.

Each NF unit (GE Osmonics PRO-100NF) is equipped with a 1.0 µm cartridge pre-filtration for membrane protection prior to a 4-2 membrane array consisting of 6 pressure vessels, each containing 4 x 200 mm diameter NF modules (OSMO PRO RO365). Each membrane element has a surface area of 33.9 m^2 which provides a total area of 813.6 m^2 per skid. Permeate production from each NF unit is designed at 379 L/min at 75% recovery, or an operating flux of 27.9 L/m^2.hr. The overall system recovery is designed at 71% recovery.

Raw water supplied to the Collins Park WTP is from Fletcher Lake. The lake is part of the Shubenacadie watershed, one of the largest and most developed watersheds in Nova Scotia. The lake receives primary inflow from the south, via Lake Thomas. Fletcher Lake is used for many recreation purposes and is largely developed along the eastern and southwestern edges with residential properties and light commercial businesses. Developments along the eastern lakefront include onsite water and wastewater systems. There are also two municipal wastewater treatment plants located along the southern lakefront which discharge treated effluent into the lake. Storm water flows from properties, highways, and the surrounding catchment area also discharged to the lake. As source water for municipal drinking water, the general water characteristics of Lake Fletcher is typical of that found in many similar surface supplies in Nova Scotia.

The Collins Park WTP treatment train includes an integrated UF-NF membrane system with redundant UF trains and a single NF train. Raw water is pumped from the lake through 50 micron self-cleaning strainers and into two parallel UF module racks. Each rack contains 4 HYDRAcap UF modules (Nitto Denko/Hydranautics Corporation, Oceanside, USA) having an active membrane surface area of 46.5 m^2 per module. The modules operate in a dead-end filtration mode at a design flowrate of 191.2 L/min per rack at a flux of 93 $L/m^2.hr$ and recovery of 95.7%. Permeate from the UF modules is stored in an intermediate transfer tank that is used as NF feed water.

The treatment process at the Collins Park WTP includes an integrated UF-NF membrane system with redundant UF trains and a single NF train. Raw water is pumped from the lake through 50 micron self-cleaning strainers and into two parallel UF module racks. Each rack contains 4 HYDRA cap UF modules (Nitto Denko/Hydranautics Corporation, Oceanside, USA) having an active membrane surface area of 46.5 m^2 per module. The modules operate in a dead-end filtration mode at a design flowrate of 191.2 L/min per rack at a flux of 93 $L/m^2.hr$ and recovery of 95.7%. Permeate from the UF modules is stored in an intermediate transfer tank that is used as NF feed water.

The NF system consists of pre-filtration through a 5 µm cartridge filter and a 1-1 membrane array of two pressure vessels, each containing 4 x 200 mm NF modules (Hydranautics ESPA4). Each NF module has a surface area of 37.1 m^2 providing a total of NF membrane area of 296.8 m^2. The permeate production rate from the system is 110 L/min at a recovery of 80% and average per module flux of 22.1 L/m^2.hr.

5.3.2 Bench-Scale NF Membrane Fouling Tests

Bench-scale commercially available DK-NF membrane test sheets (GE Osmonics, Minnetonka, CA) were used in this study. The properties of this membrane are presented in Table 5.3.

Table 5.3 Properties of DK-NF Test Membrane

Properties	**Value**
Skin layer material	Cross-linked aromatic polyamide
Typical flux/psi	22GFD@100psi[a]
pH range	2-11[a]
Salt rejection	98% $MgSO_4$[a]
Molecular weight cut-off	400 Da[b]
Contact angle	40.6 ± 5.2 ^{o}[c]
Root mean square roughness	16.4 ± 3.1 nm[c]
Zeta potential at pH 9	-18.5 mV[c]

[a] nominal value reported by manufacturer

[b] Li et al. (2008)

[c] Tang et al., (2009)

The DK-NF membrane is a thin-film composite membrane having a three-layered structure with a porous polysulfone support and an active polyamide layer. The properties of the DK-NF membrane test sheets were purchased in a flat sheet and pre-cut form (14.6 cm × 9.5 cm) from the manufacturer.

A bench-scale, cross-flow filtration unit (SEPA II, GE-Osmonics, Minnetonka, MN, USA) was used in the NF fouling experiments. The membrane cells were fitted with feed and permeate spacers in an attempt to simulate the hydrodynamics of spiral-wound membrane elements. Specifically, the thickness of the feed spacer was set at approximately 0.2 mm (65 mil). Virgin test membrane sheets used in the experiments were soaked in milli-Q water for 24 hours prior to loading into the bench-scale NF module. The milli-Q water was refreshed four times during this membrane pre-soak procedure. The membrane test sheets were then pre-compacted with milli-Q water overnight in the test-unit prior to commencing the fouling experiments.

The source water from the French River and Fletcher Lake used in the fouling experiments was pre-filtered through a mixed cellulose ester 0.45 μm membrane (GN-6 Metricel, Pall, East Hills, NY, USA) to remove larger particles prior to NF treatment at the bench-scale. The filtered water was pumped at a flowrate of 1.3×10^{-5} m^3/s (800 mL/min) (cross-flow velocity = 0.09 m/s) into the NF membrane cell body with a constant flow diaphragm pump (Hydracell, Wanner Engineering, Inc., Minneapolis, MN) equipped with variable speed motor and variable frequency drive (Baldor Electric Co., Forth Smith, AR). The bench-scale NF test unit was operated at constant pressure, variable flux mode with a TMP of 4.96 bar (72 psi) maintained during the entire filtration cycle of each experiment.

The bench-scale NF apparatus was operated in recycle mode, in which concentrate and permeate were returned to the feed water tank. To maintain constant temperature ($24^{o} \pm 2^{o}C$) of the feed water, the concentrate line was passed through a water refrigerated bath (Thermo Scientific NESLAB RTE Series, P/N U00694) before recycling into the feed tank. The membrane fouling experiments were conducted for four days (96 hours) for both source waters. The permeate flow rate was monitored regularly by measuring the volume of water collected in each hour in a graduated cylinder. Full scale data were normalized by membrane specific temperature correction factor (TCF). Because the temperature correction factor is dependent on membrane and manufacturer (USEPA, 2003), two different equations were used for calculating TCF. Collins Park and Tatamagouche NF membrane permeate flow rates were corrected according to Equations (1) (GE Infrastructure 2008) and (2) (Sharma et al., 2003) respectively.

$$\mathrm{Q_{25^{\circ}C} = Q_T \times [0.35 + (0.026 \times T)]} \quad (5.1)$$

$$\mathrm{Q_{25^{o}C} = Q_T \times exp\left[2918\left[\frac{1}{298} - \frac{1}{273+T}\right]\right]}. \quad (5.2)$$

Here T is the membrane operating temperature, Q_T is the permeate flow rate at temperature T and Q_{25^oC} is the permeate flow rate at 25°C.

Water samples were collected from the permeate, concentrate and feed tank process lines of the bench-scale NF apparatus every two hours to measure UV_{254}, DOC, conductivity, THMFP and HAAFP. Percentage DOC rejection was calculated as follows:

$$\text{Percent DOC rejection} = \left(1 - {Cp}/{Cf}\right) \times 100\,, \qquad (5.3)$$

where, C_p and C_f are the DOC concentrations of NF permeate and feed waters respectively.

5.3.3 Water Quality Analysis

Water samples (feed water and permeate) were characterized in terms of pH, UV_{254}, DOC, conductivity, THMFP, HAAFP, cations (sodium, calcium, magnesium) and anions (phosphate, chloride, nitrate). The description of analytical procedure for the measurement of water quality parameters such as pH, UV_{254}, DOC, THMs and HAAs are described in Section 3.7 of Chapter 3. The concentrations of anions were measured using an Ion Chromatogram (Metrohm 761 Compact IC, Fisher Scientific) and dissolved metals were measured using ICP-MS (Thermo Scientific X-Series 2). HPSEC (Perklin Elmer, Series 200) with UV/VIS detector was used to determine molecular weight distribution of

NOM present in two source waters following the procedure described in Section 3.7 of Chapter 3.

5.3.4 Microbiological Enumeration and Microscopy

Heterotrophic plate counts (HPCs) of the feed waters and the fouled membrane layers were determined using the spread plate method on R2A agar (APHA, 1995). Serial dilutions were prepared from each sample analyzed to yield 30 to 300 colonies per plate. The petri plates were incubated at room temperature (20^{o}C) for 7 days and then enumerated number of colonies.

At the end of the fouling experiments (i.e., after four days), the membrane test sheets were carefully removed from the SEPA-Cell test unit and cut in half using sterilized gloves and tools. One half of the fouled membrane test sheet was placed in 250 mL Erlenmeyer flasks containing 200 mL of sterilized water then covered with aluminum foil and placed on a shaker table (Barnstead E-Class, Model 2000, Fischer Scientific) operated at a speed of 1,200 rpm for 1 minute. A 1 mL of sample was collected and serial dilutions were prepared and 1 μL of each diluted samples were poured into R2A agar plates (APHA, 1995). The normalized HPC results are presented as numbers of microbes per unit membrane area (cells/m^2) as reported in previous studies (Baker and Dudley, 1998; Speth et al., 1998). Control runs were made with the virgin membrane samples.

The second half of the membrane was stored in a sterilized beaker and covered with aluminium foil. The small pieces of membrane coupons were subjected to SEM and AFM analysis. For SEM analysis, sections of the virgin and dried fouled test membranes were first coated with Gold/Palladium by utilizing a SC7620 Mini Sputter Coater under vacuum. The thickness of the coating was approximately 367 Å. A model Hitachi S-4700 field emission scanning electron microscope equipped with Oxford Inca x-sight EDS system was used to observe and analyze the surface morphology of virgin and fouled membranes.

AFM analysis was used to obtain images and roughness of the surfaces of the test membrane sheets. The analysis was performed in acoustic mode at a scanning speed of 1 Hz with an Agilent 5500 instrument (Agilent, Santa Barbara, CA) using high frequency (300 kHz) silicon cantilevers with a tip radius of 2-5 nm (TESP-SS, Veeco, Sanata Barbara, CA). Images were analyzed using the software *Gwyddion* (http://gwyddion.net/). Surface roughness of the membrane test sheets was quantified as average roughness, which is defined as the arithmetic average of the absolute values of the surface height deviations measured from the centre plane. The root mean squared (RMS) roughness is the average of the measured height deviations from the mean surface taken within the evaluation area. Three different images were taken at 10 µm × 10 µm scan at different spots of the membrane with a resolution of 512 × 512 points and average roughness values were calculated.

5.4 Results and Discussion

5.4.1 Impact of Feed Water Characteristics on Membrane Fouling and NOM Rejection

Figure 5.1 shows permeate flux declines for the two source waters evaluated in this study (French River and Fletcher Lake) monitored at bench-scale with the DK-NF test sheet membranes at constant pressure of 4.96 bar (72 psi). The initial permeate flux for both source waters was approximately 37 L/m^2·hr. The flux decline trend with the two different source waters was almost identical during the first 12 hours of filtration through the bench-scale NF membrane apparatus. After 24 hours of operation, the Fletcher Lake source water showed slightly more flux decline than the French River water, with subsequent membrane filtration time increasing this difference in permeate flux decline observed between the two source waters evaluated.

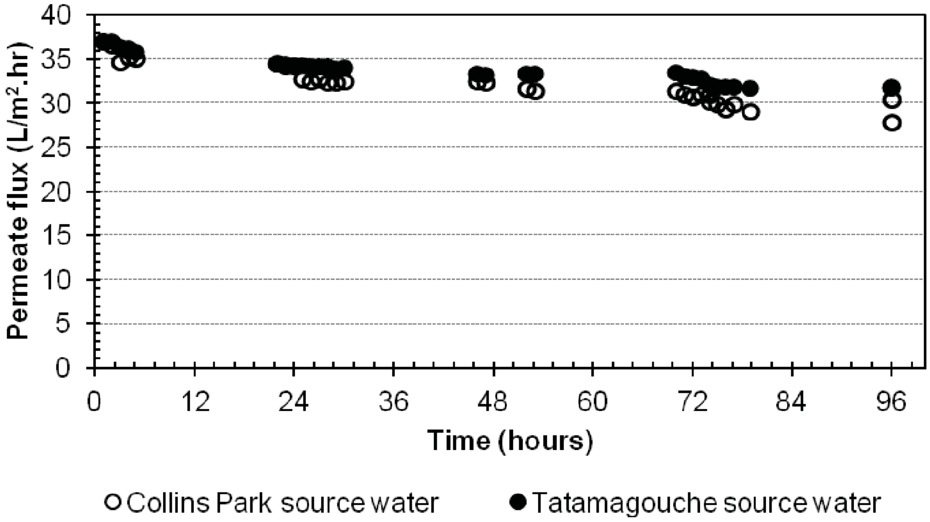

Figure 5.1 Permeate Flux during Bench-Scale NF Experiments.

At the completion of the 96-hour filtration run time, the percent flux decline for the Fletcher Lake water (i.e. 25%) was found to be higher than that of the French River water (i.e. 15%). The higher organic content of the Fletcher Lake water compared to the French River water may have influenced the flux decline patterns observed. The Fletcher Lake water has higher DOC concentration (4.5±0.1 mg/L) and SUVA value (3.6±0.07 $Lm^{-1}mg^{-1}$) than the French River water (DOC = 2.8±0.04 mg/L and SUVA = 2.2±0.04 $Lm^{-1}mg^{-1}$). Braghetta et al. (1998) also observed increased flux decline with increased TOC concentration in bench-scale NF fouling experiments conducted with Suwanne River humic acid as a model foulant. The conductivity of the Collins Park source water was slightly higher (96.6 μS/cm) than that of the Tatamagouche source water (86.1 μS/cm). Li and Elimelech (2004) observed increased rates of NF fouling with increasing ionic strength (i.e., conductivity) due to a reduction in the repulsive electrostatic forces between the colloids and the membrane surface. At high ionic strength, the electric potential and energy of interaction decrease due to double layer compression and charge screening resulting in a decrease in electrostatic repulsion between the membrane surface and NOM.

The higher concentration of selected cations (i.e., Ca^{2+}, Mg^{2+} and Na^{+}) observed in the Collins Park source water compared to the Tatamagouche source water may also have contributed to increased flux decline observed in the Fletcher Lake experiments compared to the French River experiments through the combined effect of NOM complexation with those cations. As presented in Table 5.2, calcium, magnesium and sodium concentrations were 16, 24 and 77% higher, respectively, in the Collins Park source water compared to those measured in the Tatamagouche source water samples. Li and Elimelech (2004) reported the synergetic effect of model dissolved organic carbon and calcium and magnesium cations on permeate flux decline. Other studies have also found increased flux decline rates in the presence of Ca^{2+}, Mg^{2+} and Na^{+} and emphasized the dramatic effect of Ca^{2+} in enhancing the flux decline rates by an intermolecular bridging mechanism (Hong and Elimelech, 1997a; Li and Elimelech, 2004). Another possible explanation for the differences observed in flux decline may be potential differences in NOM composition between the two source waters.

Table 5.4 NOM Removal during NF Fouling Experiments with the French River Water and the Fletcher Lake Water

WTP		French River water	Fletcher Lake water
UV_{254} (cm^{-1})	Feed	0.122 ± 0.011	0.186 ± 0.017
	Permeate	0.0005 ± 0.0007	0.001 ± 0.0007
Conductivity (µS/cm)	Feed	78.3 ± 5.1	158.8 ± 15.9
	Permeate	4.1 ± 2.9	5.3 ± 0.9
DOC (mg/L)	Feed	4.0 ± 0.6	5.3 ± 0.5
	Permeate	0.8 ± 0.22	0.9 ± 0.08
THMFP (µg/L)	Feed	236.0 ± 4.6	306.3 ± 4.4
	Permeate	19.1 ± 0.3	9.0 ± 0.1
HAAFP (µg/L)	Feed	203.1 ± 50.8	272.7 ± 10.0
	Permeate	1.6 ± 2.0	0.5 ± 0.7

The NOM rejection achieved with treatment of the source waters through the bench-scale NF apparatus was evaluated in terms of DOC, UV_{254}, conductivity, THMFP and HAAFP for the Fletcher Lake and the French River waters (Table 5.4).

Samples were taken every two hours during the day time operation of the bench-scale NF apparatus over a 4 day operational period and values were averaged. For both source waters, significant DOC rejection was achieved. Results of the Fletcher Lake water experiments showed a slightly higher rejection (up to 83%) of DOC than that found in the French River water experiments (80%). Results of the bench-scale NF study also showed significant reduction (i.e., ≥ 99%) of UV absorbing organics with both source waters. The reduction of SUVA is the indication of removal of humic and/or larger molecular weight NOM over non-humic and/or lower molecular weight NOM. Siddiqui et al. (2000) observed similar results in bench-scale NF fouling experiments with low turbidity surface waters.

As expected with the significant decreases in DOC and UV_{254} after NF treatment, significant reductions in DBP formation was observed on NF permeate samples of both source waters. The results of UFC tests showed 92% and 97% reductions in THMFP for the French River and Fletcher Lake source waters, respectively. Results of this study are consistent with the 90% to 99% reduction of THMFP and HAAFP observed in other NF studies with the natural source waters (Ates et al., 2009; Conlon and MCClellan, 1989; Edwards E., 1988; Siddiqui et al., 2000). Lower reductions in THMFP (65% to 70%)

have been reported in a NF bench-scale study of Colorado River water (Amy, 1990). However, the lower rejections found in that study were concluded to be related to the low MW characteristics of organic precursor material in that source water (i.e. significant amount of precursor material corresponded to MW≤ 500 Da).

5.4.2 Molecular Weight Distribution Analysis

Figure 5.2 presents the HPSEC chromatogram measured with UVA detector as a function of retention time for the two source water samples used in this study. Although the intensity of the peak for the Collins Park source water was higher than that of the Tatamagouche source water, the overall trend of the spectra (i.e., presence of peaks at set retention times) was found to be the same for both source waters. The higher molecular

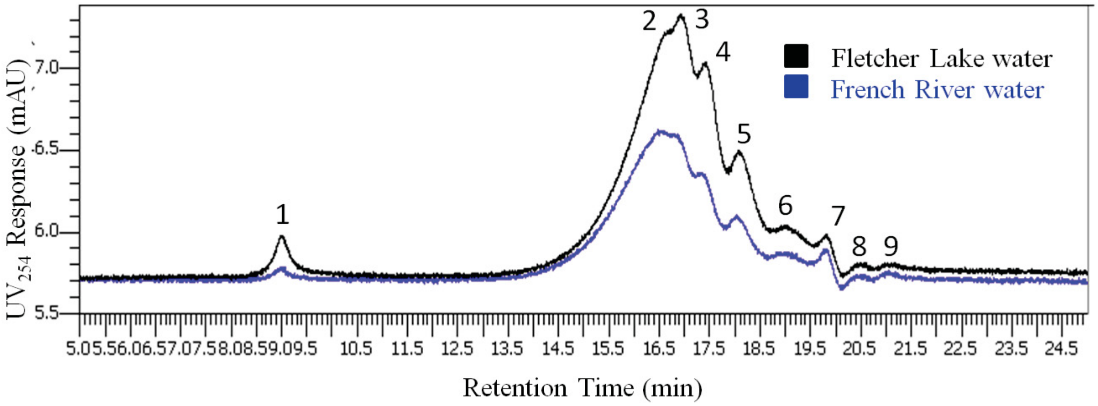

Figure 5.2 Molecular Weight Distribution of Organic Compounds: Comparison of Molecular Weight Distribution of the French River Water and the Fletcher Lake Water as Measured by HPSEC with a UVA Detector.

weight UV absorbing organics were eluted in the column first before the lower MW UV absorbing organics. Note that since the UV detector can only measure the UV absorbing organic compounds, the HPSEC results presented in this study is limited for UV absorbing organics only.

Table 5.5 shows the MW of each peak for both samples. The first peak with high MW organics (~58,000 Da) most likely represents protein type organic molecules as polysaccharides are not detected by UV detection.

Table 5.5 Molecular Weights of Assigned Peaks in HPSEC Analysis

PeakNumber from Chromatogram	**Molecular weight (Da)**	
	French River water	**Fletcher Lake water**
1	58300	58600
2	2060	1930
3	1210	1180
4	912	864
5	637	625
6	405	410
7	290	291
8	213	206
9	145	154

Peaks 2 and 3 may be associated with fulvic acids like substances (Her et al., 2002; Wu et al., 2007). Wu et al. (2007) identified the humic acid and fulvic acid fractions in Harp Lake, Ontario water based on MW calibration, and determined that the MW of humic acid was higher than 4,500 Da and that of fulvic acid was approximately lower than 4,500 Da. MW results found in this study indicate that both the source waters have a high percentage of low MW organics (i.e., < 4,500 Da) possibly representing higher constituents of fulvic acid fractions. Previous studies have demonstrated strong relationship between the MW profile and the physical-chemical properties of DOC and humic/fulvic substances (Chin et al., 1994; Her et al., 2002). Those studies demonstrated that larger MW fractions have been related to higher levels of hydrophobicity while smaller MW fractions have been related to higher hydrophilicity (Cabaniss et al., 2000). Further, a previous study that focused on NOM fractionation of water samples taken from the French River showed that a higher percentage (~58%) of the organic material were hydrophilic in nature (Lamsal et al., 2012).

5.4.3 Thickness of Foulant Layer by AFM Analysis

The AFM images for virgin and fouled membrane samples are presented in Figure 5.3a-c. The three-dimensional images were taken in each case with scan size of 10 µm × 10 µm. A significant difference was observed between the surface morphologies of the virgin and fouled membranes. The virgin membrane exhibited an average roughness (Ra) and root mean squared (RMS) roughness of 46.0 nm and 55.0 nm respectively. The test membrane that had been fouled through NF filtration runs with the Tatamagouche source water resulted in Ra and RMS roughness of 100.3 nm and 119.5 nm, respectively (Figure 5.3b); whereas, the test membrane samples that were fouled with the Collins Park source water had Ra and RMS of 173 nm and 211 nm, respectively). The maximum height of the peaks on the fouled layer (Ry) was also found to be higher (i.e., 1.07 μm) for the membrane samples fouled during the Fletcher Lake experiments. The Ry for the French River membrane samples were 0.78 μm (Figure 5.3b). Visually, the foulant layer was noticeably thicker on the NF test sheet that processed the Fletcher Lake water than the test sheets that processed the French River water sample.

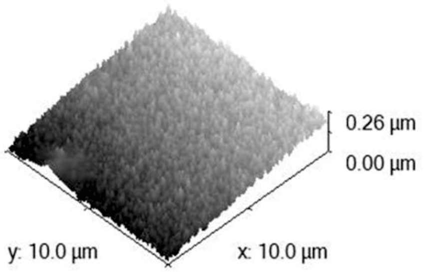

(a) Virgin Membrane

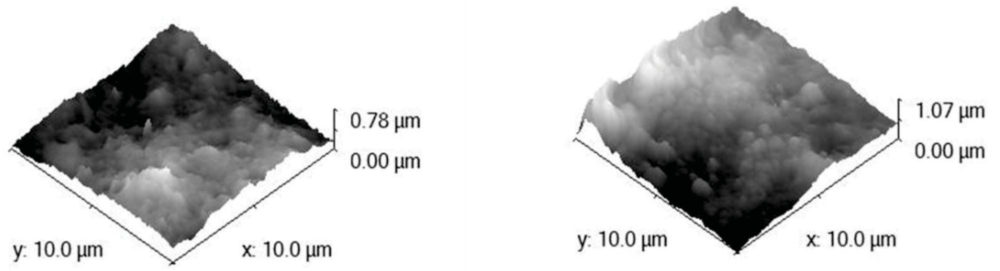

(b) Fouled with Tatamagouche source water (c) Fouled with Collins Park source water

Figure 5.3 AFM Images (a) Virgin NF Membrane (b) Fouled NF Membrane Fed with the French River Water (c) Fouled NF Membrane Fed with the Fletcher Lake Water.

5.4.4 Morphological Analysis of Foulant Layer by SEM

Figure 5.4 provides the SEM images of the virgin and fouled test sheet membranes after 96-hours of treatment with the Fletcher Lake water and the French River water. The SEM images of the virgin membrane demonstrates the network-like structure typical of a

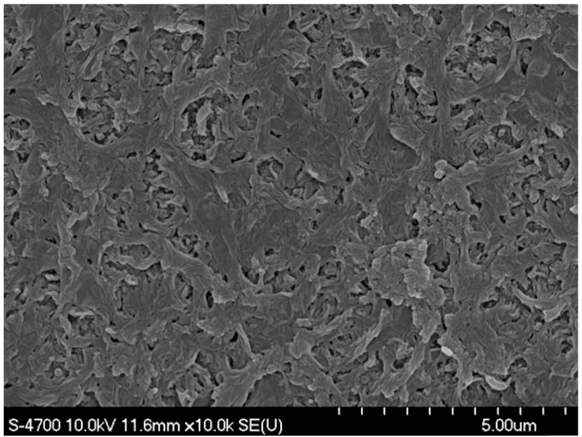

(a) Virgin membrane

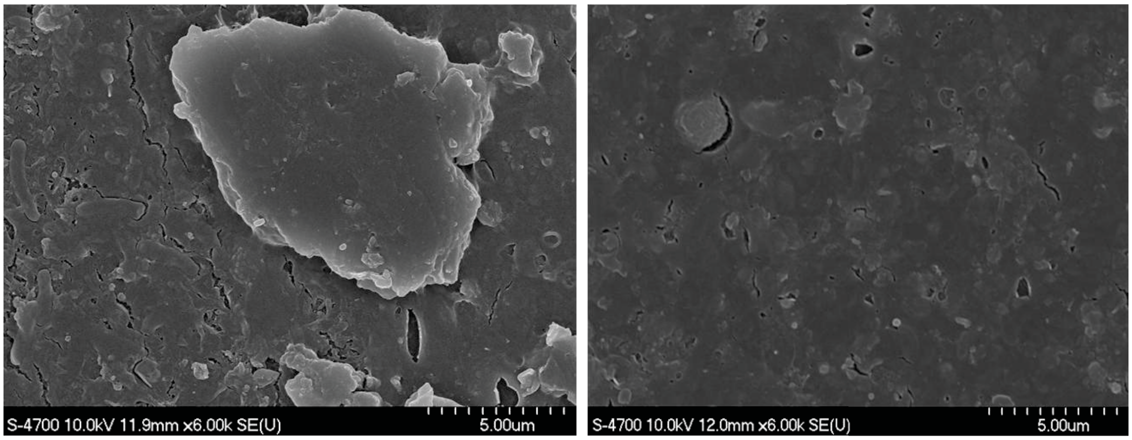

(b) Fouled with the French River water (c) Fouled with the Fletcher Lake water

Figure 5.4 SEM Images (a) Virgin NF Membrane (b) Fouled Membrane Fed with the French River Water and (c) Fouled Membrane Fed with the Fletcher Lake Water.

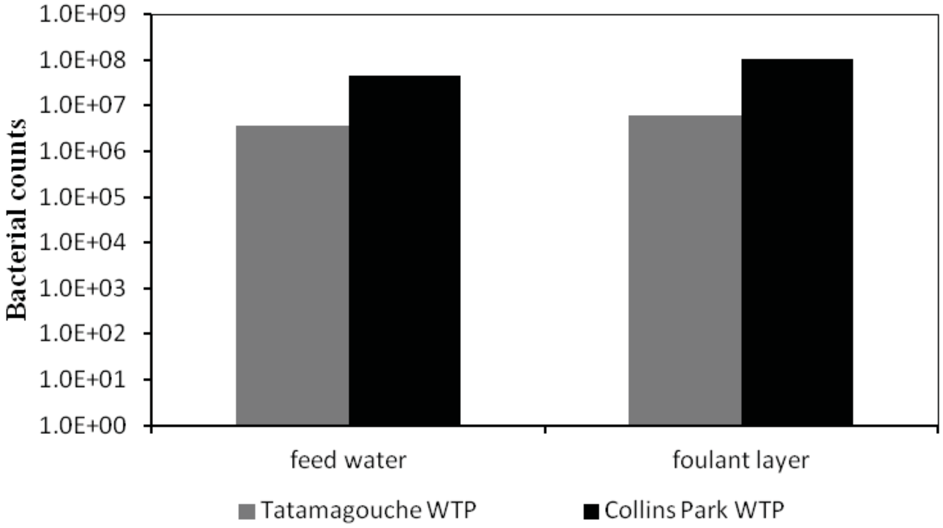

Figure 5.4 Heterotrophic Bacteria (CFU/mL) in the Feed Waters and Microbial Cell Counts in the foulant Layers (CFU/m^2).

membrane polyamide layer (Mukherjee et al., 1996), while images of the fouled membranes showed different morphologies. The visual observations obtained from this SEM photos support the theory that surface adsorption is the dominant mechanism in NF fouling (Li and Elimelech, 2004). The SEM images of the membrane fouled after treatment of the Fletcher Lake water showed a more homogeneous and dense foulant layer than the membrane fouled with the French River water. This observation was consistent with observed large surface roughness of membrane with the Fletcher Lake water as described in Section 3.4.

5.4.5 Microbiological Analysis

HPC data of the NF feed water and membrane foulant layers during the Fletcher Lake and French River bench-scale experiments are presented in Figure 5.5. HPCs of the source waters were observed in the range 10^6 - 10^7. HPCs in both source waters are consistent with the range of values of HPC reported by Baker and Dudely (1998) and Speth et al. (1998) for surface waters. HPCs of the Collins Park source water were found to be more than an order of magnitude higher than that of the Tatamagouche source water. Attached HPCs enumerated in the fouled membrane with the Collins Park source water were also an order of magnitude higher than HPCs quantified from the fouled membrane with the Tatamagouche source water.

5.4.6 Full Scale NF fouling Analysis

Plant operational data were collected from October 26 to December 19, 2010 from both the Tatamagouche and Collins Park WTPs to evaluate NF fouling behaviour of the two source waters at full-scale. Data were collected in real-time by the plant Supervisory Control and Data Acquisition (SCADA) system (VTSCADA, Trihedral Engineering Limited, Bedford, Nova Scotia) and online instrumentation. Data was collected every two hours. The operational hours of the Collins Park NF membrane were much longer (412 hours) than for the Tatamagouche NF membrane (244 hours). Feed water temperature, membrane operating pressures and permeate flux data collected for this study from both plants are presented in Figure 5.6.

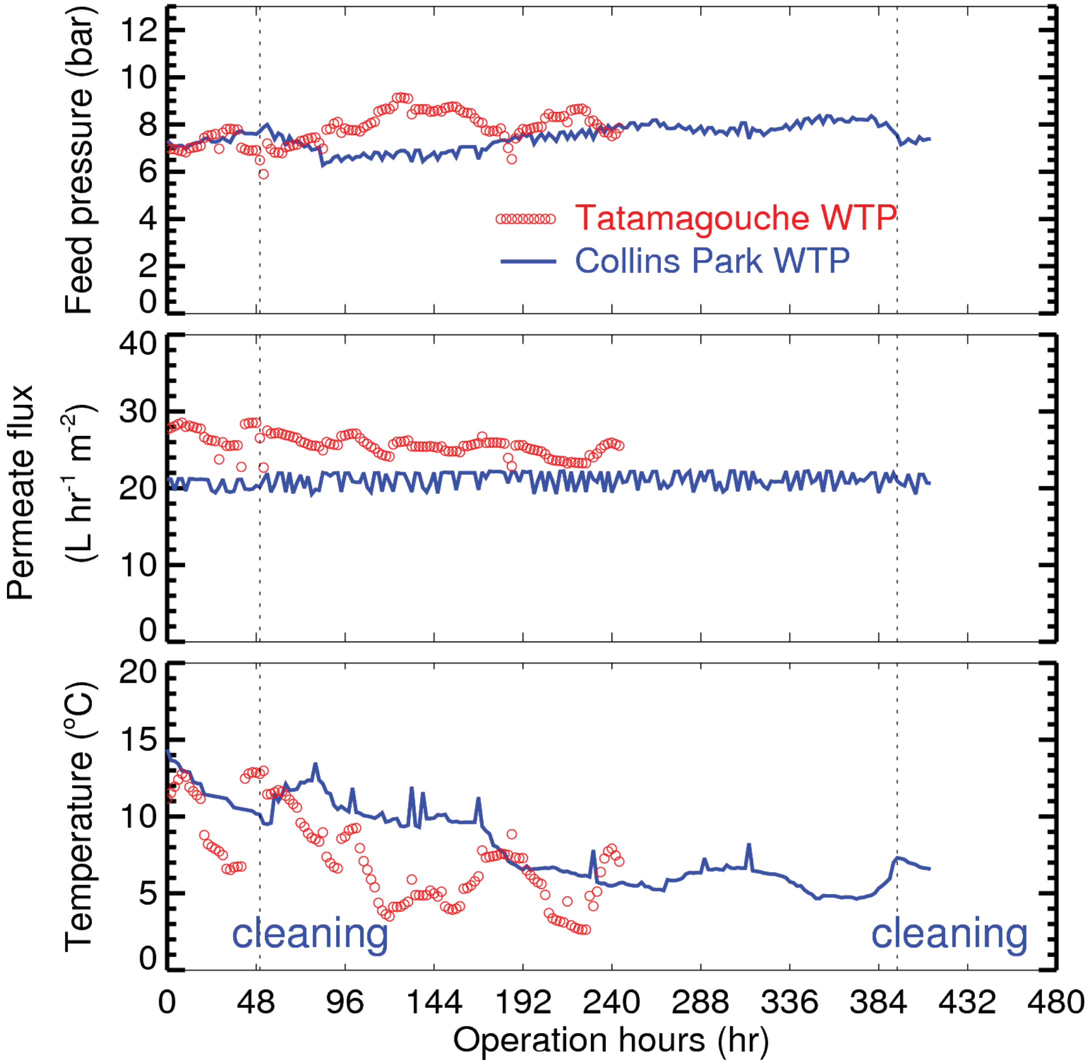

Figure 5.5 Actual Feed Pressure and Permeate Flux of NF Units at Collins Park and Tatamagouche Water Treatment Plants.

As evident in Figure 5.6, the NF membrane at Collins Park WTP was cleaned twice (on Nov. 4 and Dec.15) and the membrane at the Tatamagouche WTP was not cleaned. The Collins Park and Tatamagouche WTPs at the time of this study were operated at design flow rates of 105 L/min and 375 L/min, respectively (Table 5.1). In principle, the NF system is designed to operate at constant permeate flux, the feed pressure is adjusted to compensate for water flux changes when temperature changes. However, permeate flux at Tatamagouche WTP appears to be changing over time following the trend of water temperature (approx. 0.58 correlation) as shown in Figure 5.6.

The overall increase in feed pressure of the NF membranes in Collins Park and Tatamagouche WTPs were 25 and 5% respectively (Figure 5.6). The feed pressure of NF membrane in Collins Park increased from 6.3 bar (on Nov 9) to 8.4 bar (on Dec 13) in 296 hours of operation within one cleaning cycle. A cleaning was performed on Dec 15 since the feed pressure exceeded the maximum operating pressure 8.27 bar (i.e. 120 psi). The temperature corrected feed pressure during this period was nearly constant (Figure 5.7) suggesting that the increase in feed pressure was mostly associated with the decrease in water temperature since it is more restrictive due to increase in water viscosity (Sharma et al., 2003). Although there was not an actual increase in normalized feed pressure, a second membrane cleaning was performed on Dec 15 as the feed pressure was higher than the maximum practical pressure (i.e. 120 psi). The feed pressure in the Tatamagouche WTP was varied from 5.9 bar to 9.1 bar in 244 hours of operation within the study period (i.e. Oct 26 to Dec 19). The temperature corrected feed pressure was almost constant to 4.2 bar in the Tatamagouche WTP, suggesting that there was no significant NF fouling during the study period.

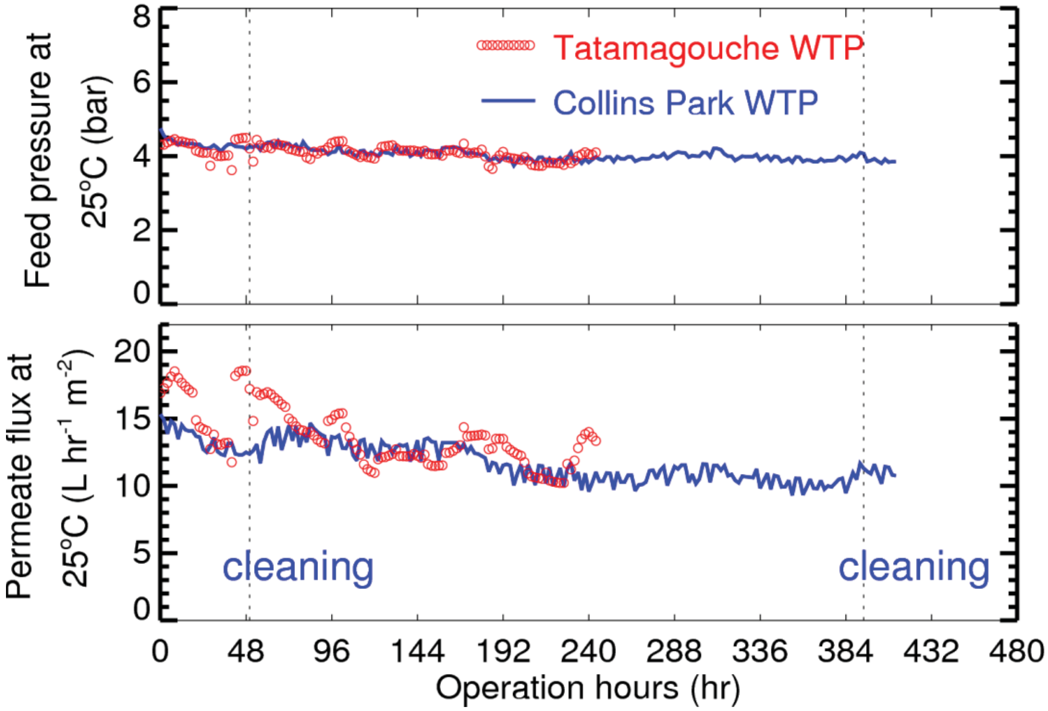

Figure 5.6 Normalized Permeate Flux and Feed Pressure of NF Units at Collins Park and Tatamagouche Water Treatment Plants.

The normalized permeate flux at 25°C for the Collins Park and Tatamagouche WTPs are presented in Figure 9. Before the first cleaning, the average permeate flux of the NF membrane in Collins Park WTP was 12.5 Lhr^{-1}m^{-2}. The permeate flux increased to 13.8 Lhr^{-1}m^{-2} after the first cleaning was performed. This was followed by a gradual decrease in permeate flux to 10.3 Lhr^{-1} m^{-2} on Dec 13 (in 380 hours of operation). After the second cleaning (i.e. on Dec 15) the permeate flux was recorded as 10.9 Lhr^{-1} m^{-2} (on Dec 16) which indicates that the cleaning procedure did not immediately return the permeate flux back to the initial value (i.e.13. 8 Lhr^{-1} m^{-2}). This likely indicates that there was irreversible NF fouling in the Collins Park WTP. Data collected from the Tatamagouche

WTP also showed decreases in the normalized permeate flux at 25°C. Review of the operator logs from both of the full-scale UF-NF facilities has shown that the NF membranes in the Collins Park WTP have been chemically cleaned almost every month in spring and fall period, whereas the NF modules in the Tatamagouche WTP have been cleaned only once in the last 2 years of operation. Anecdotally, this showed that the source water quality contributed to membrane fouling at the Collins Park WTP. Based on the cleaning regime in full-scale, the primary NF fouling in the Collins Park WTP is due to organics or/ and biological growth. The bench-scale NF fouling results provide evidences that biofouling could be a mechanism of fouling at the Collins Park WTP.

5.5 Conclusions

This study examined the impact of feed water characteristics on fouling behaviour of polyamide NF membranes using the Collins Park and Tatamagouche WTPs in Nova Scotia, Canada. Bench-scale NF fouling experiments were performed with a cross-flow NF membrane unit under similar conditions for both source waters. The rate of fouling and various water quality parameters were measured and autopsies of virgin and fouled membrane were performed using different techniques to compare the fouling propensity of two source waters. Full-scale NF fouling data from two IMS plants were compared to relate with bench-scale observations which help isolate the role of water quality in observed differences in full-scale data.

Bench-scale NF fouling results showed that Collins Park source water caused more NF fouling (25% flux decline) than the Tatamagouche source water (15% flux decline). Evidence suggest that increase in flux decline with the Collins Park source water was due to the higher concentration of DOC, conductivity and concentrations of ionic species. AFM studies showed that average roughness of the fouled membrane with Collins Park source water was 72.7 nm higher than that with the Tatamagouche source water. The number of heterotrophic bacteria in the Collins Park source water was more than an order of magnitude higher than the number of bacteria in the Tatamagouche source water suggesting that biofouling could be an additional mechanism for NF fouling at this facility.

In actual full-scale NF systems, the overall trend of increase in the feed pressure of Collins Park WTP was 25% compared to 5% in increase of the Tatamagouche WTP. The feed pressure of NF membrane in the Collins Park WTP exceeded the maximum operating pressure 8.27 bar (i.e. 120 psi) in 296 hours of operation within one complete cycle demanding membrane cleaning. Decrease in normalized permeate flux from 13.8 $Lhr^{-1}m^{-2}$ to 10.3 $Lhr^{-1}m^{-2}$ indicates that there is a real NF fouling issue in the Collins Park WTP. No clear fouling was observed in the Tatamagouche WTP.

Both the bench- and full- scale NF fouling studies suggested that the Collins Park WTP had more NF fouling than the Tatamagouche WTP. These observations support the current practices of regular membrane cleaning almost every month in the Collins Park

WTP. The NF membrane in Tatamagouche was cleaned only once after 2 years of operation. The higher values of all water quality parameters (DOC, SUVA, conductivity, concentration of ions, and the number of heterotrophic bacteria) suggested that water quality may be playing a major role for the higher NF fouling rate at the Collins Park WTP.

CHAPTER 6 COMPARISON OF ADVANCED OXIDATION PROCESSES FOR THE REMOVAL OF NATURAL ORGANIC MATTER[3]

6.1 Abstract

This study examined the impact of UV, ozone (O_3), and AOPs including O_3/UV, H_2O_2/UV, and H_2O_2/O_3 in the change of molecular weight distribution (MWD) and DBP formation potential. Bench-scale experiments were conducted with surface river water and changes in UV_{254}, TOC, THMFP, HAAFP and MWD of the raw and oxidized water were analyzed to evaluate treatment performance. Combination of O_3 and UV with H_2O_2 was found to result in more TOC and UV_{254} reduction than the individual processes. The O_3/UV process was found to be the most effective AOP for NOM reduction, with TOC and UV_{254} reduced by 31% and 88%, respectively. Application of O_3/UV and H_2O_2/UV treatments to the source waters organics with 190 Da to 1500 Da molecular weight resulted in the near complete alteration of the molecular weight of NOM from >900 Da to <300 Da. H_2O_2/UV was found to be the most effective treatment for the reduction of THM and HAA formation under uniform formation conditions. These results could hold particular significance for drinking water utilities with low alkalinity source waters that are investigating AOPs, as there are limited published studies that have evaluated the treatment efficacy of five different oxidation processes in parallel.

---

[3] Note: This work has been published in Journal of *Water Research*.
Lamsal, R., Walsh, M. E, and Gagnon, G. A., 2011. Comparison of Advanced Oxidation Processes for the Removal of Natural Organic Matter, *Water Research*, 45: 3263-3269.

6.2 Introduction

Natural organic matter (NOM) is a complex heterogeneous mixture of different organic compounds with varying molecular size and properties. A common drinking water treatment goal is to remove NOM as it is a precursor for unwanted DBPs during chemical disinfection processes, such as chlorine (Edwards E., 1988; Mosteo et al., 2009) and ozone (Gagnon et al., 1997; Schechter and Singer, 1995). NOM has also been shown to contribute to fouling on membrane surfaces (Her et al., 2008a; Hong and Elimelech, 1997a), production of biologically unstable water (Rittmann and Snoeylink, 1984) and other unwanted water quality issues such as metal complexes (Ravichandran et al., 1998; Schmitt et al., 2002).

The application of AOPs has gained significant interest in the drinking water industry as an additional tool for removing NOM and minimizing the formation of DBPs in drinking water (Chin and Bérubé, 2005; Zhou and Smith, 2001). Previous studies have focused on O_3 (Gagnon et al., 1997), UV (Chin and Bérubé, 2005; Thomson et al., 2002) and AOPs including H_2O_2/UV (Toor and Mohseni, 2007; Wang et al., 2006), O_3/UV (Amirsardari et al., 2001; Chin and Bérubé, 2005) and H_2O_2/O_3 (Kleiser and Frimmel, 2000) to evaluate the potential for NOM reduction and the mitigation of DBP formation in finished water. Matilainenm and Sillanpää (2010) have provided a thorough review of published oxidation and AOPs studies that have been conducted on both natural and synthetic test waters. However, these studies have primarily focused on evaluating one or two oxidation or AOPs for NOM reduction. This study goes beyond the previously published studies by directly comparing the treatment efficacy of five different oxidation processes in parallel, in terms of changes to MWD of the source water, NOM reduction and subsequent minimization of DBP formation potential from a low turbidity, highly coloured surface water.

During advanced oxidation treatment, hydroxyl (HO•) radicals are formed which act as a strong oxidant and transform NOM. Westerhoff et al., (2007) directly measured the rate constants for reactions between HO• radicals and seven DOM isolates from different sources and observed rate constants in range from 1-5×10^8 $M^{-1}S^{-1}$, which is three to four orders of magnitude higher than for chlorine and ozone (Crittenden et al., 1999). HO• radicals produced during AOPs are capable of reducing TOC concentrations and DBPFP of raw water (Amirsardari et al., 2001; Chin and Bérubé, 2005; Glaze et al., 1982; Kusakabe et al., 1990; Sierka and Amy, 1985). Under strong advanced oxidation conditions (i.e. long irradiation time and/or higher H_2O_2 concentrations) NOM is mineralized, indicated by a decrease in TOC and DBPFP (Kleiser and Frimmel, 2000; Toor and Mohseni, 2007; Wang et al., 2006). However, such strong treatment conditions may not be economically feasible, and in commercial applications, low or moderate advanced oxidation conditions are applied. Under these conditions, NOM is partially oxidized and higher molecular weight compounds are transformed into smaller and more biodegradable compounds such as aldehydes and carboxylic acids (Backlund, 1994; Edwards and Benjamin, 1992; Gagnon et al., 1997; Sarathy and Mohseni, 2007). Such changes in the chemical characteristic of NOM also result in reducing TOC concentrations and/or alter the characteristics of the DBP precursor material potentially reducing its reactivity with chlorine.

The objective of this study was to compare O_3, UV and three AOPs including H_2O_2/O_3, H_2O_2/UV and O_3/UV for NOM removal and assess the impact on modifying the MWD of NOM following treatment. This study was conducted using laboratory-controlled conditions with a natural surface water source that has a low alkalinity (< 5 mg/L as $CaCO_3$) and moderate level of total organic carbon (TOC of 3 to 4 mg/L). The effectiveness of each treatment process was evaluated by traditional metrics for NOM; namely, UV_{254}, TOC concentration, SUVA, THMFP and HAAFP. In addition, the MWD following each treatment was assessed using HPSEC analysis. HPSEC has been demonstrated to be an effective technique for determining the MWD of NOM (Pelakani et al., 1999). Determination of the MWD of NOM provides information on the specific fraction of NOM that plays important role in DBP formation (Amy et al., 1987b; L.Chang and Young, 2000) and membrane fouling potential during water treatment (Her et al., 2008a).

6.3 Materials and Methods

6.3.1 Source Water Characterization

Surface water collected from the French River, which provides the drinking water in a northern shore community in Nova Scotia, Canada, was used for the bench-scale study.

The average water quality of the French River is characterized by its low alkalinity (< 5 mg $CaCO_3$/L), low turbidity (<1.5 NTU), and high colour level (> 35 Pt-Co). The French River has general characteristics that are similar to other surface water sources in Nova Scotia and Atlantic Canada (Waller et al., 1996).

6.3.2 Experimental Set-up

The laboratory scale batch set up for the ozone experiments used in this study is shown in Figure 3.3 in Section 3. It consists of a compressed air system, ozone generator, a contactor (reactor) and off gas collection system. The reactor was a glass tank with a working volume of 10 L (0.305 m diameter × 0.41 m height). The inflow and outflow of the ozone gas line in the reactor was fitted with a laboratory stopper (Fisher scientific # 14141R) at the top of the reactor and sample was taken from the bottom of the reactor. Compressed air with a flow rate of 2 L/min was passed into the ozone generator (VMUS-4), where high voltage corona discharge causes break down of oxygen molecules into radicals that combine with oxygen molecules to form ozone. Ozone was bubbled into the base of the reactor using a fine bubble diffuser at a flow rate of 2 L/min and pressure of 15 psi. A potassium iodide solution (20 gm KI in 1L water) was used to collect the residual ozone in the off-gas from the reactor. The ozone experiments were conducted in a semi-batch mode by continuously passing O_3 gas in a 10 L reactor directly with 3 L sample volume at room temperature ($23 \pm 1^{o}C$) for 5, 15, 30, 45 and 60 min. Ozonation for 30 min showed better performance than for lower treatment times (e.g., 5 min and 15 min) and similar performance to higher treatment times (45 min and 60 min). The concentration of ozone consumed during the 30 min reaction time was 4.04 ± 0.11 mg/L. The detailed procedure for ozone dose calculation was provided in Section 3.2 in chapter 3. For the H_2O_2/O_3 experiments, 23 mg/L of hydrogen peroxide solution (50% Fisher Scientific) was mixed with 3 L of the raw water for approximately 5 minutes and the mixture was ozonated for 30 min, similar to the treatment times used in the ozone experiments. The optimum concentration of H_2O_2 (i.e. 23 mg/L) for the source water was determined during H_2O_2/UV process with UV dose of 1140 mJ/cm^2. Removal of TOC and UV_{254} with different concentration of H_2O_2 is provided in Appendix C.

A low pressure ultraviolet lamp (Trojan UV Max.) with 43 Watt power was used during the UV experiment. The dimension of the chamber assembly was 0.495 m × 0.09 m, and the length of the lamp (i.e., sleeve length) was 0.405 m. The UV reactor is a glass tube with a working volume of approximately 2 L. Raw water was pumped into the reactor at a flowrate of 167 mL/min using a masterflex pump to achieve the maximum UV dose delivered by the lamp. The delivered UV dose in the UV and UV based AOP experiments was 1140 mJ/cm^2, which was determined by using potassium ferrioxalate actinometer. Since flow rate in the reactor was low the dose distribution within the reactor may vary. Additional information on the UV dose calculation was described in Section 3.2 of Chapter 3. For the H_2O_2/UV AOP experiments, 23 mg/L of H_2O_2 was first mixed with 3 L of the raw water for 5 minutes. The mixture was then pumped through the UV reactor at the same flow rate as that of UV experiments. For the O_3/UV combined AO process, the raw water sample was ozonated for 30 min and then pumped through the UV reactor to achieve the 1140 mJ/cm^2 UV dosage. The oxidation processes evaluated in this study utilized higher dosages of oxidants than typically applied in drinking water treatment for optimum removal of NOM and DBPFP, consistent with earlier studies (Chin and Bérubé, 2005; Toor and Mohseni, 2007).

6.3.3 Analytical Methods

In this study, NOM was quantified by measuring UV_{254}, TOC, and DOC concentrations. SUVA which can be used as a surrogate parameter to monitor the changes in aromatic nature of NOM in water was calculated from UV_{254} and DOC as outlined by Edzwald et al. (1985). In addition, DBPFP was determined for THMs and HAAs using UFC methodology (Summers et al. 1996). Finally, NOM characterization included analysis using HPSEC (PerkinElmer, Series 200) with a UV/VIS detector to determine the molecular weight distribution of NOM. A detailed description of the analytical test procedures used for this research is provided in Section 3.1 of Chapter 3.

6.4 Results and Discussions

6.4.1 Characterization of the Source Water

The majority of organic carbon of the French River was in the dissolved fraction, as demonstrated by the TOC (3.10 ± 0.325 mg/L) and DOC (2.85 ± 0.131 mg/L) measurements. The UV_{254} value was 0.090 ± 0.003 cm^{-1} (Table 6.1). The SUVA for the

French River water was 3.2 m^{-1}/ (mg/L), which indicates that the source water contained a mixture of hydrophobic and hydrophilic NOM fractions (Owen et al., 1995b).

The chromatogram used to determine the MWD of the source water is presented in Figure 6.1. The total area of the sample was integrated using Totalchrom software (PerkinElmer, Ontario, Canada) to obtain the entire MWD of NOM in the sample (Figure 6.2). The relationship between the molecular weight of organic compounds and their retention time was determined by log-linear regression between log molecular weight and retention time. HPSEC analysis showed that the French River raw water consists of four different MW fractions: 1246, 690, 478 and 292 Da. The highest percentage area of chromatogram (i.e., 66%) was observed with the 1246 Da MW fraction. Earlier studies have proposed that compounds having 1000 to 1500 Da MW range likely represent humic and fulvic acids (e.g. Huber and Frimmel, 1996), which is supported by the measured SUVA value (3.19 Lmg-1m-1) in the French River. The lower proportion of intermediate and MW low fractions present in the French River water may represent simple aromatic compounds or fulvic acids as described by Her et al. (2000, 2003).

Table 6.1 Mean and Standard Deviations of Water Quality Parameters and Dosages Used in Each Treatment Processes

	UV_{254} (cm^{-1})	**TOC (mg/L)**	**DOC (mg/L)**	**SUVA (m^{-1}/(mg/L))**	**Dosages***
Raw	0.092 ± 0.003	3.10 ± 0.325	2.85 ± 0.131	3.16 ± 0.170	
UV	0.080 ± 0.003	2.99 ± 0.049	2.73 ± 0.072	2.93 ± 0.131	1140
O_3	0.039 ± 0.007	2.92 ± 0.053	2.79 ± 0.175	1.43 ± 0.023	4.04 ± 0.11
O_3/UV	0.011 ± 0.004	2.12 ± 0.116	2.0 ± 0.723	0.55 ± 0.006	(4.04 ± 0.11)/ 1140
H_2O_2/UV	0.037 ± 0.010	2.38 ± 0.188	2.35 ± 0.585	1.70 ± 0.041	23/1140
H_2O_2/O_3	0.035 ± 0.007	2.78 ± 0.081	2.69 ± 0.531	1.30 ± 0.037	23/(4.04 ± 0.11)

*UV dose is expressed in mJ/cm^2 and O_3 and H_2O_2 are expressed in mg/L.

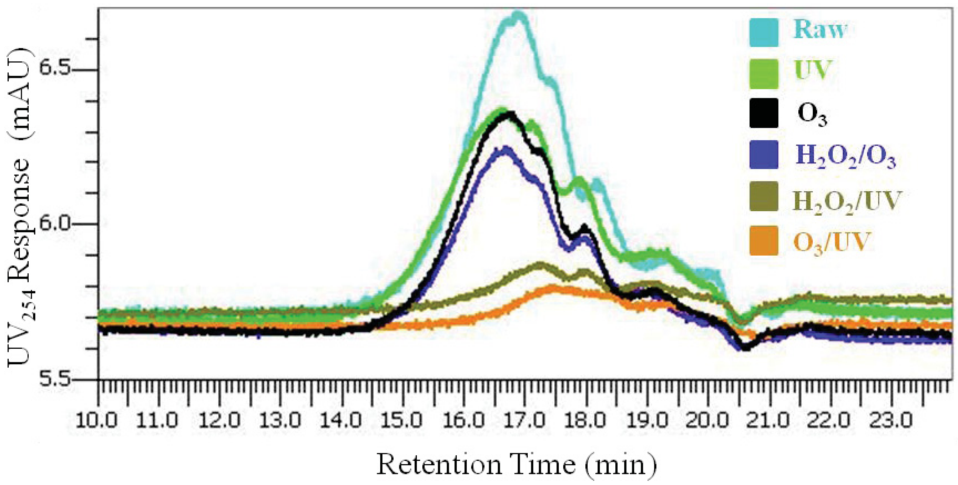

Figure 6.1 High Performance Size Exclusion Chromatograms of Raw and Oxidized Waters.

6.4.2 Impact of Oxidation on TOC and SUVA

In the AOP experiments, the reduction of NOM was attributed to chemical oxidation of NOM present in the raw water by HO• radicals. However, these HO• radicals can also react with carbonate and bicarbonate ions which are typically present in raw water. This reaction significantly reduces the amount of HO• radicals available for oxidation of NOM (Gottschalk et al., 2000). Since the source water used in this study has low alkalinity, the impact of carbonate and bicarbonate ions on the resulting concentration of HO• radicals was expected to be negligible.

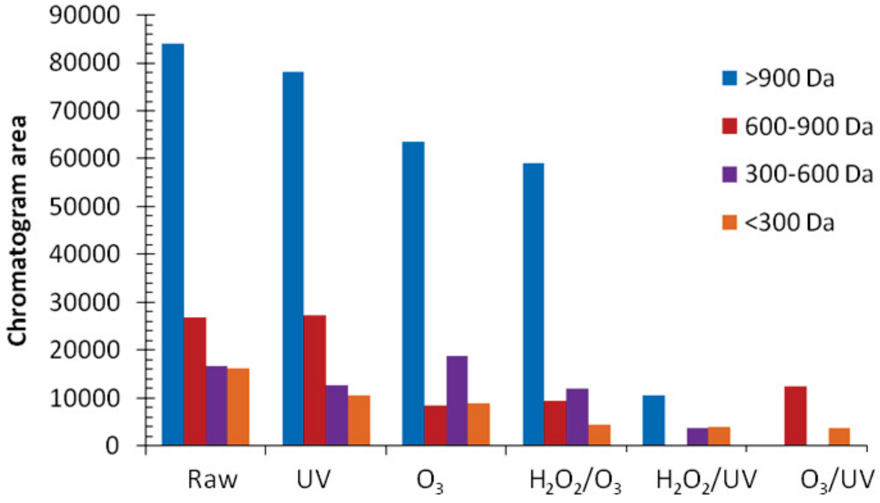

Figure 6.2 Chromatogram Area Counts for Raw and Oxidized Waters for Different Molecular Weight Compounds. Each Bar Represents the Average of Two HPSamples.

A reduction in UV_{254} absorbance was observed after each treatment process is presented in Table 6.1. UV radiation at 254 nm is mainly absorbed by aromatic compounds and conjugated double bonds (Singer 1999). Therefore, reduction in UV_{254} indicates a loss of aromatic and conjugated double bond structures of NOM (Owen et al., 1995). However, the observed impact of the treatment processes on TOC concentration was less because of the partial oxidation of NOM to other intermediate byproducts (Table 6.1). UV treatment on its own had minor impact upon the UV_{254} absorbance and almost no impact on TOC concentration. The impact of UV or H_2O_2 alone has been found to be negligible for NOM reduction in other studies (Chin and Bérubé, 2005). The rate of UV_{254} and TOC reduction increased significantly when H_2O_2 was combined with UV. UV in combination with H_2O_2 promotes the formation of HO• radicals, as reported by other researchers (Wang et al., 2006; Toor and Mohseni, 2007). The UV_{254} absorbance and TOC concentrations decreased from 11 to 60% and 3 to 23%, respectively, with UV treatment in the presence of H_2O_2 compared to UV treatment on its own. Sarathy and Mohseni (2007) also observed significant reduction of UV_{254} without TOC reduction in experiments with H_2O_2/UV AOP with a UV dose of 1500 mJ/cm^2 and H_2O_2 concentrations up to 20 mg/L.

The ozone and H_2O_2/O_3 treatment processes reduced the raw water TOC concentration by 6 and 10%, respectively. However, as presented in Table 6.1, UV_{254} absorbance was observed to be reduced by 57% with O_3 treatment and 59% with H_2O_2/O_3 treatment. The higher reduction of UV_{254} absorbance with less reduction of TOC demonstrates the removal of conjugated double bonds with minimal mineralization. Increased NOM oxidation in H_2O_2/O_3 process, as compared to the O_3 process alone, was a result of more HO• formation.

O_3/UV reduced TOC and UV_{254} by 31% and 88%, respectively. The higher reduction of UV_{254} achieved can be explained by the NOM reaction with O_3. In O_3/UV AOP systems evaluated in other studies, mineralization of organic carbon was also observed (Amirsardai et al., 2001; Kusakabe et al., 1990, Glaze et al., 1982; Sierka and Amy, 1985). Chin and Bérubé (2005) evaluated the O_3/UV AOP with an O_3 dose of 4 mg/L and a UV dose of 0.13 Ws/cm^2 on raw water characterized with 1.3 to 3.2 mg /L TOC concentrations. That study found approximately 15% mineralization of the TOC in the raw water after O_3/UV treatment, although the UV dose evaluated (approx. 130 mJ/cm^2) was much lower than that used in this study (i.e., 1140 mJ/cm^2). The increased mineralization observed in O_3/UV AOP compared to H_2O_2/O_3 and H_2O_2/UV AOPs may be due to a larger yield of hydroxyl radical per oxidant compared to other advanced oxidation processes (Gottschalk et al., 2000; Oh et al., 2003). Since production yields of HO• radicals in each oxidation process were not measured during this study, further work would be required to verify this theory.

6.4.3 Impact of Oxidation on NOM Molecular Weight

HPSEC chromatograms for the AOP test waters are presented in Figure 6.1. Higher MW organics are eluted from the column first and lower MW organics are eluted later. The peak area of chromatogram represents the intensity of UV absorbance of the sample detected by the UV detector at 254 nm. Therefore, these peaks are indication of the presence of aromatic or double bond organic compounds. Prior to application of the treatments evaluated in this study, the HPSEC chromatogram of raw water featured a large peak, and the total area under the HPSEC chromatogram decreased with the application of the different treatment processes. These results demonstrate the oxidation of aromatic or double bond organic matter into lower molecular weight compounds after treatment.

The MWD of each process observed in Figure 6.1 was translated into quantitative terms using Totalchrom software available with the HPSEC instrument and is presented in Figure 6.2. The UV treatment process showed minor impact on the MWD of the source water NOM. Ozone was found to reduce the > 900 Da and 600 to 900 Da MW fractions of organics by 25% and 68%, respectively. As described earlier, UV_{254} and TOC were found to be reduced by 57% and 6%, respectively, after O_3 treatment, demonstrating that NOM oxidation occurred with removal of conjugated double bonds with minimal mineralization. Frimmel et al. (2000) also observed that ozone treatment decreased the absorbance of Ruhr River water with minimal mineralization and found decreases in the higher MW fractions with concomitant increase in the lower MW fractions. However, minimal increase in the lower MW (i.e. 13% of 300-600 Da) fraction of NOM was observed during this study.

Figure 6.2 shows that the reduction of larger MW NOM was higher than that of lower MW NOM. The preferential reduction of larger MW organic matter, in comparison to lower MW organic matter, could be a result of the higher reaction rate constant between HO• and the larger MW compounds (Thomson et al., 2004). Higher MW compounds tend to be more aromatic in nature, so they may have a larger number of reaction sites than smaller MW compounds. Thomson et al., (2004) also explained that higher MW compounds react fastest as they have higher molar absorptivity than lower MW compounds. Westerhoff et al (1999) observed the positive correlation between molecular weights and aromaticity and the reaction rate constant between HO● radicals and NOM.

Ozone in combination with UV showed complete removal of MW NOM >900 Da. However, there was no observed increase in the formation of lower MW NOM. Similarly, when H_2O_2 was combined with the UV process, the H_2O_2/UV AOP reduced the >900 Da MW fractions by 85% and the 600-900 Da MW fractions by 100% without any observed increase in lower MW fractions of the NOM. This is in contrast to previous studies that have shown significant reduction of larger MW NOM in combination with an increase in lower MW NOM (Sarathy and Mohseni. 2007). However, that study performed HPSEC analysis at 260 nm to detect the chromophoric NOM only. Observation of 23% TOC reduction versus 60% UV_{254} reduction with the H_2O_2/UV AOP implies increase in lower MW NOM. However, the HPSEC analysis used in this study did not provide further information for single bond organic carbon since the UV detector of the HSPEC instrument only measures the aromatic or double bond organics, making the direct relationship and quantification between HPSEC and TOC results difficult.

6.4.4 Impact of Oxidation on DBP Formation

THMFP and HAAFP of the raw and oxidized waters are shown in Figures 6.3 and 6.4, respectively. In general, THMFP removal was greater than HAAFP in the oxidation processes studied. The precursor materials for THMs tend to be aromatic whereas HAAs precursor materials are aliphatic as discussed in detail in Bond et al. (2009) and Hong et al. (2009). The treatment by AOPs tends to decrease the aromaticity of NOM; therefore, the decrease in THMFP is greater than that of HAAFP caused by the larger removal of THMs precursor materials. In both the raw and oxidized waters, chloroform formed the majority of trihalomethane species, followed by dichlorobromomethane and dibromochloromethane. The concentrations of bromoform were below the detection limit (zero) in all samples.

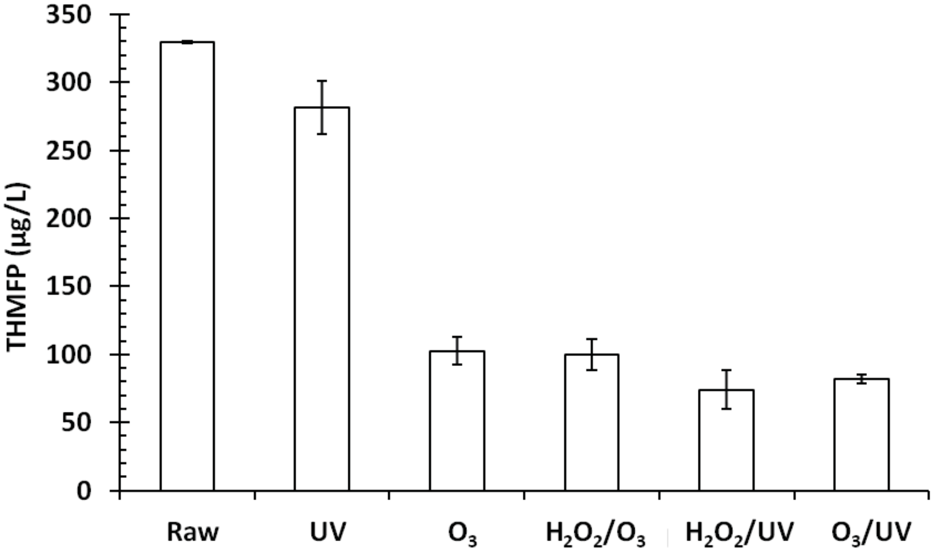

Figure 6.3 THMs for Raw and Oxidized Waters. Vertical Bars Represent 2σ Levels.

The majority of HAA species measured in the raw water were dichloroacetic acid, bromochloroacetic acid, chloroacetic acid. Dibromoacetic acid and bromodiacetic acid concentrations were found to be below detection limit.

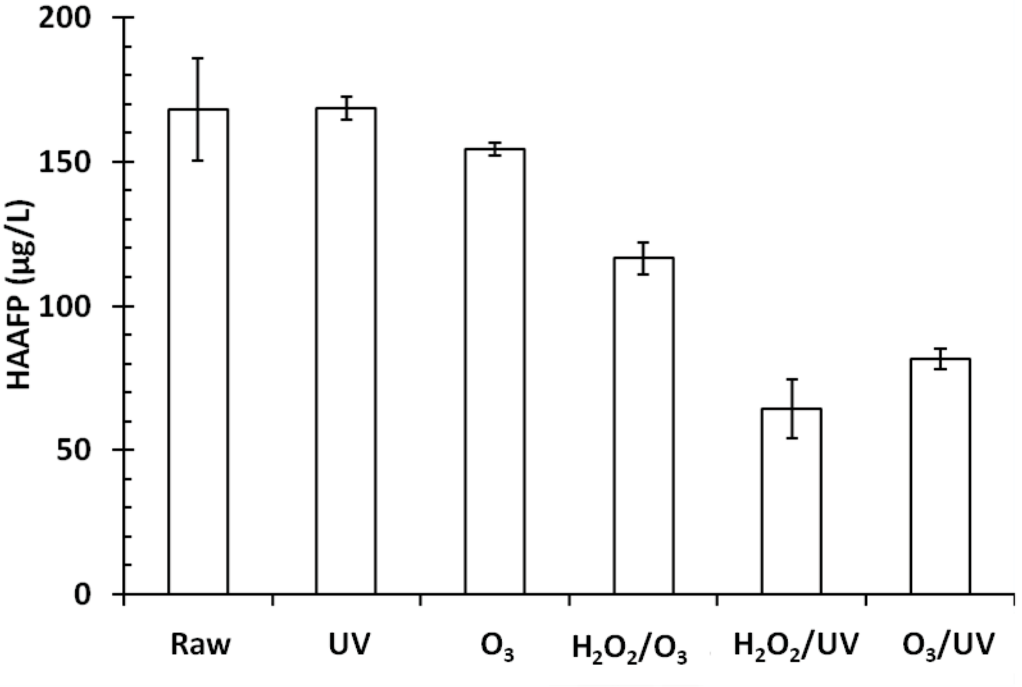

Figure 6.4 HAAs of Raw and Oxidized Waters. Vertical Bars Represent 2σ Levels.

The results of the UV treatment process showed 15% reduction of THMFP and no reduction of HAAFP. The little to no reduction of THMFP and HAAFP may be due to the minor impact of UV radiation on UV_{254} reductions and changes in MWD of organics. These observations are consistent with those found in other studies (e.g., Chin and Bérubé, 2005), where it has also been demonstrated that UV treatment on its own is ineffective at reducing THMFP and HAAFP. When H_2O_2 was combined with UV, THMFP and HAAFP were reduced by 77% and 62%, respectively. The increased reduction of THMFP and HAAFP observed with the H_2O_2/UV AOP agrees with the increased reduction of UV_{254} achieved with H_2O_2/UV treatment (e.g., 60%) compared to the moderate 11% reduction in UV_{254} achieved with UV treatment alone. MWD results also showed that H_2O_2/UV AOP resulted in increased reduction of >900 Da MW fractions by 85% and the complete reduction of 600-900 Da MW fractions of NOM. Such a decrease in THMFP and HAAFP was also observed with 23 mg/L initial H_2O_2 concentration and UV dose higher than 1500 mJ/cm^2 in a study conducted by Toor and Mohseni (2007) with similar source water qualities. Liu et al. (2002) reported reduction of both THMFP and HAAFP with UV dose of 1000 mJ/cm^2 or higher and initial H_2O_2 concentration of 100 mg/L. These studies have suggested that a combination of high UV dose and H_2O_2 concentration is required for the potential generation of higher levels of HO• radicals and hence the reduction of THMFP and HAAFP. The study conducted by Toor and Mohseni (2007) also demonstrated a significant reduction of H_2O_2 concentration in the solution, indicating the generation of HO• radicals that consequently oxidized DBP precursors and reduced the THMFP and HAAFP of the source water. Significant reduction of THMFP and HAAFP with H_2O_2/UV treatment was also observed in this study, which indicates a decrease in H_2O_2 concentration in the solution.

In contrast to UV treatment alone, ozone treatment showed a higher reduction of THMFP and HAAFP (i.e., 69% and 8%, respectively). The increased percent reduction of THMFP with the O_3 process is supported by increased reduction of UV_{254} (57%), indicating strong correlation between UV_{254} and THMFP reductions (Edzwald et al., 1985). The MWD results also showed the increased reduction of UV absorbing organics. These results are consistent with previous studies (e.g., Hu et al., 1999; Westehoff et al., 1999; Galapate et al., 2001). The reduction of THMFP and HAAFP of the ozonated samples can be explained by the reaction pathway for DBPs. Similar to chlorine, ozone reacts by addition to the aromatic system and once the aromatic double bonds are consumed by ozone, fewer sites are available for chlorine addition. Chlorine addition to the double bond is a main pathway for DBP production.

In the H_2O_2/O_3 AOP experiments, the THMFP and HAAFP were reduced by 70% and 31%, respectively. For treatments involving O_3 in combination with UV, THMFP was reduced by 75% and HAAFP was reduced by 52%. Glaze et al. (1982) observed that the combined application of O_3 and UV was more effective than ozone alone for the destruction of THM precursors in two southern U.S. surface-water sources. Other researchers have also reported significant reduction of THMFP and HAAFP during treatment with the O_3/UV process (Sierka and Amy, 1985; Chin and Bérubé, 2005). Overall, the results of this study found that H_2O_2/UV showed improved precursor reduction of 77% for THMFP and 62% for HAAFP, compared to the reduction of 75% for THMFP and 52% for HAAFP in O_3/UV, and the reduction of 70% for THMFP and 31% for HAAFP in H_2O_2/O_3.

6.5 Conclusion

This study evaluated O_3, UV, and three advanced oxidation processes including H_2O_2/O_3, H_2O_2/UV and O_3/UV for the removal of natural organic matter and reduction in DBP formation potential of the treated source water. Bench-scale experiments demonstrated that the ozone and UV treatment processes alone showed less impact on TOC reduction compared to the combined AOPs of H_2O_2/O_3 and H_2O_2/UV. However, O_3 showed significant reduction of UV_{254}. The O_3/UV AOP showed increased performance reducing UV_{254} by 88% and TOC by 31% compared to the other oxidation processes evaluated. The H_2O_2/UV process reduced UV_{254} by 60% and TOC by 23%, achieving somewhat lower reductions than the O_3/UV process. Further study with measurement of product yield in each oxidation process would help for better explanation of the results.

The HPSEC analysis showed that the molecular weight (MW) of the organic compounds that are able to absorb UV light at 254 nm in the source water ranged from 190 to 1500 Da. Overall, the application of the oxidation processes evaluated in this study resulted in the reduction of higher MW NOM, with the O_3/UV and H_2O_2/UV AOPs having the largest impact on MW transformation of the source water. Treatment with the H_2O_2/UV AOP resulted in the largest reduction of THMFP (77%) and HAAFP (62%) compared to the other treatment processes evaluated. Similarly, treatment with the O_3/UV AOP showed comparable reduction of THMFP (75%) and HAAFP (52%). Results from this study suggest that O_3/UV and H_2O_2/UV are viable options for maximum reduction of NOM from low alkalinity drinking water sources characterized with low turbidity and medium SUVA, and could hold particular significance for plants that are investigating alternative AOPs currently available in the drinking water marketplace. However, further studies that focus on measurement of product yield and include cost analysis for each oxidation process would be necessary for appropriate selection of AOPs.

CHAPTER 7 USE OF RAMAN AND SURFACE ENHANCED RAMAN SPECTROSCOPY FOR STUDYING FOULING ON NANOFILTRATION MEMBRANE[4]

7.1 Abstract

Membrane fouling is a key constraint for the widespread application of membrane-based technologies in water and wastewater treatment because it reduces the production volume of water, thereby increasing operating and maintenance costs. Characterization of membrane materials and foulant layers is crucial for an accurate understanding of fouling processes. This study used surface-enhanced Raman spectroscopy (SERS) and normal Raman spectroscopy as a novel technique to examine fouling caused by naturally occurring organics on a polymeric NF membrane, which is used for the treatment of drinking water. The results from this study suggest that normal Raman spectroscopy is useful for characterization of polyamide NF membranes used in drinking water treatment, but is not sensitive enough to resolve the foulant materials present on the membrane surface. SEM analysis of virgin and used membrane suggests significant membrane fouling. The observed SERS peak of fouled membrane at wavenumber 1543 cm^{-1} suggests the presence of protein and those at 1444, 1305, and 1239 cm^{-1} indicate the possible presence of carbohydrate on the membrane surface. These results demonstrate that SERS has the potential for identification functional groups of organics involved in NF membrane fouling in water treatment that could lead to improved strategies for membrane fouling reduction.

---

[4] This work has been published in Journal of *Separation and Purification Technology.*

Lamsal, R., Harroun, S. G., Brosseau, C. L. and Gagnon, G. A., 2012. Use of Surface Enhanced Raman Spectroscopy for Studying Fouling on Nanofiltration Membrane, Separation and Purification Technology, 96: 7-11.

7.2 Introduction

Membrane fouling is a critical operational challenge in the water industry because it reduces the production volume of water and increases operating and maintenance costs. Fouling results mainly from the deposition of retained substances on the membrane surface and the accumulation of small molecules in the membrane pores. One of the most significant problems limiting the control and prevention of membrane fouling is the inadequate understanding of materials that lead to fouling. Improved knowledge of the foulant composition and organization will greatly facilitate the development of strategies for membrane fouling prevention and control (Flemming et al., 1997; Violleau et al., 2005).

In drinking water treatment processes, NOM is an important contributor to membrane fouling (Hong and Elimelech, 1997a; Nilson and DiGiano, 1996). A variety of NOM characterization approaches have been investigated in the past several years; such methods include hydrophobicity determination (Nilson and DiGiano, 1996), molecular weight distribution (Cho et al., 1998a) and functional group chemistry (Tang et al., 2009). Functional group that controls the reaction between organics and other constituents present in source water contributes to membrane fouling. In natural water sources, the major chemical functional groups encountered in NOM are carboxylic acids, hydroxyls, phenolics, and carbonyl groups with carboxylic acid as the dominant functional group (Thurman, 1985).

Fourier Transform Infrared (FTIR) and Raman spectroscopy are non-invasive, *in-situ* vibrational spectroscopic techniques that can characterize the functional groups of molecules. FTIR has been used to characterize the membrane surface (Tang et al., 2009) and to examine functional groups of organic molecules adsorbed on the membrane surfaces (Her et al., 2000; Howe et al., 2002; Kimura et al., 2004; Rabiller-Baudry et al., 2002). However, this technique suffers from limited sensitivity and has a large sampling depth (> 100 nm) (Khulbe et al., 1996). Another disadvantage of FTIR spectroscopy isits inability to work with aqueous samples (e.g. FTIR shows overwhelming peak of water at 3000 cm^{-1}).

Raman spectroscopy, a complimentary method to infrared spectroscopy, is an alternative technique for molecular identification. In particular, Raman spectroscopy provides information about functional groups (e.g., –C-S-, -C-C, -N≡N-, -C=C-, –C-H) which are important in membrane technology (Khulbe et al., 1995). Raman spectroscopy has been used to examine changes in polymer structure in the membrane and to characterize membrane morphology that together help reveal the mechanism of mass transport in the membrane (Khulbe et al., 1995; Khulbe and Matsuura, 2000; Khulbe et al., 1997; Oust et al., 2006). Moreover, Raman spectroscopy has been used for characterizing bacterial strains (Oust et al., 2006). Raman techniques require no special sample preparation and produce cleaner, narrower spectra than infrared, making band interpretation more robust (Albrecht and Creighton, 1977). However, because of the inherently weak signals and interference from fluorescence, the technique has not gained significant attraction for identification of organic compounds. As an example, Khulbe et al. (1995) studied polyphenyleneoxide (PPO) and polyamide (PA) membranes using Raman scattering, but they could not observe Raman spectra of the PA membrane due to high background fluorescence.

SERS is an extension of Raman spectroscopy that allows both an enhanced Raman signal and substantial quenching of fluorescence through the use of coinage metal nanostructures (silver, gold, etc), thus offering highly specific molecular level identification of extremely small samples and samples capable of fluorescence (Albrecht and Creighton, 1977; Birke and Lombardi, 1988; Moscovits, 1985; Moskovits, 2006). It allows non-destructive characterization of organics. The theory of SERS is based on electronic and chemical interactions among the incident laser excitation, analyte of interest, and plasmonic properties of roughened/nanostructured metal surfaces (Moskovits, 2006). The magnitude of the SERS signal is distance dependent being the effect confined to the surface of the nanoparticles, and therefore, the target analyte has to be on or in very close proximity to the metal surface in order to experience an enhancement (Liu et al., 2006). The enhancement factor of the Raman signal for an analyte located in a “hot spot” on a metal substrate can be as much as 10^{14}-10^{15} because of combined electromagnetic, charge transfer, and resonance signal enhancement mechanisms (Qian and Nie, 2008). SERS has been used for quantification and identification of organic contaminants (Brosseau et al., 2009b; Brosseau et al., 2009a), inorganic contaminants (Baker and Moore, 2005; Bao et al., 2003), and pathogens (Rule and Vikesland, 2009; Sengupta et al., 2006) in environmental samples. Recently, Cui *et al.* (2011) examined the possibility of using SERS for the detection of fouling on polyvinlylidene fluoride (PVDF) membranes using modelled protein foulants.

This study used SEM to examine the nature and morphology of foulant materials and SERS and normal Raman to determine the identity of foulant materials. To our knowledge, this is the first study that used SERS to examine fouling caused by naturally occurring organic molecules on a polymeric NF membrane used for drinking water treatment. The efficiency of normal Raman spectroscopy (in the absence of nanoparticles) and SERS (by coating the membrane surface with silver nanoparticles) to characterize the membrane and membrane foulants was compared. The surface sensitive nature of SERS provides more precise information on foulants deposited directly onto the membrane surface. Two replicate analyses were carried out for bench scale virgin, fouled and cleaned NF membranes. Analysis of fouled and cleaned membranes using SERS was done in an effort to provide information on the nature of reversible and irreversible fouling caused by organic material. No attempt is made here to distinguish internal (inside pores) and external (attached onto surface) membrane fouling.

7.3 Materials and Methods

7.3.1 Membrane

The bench scale commercially available NF membrane (DK-NF) was purchased as a flat sheet from GE Osmonics, Minnetonka, CA. The DK-NF membrane is a thin-film negatively-charged composite membrane consisting of a proprietary active nanopolymer layer based on polypyperazinamide (Figure 7.1). It shows the chemical structure of the membrane material, which is important for assigning vibrational modes in the Raman and SERS spectrum. The active top layer of the membrane consists of three sub-layers with amine and carboxylate end groups (Ahmed et al., 2007). The detail characteristics of the membrane were provided in Table 5.3 of Chapter 5.

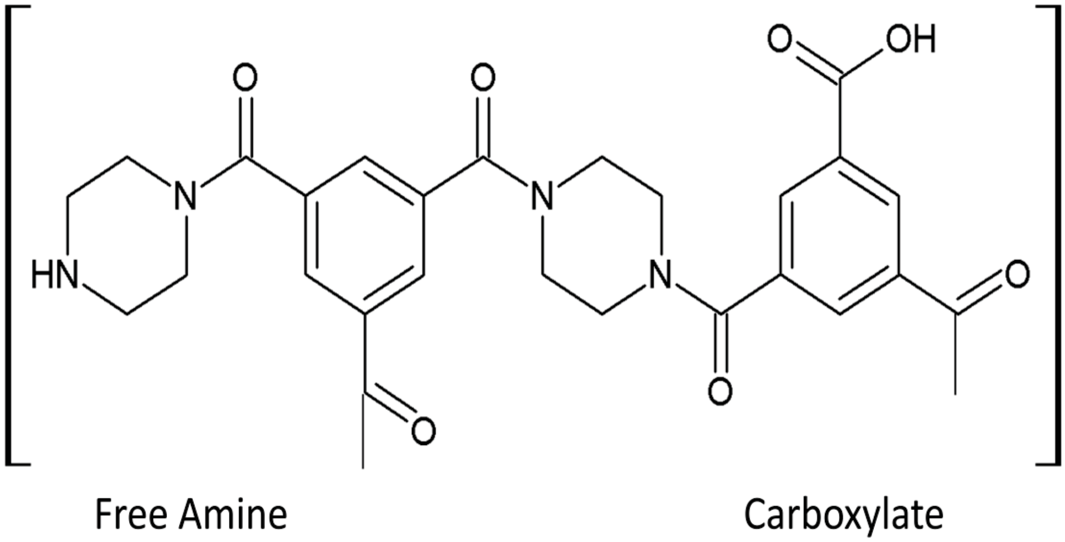

Figure 7.1 Typical Chemistry for Interfacially Formed Thin Film NF Membranes. The Active Nanopolymer Layer is based on Polypiperazinamide in DK-NF Membrane with Amine and Carboxylates End Groups (Al-Amoudi et al., 2007).

7.3.2 Preparation of Fouled and Cleaned Membranes

Surface waters from the French river, which provides drinking water for the northern shore communities of Nova Scotia, Canada, were filtered through DK-NF membranes and fouled membranes were examined by Raman spectroscopy. Filtration was done with 14.6 cm × 9.5 cm (~140 cm^2) membrane coupons using a bench scale cross-flow filtration unit (SEPA II, GE-Osmonics, Minnetonka, MN, USA). Before filtration with source water, membrane coupons were soaked with milli-Q water (>18.2 MΩ cm) for 24 hours and loaded into the unit and compacted overnight with milli-Q water. Feed water was pumped into the membrane cell unit with a Hydracell constant flow diaphragm pump (M03SASGSSSPA, Wanner Engineering, Inc., Minneapolis, MN) with a variable speed motor, and a variable frequency drive (ID15J101-ER, Blador Electric Co., Fort Smith, AR) with a flow rate of 800 mL/min (cross-flow velocity = 0.09 m/s). The membrane system was operated in recycle mode in which all of the concentrate is returned to the feed tank. To prevent an increase in water temperature resulting from the use of the diaphragm pump, the concentrate line was passed through a water refrigerated bath (Thermo Scientific NESLAB RTE Series, P/N U00694) before entering into the feed tank. The temperature in the feed tank was kept constant at ~24±2 °C by recirculation of concentrate water from water refrigerated bath to feed tank. Fouling experiments were conducted at constant pressure, declining permeate flux mode. In order to prepare the cleaned membrane (cleaned after fouling), the fouled membrane was flushed with mill-Q water in the bench scale NF filtration unit for 8 hours under the same conditions as that of fouling experiment. Fouled and cleaned membranes were put in a sterilized beaker and covered with aluminium foil before SEM and Raman spectroscopic analysis.

7.3.3 SEM Analysis

For SEM analysis, small pieces of virgin, fouled and hydraulically clean membranes were first coated with gold/palladium by utilizing a SC7620 Mini Sputter Coater under vacuum. The thickness of the coating layer was approximately 367 A^o. The coated membranes were analyzed in a Hitachi S-4700 field emission scanning electron microscope equipped with Oxford Inca x-sight EDS system. Six fields per sample were analyzed and the most representative images are presented.

7.3.4 Preparation of Citrate-Reduced Colloids

Silver nitrate (99+%) and sodium citrate were purchased from Sigma Aldrich (St. Louis, MO). Citrate-reduced silver colloids were prepared following the standard method (Lee and Meisel, 1982), having a peak absorption wavelength of ~420 nm and a full width at half-maximum (FWHM) of ~100 nm. The colloids prepared this way were stable at room temperature (stored in the dark) for up to 3 weeks. Figure 7.2 shows an SEM image of the silver colloidal nanoparticles (deposited on virgin DK-NF membrane) after centrifugation. The predominant shape for the colloidal nanoparticles prepared by this method was observed to be spherical (diameter ~ 40 to 60 nm), however, some nanorod formation was also observed.

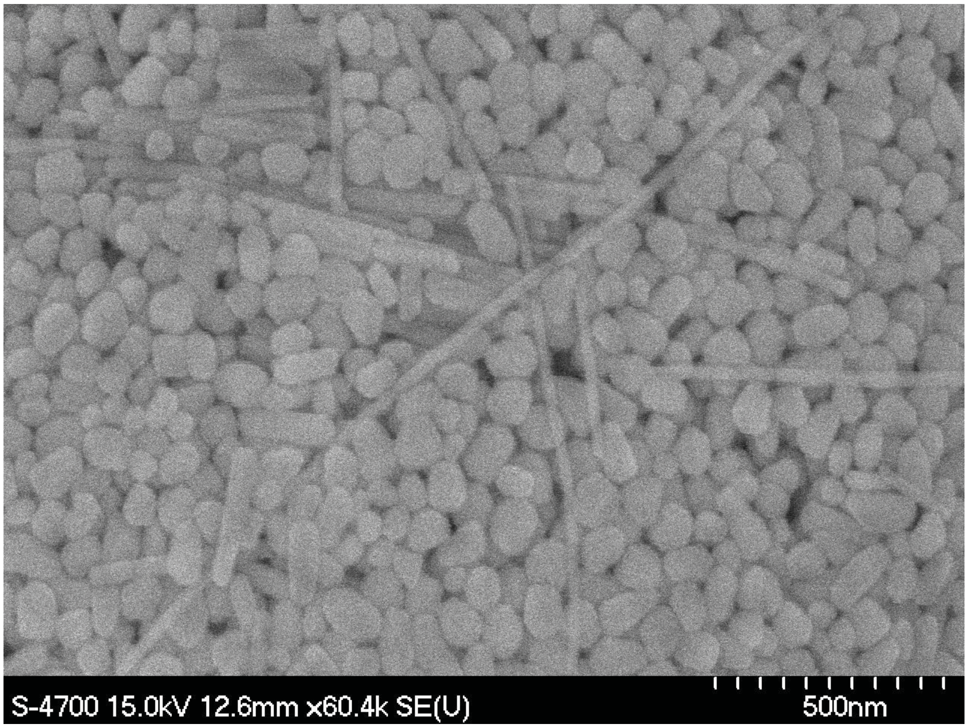

Figure 7.2 SEM Image of Citrate Reduced Silver Colloidal Nanoparticles Produced by the Lee and Meisel Method and Aggregated via Centrifugation. Image was Taken using 5 μL of Silver Nanoparticles Deposited on Virgin DK-NF Membrane.

7.3.5 Raman and SERS Analysis

All Raman and SER spectra were collected using a DeltaNu Advantage benchtop Raman spectrometer. The 785 nm excitation was obtained using a diode laser (55.9 mW at the sample), and detection of the scattered radiation was performed using an air-cooled CCD. Background correction was applied to all collected spectra using NuSpec software. For normal Raman spectroscopy measurements, a small piece of virgin, fouled and hydraulically cleaned membranes (~1 cm x 1 cm) was placed directly under the laser, and spectra were collected. For SERS analysis, 5 μL of citrate reduced colloids were added directly to the membrane coupon surface. SER spectra were recorded after the colloidal suspension had dried onto the membrane.

7.4 Results and Discussion

7.4.1 SEM Analysis

Figure 7.3 presents SEM images of three separate coupons of virgin, fouled, and hydraulically clean NF membranes.

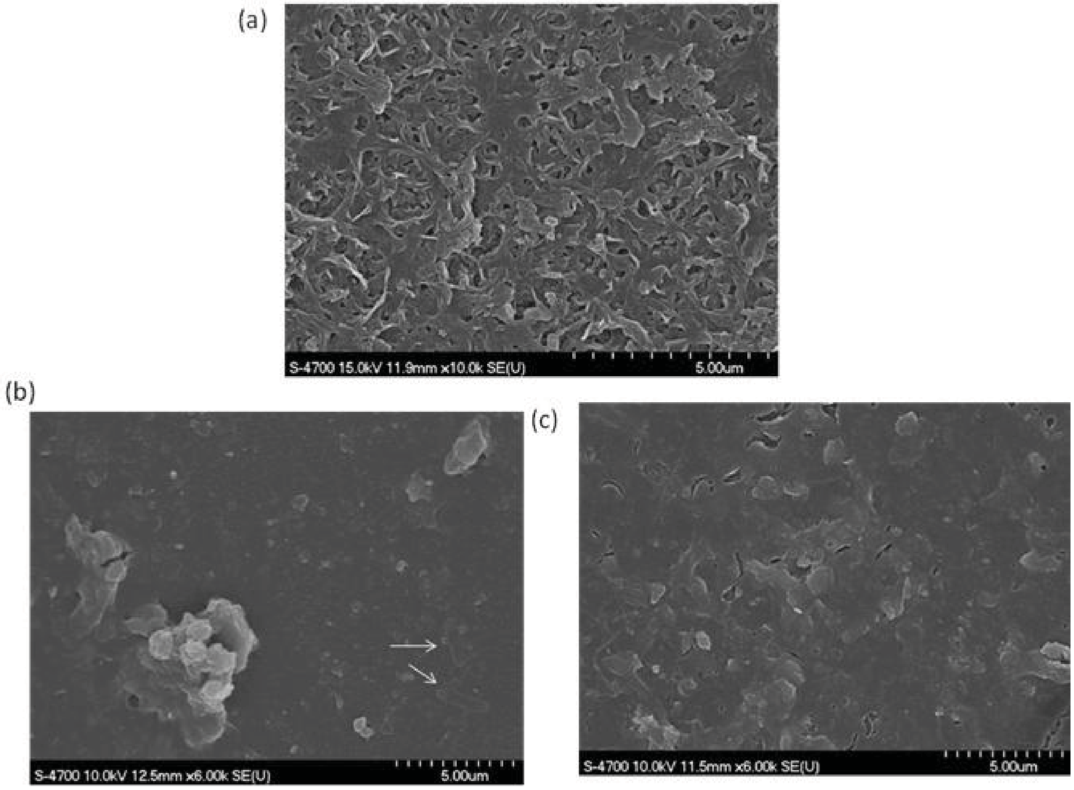

Figure 7.2 SEM Images of a (a) Virgin DK-NF Membrane, (b) Fouled Membrane with Raw, and (c) Fouled Membrane after Cleaning with Milli-Q Water. The Arrows in the Fouled Membrane Indicate the Presence of Bacterial Cells.

The virgin membrane exhibits the network-like structure typical of a membrane polyamide layer (Mukherjee et al., 1996). The SEM image of fouled membrane clearly shows the accumulation of a foulant layer onto the membrane surface. The visual observation of the SEM image indicates that surface adsorption may be the main mechanism for NF fouling (Li and Elimelech, 2004). The rod shaped structures in the fouled membrane indicate the presence of bacterial cells. The shape and surface morphology with minor colloids in the fouled membrane are indicative of organic and microbial fouling. The surface morphology in Figure 7.3c suggests that hydraulic cleaning of the membrane did not significantly remove foulant materials adsorbed onto the membrane surface thus indicating that most of the foulants adsorb irreversibly.

7.4.2 Normal Raman Analysis

Normal Raman spectra of virgin, fouled and cleaned membranes over the wavenumber range from 2000-200 cm^{-1} are presented in Figure 7.4. Major peaks are observed at 1607, 1587, 1149, 1110, 1075 and 792 cm^{-1} for all three membranes. The band at 1607 cm^{-1} is associated with aromatic amide groups (Socrates, 1994). This band was previously assigned to the aromatic in-plane ring stretching due to N-H deformation vibration and C=C ring stretching vibration in the phenyl ring (Ge et al., 1998; Khulbe et al., 1995). The peak at 1587 cm^{-1} is due to an aromatic in-plane ring bending vibration (Tang et al., 2009). The bands at 1149, 1110 and 1075 cm^{-1} are associated with C-N stretching vibrations of both the piperazine rings and the amide groups (Socrates, 1994). The band at 792 cm^{-1} is characteristic of the asymmetric C-N-C stretch of tertiary amides (Socrates, 1994). These results suggested that normal Raman spectroscopy is able to characterize the surface of polymeric NF membrane used in drinking water treatment. As mentioned previously, Khulbe *et al.* (1995, 1996) used normal Raman spectroscopy to characterize synthetic polyphenyleneoxide (PPO) and polyamide (PA) membranes but they were unable to observe the Raman spectra due to high fluorescence. Similarly, Ge *et al.* (1998) concluded that normal FT-Raman spectroscopy is not sensitive enough for analyzing thin-film polyamide samples, since they only observed spectra of thin films when silver colloids were deposited on the film surface.

As shown in Figure 7.4, all three membranes maintain the exact same peaks to the extent that they exhibit at least 0.99 correlations with each other. This indicates that the observed spectra are the representation of the polyamide membrane structure only, and do not reveal any information concerning the foulant layer, which is present on the surface at lower concentration. This lack of useful information concerning the surface foulant layer stems from the inherently poor sensitivity of normal Raman spectroscopy. Only bulk samples of the analyte of interest or reasonably concentrated solutions (>0.1M) can give sufficient signal/noise to generate useful Raman spectra.

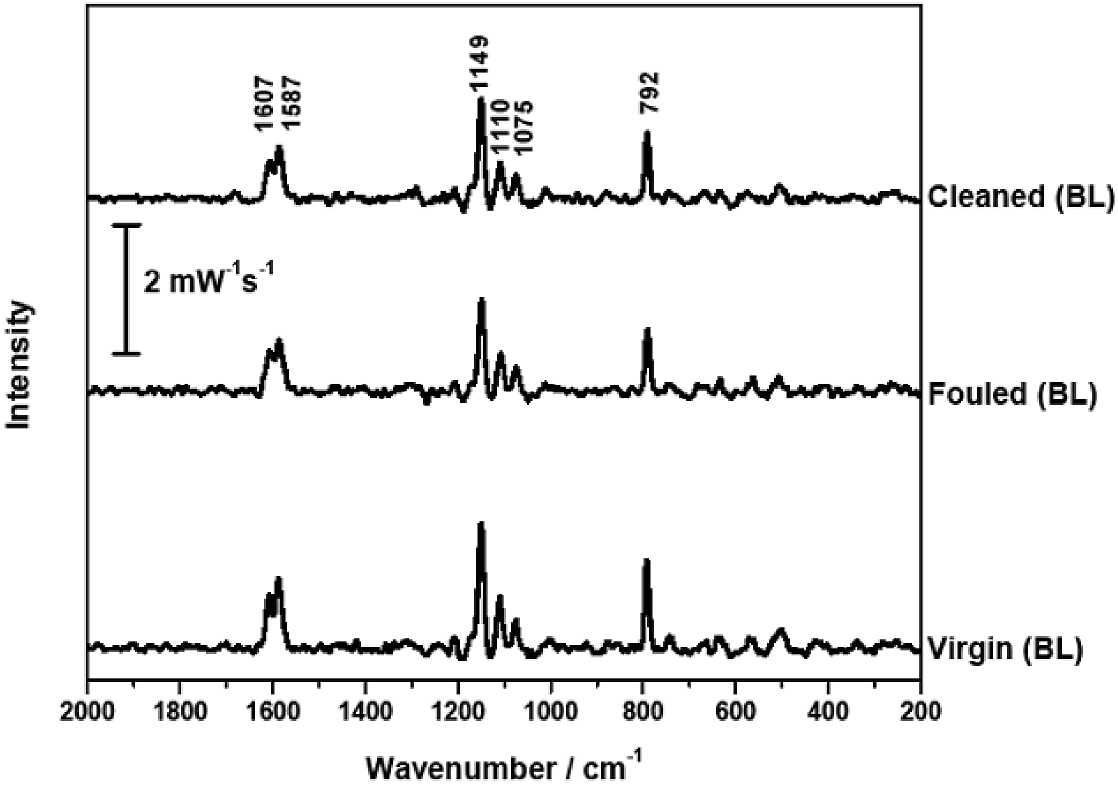

Figure 7.3 Normal Raman Spectra of Virgin, Fouled and Cleaned Membranes (Bottom to Top). Laser λex = 785 nm, Power at Sample = 5mW and Acquisition Time =30 s.

7.4.3 SERS Analysis

Figure 7.5 shows the SERS spectra of virgin, fouled and hydraulically cleaned membranes. The virgin membrane, compared to the normal Raman spectrum, exhibits a larger number of peaks, a result of a change of symmetry of the polymer species upon interaction with the silver surface. Some bands are the same as were observed in the normal Raman spectrum (peaks at 1587 cm^{-1} (weak), 1149 cm^{-1} (shoulder), 1112 cm^{-1} and 1073 cm^{-1} (both weak), as well as the band at 792 cm^{-1}. Some bands are new, however. For example, the amide I band for the poly(piperazinamide) is now present at

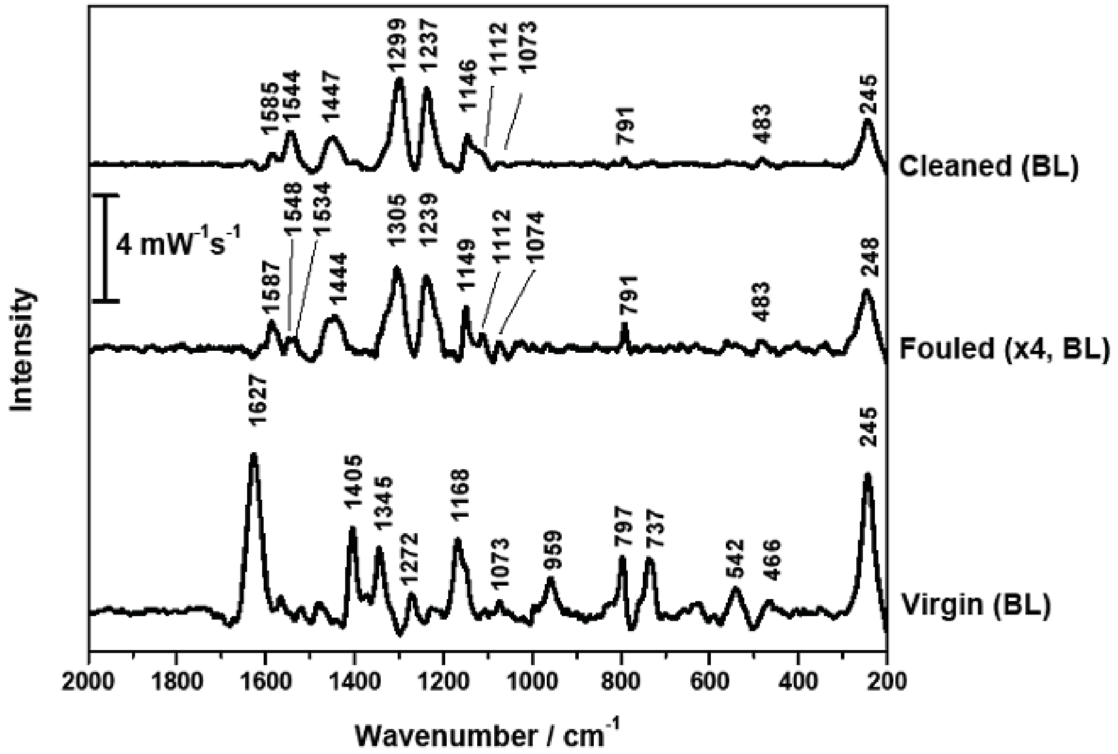

Figure 7.5 SERS Spectra of Virgin, Fouled and Cleaned Membranes (Bottom to Top).

1627 cm^{-1} (Tang et al., 2009). Comparing the virgin and fouled membranes, the only bands which appear to be due to the foulant layer and not the membrane are at ~1544, 1444, ~1300 and ~1237 cm^{-1}.

In the case of fouled and cleaned membranes the peak around 1544 cm^{-1} may be associated with N-H in plane bending and C-N-H stretching vibration of a –CO-NH-group (amide II band). Amide II vibrations are characteristic of proteinaceous substances present in NOM foulant layers (Campion and Kambhampati, 1998). The observed peak at 1444 cm^{-1} may be associated with C-H and O-H deformation vibrations, typical of carbohydrate bands, located from 1460-1200 cm^{-1}, and could also be due to a CH_2 deformation vibration (perhaps from cellulose). The peaks at ~1300 and ~1237 cm^{-1} correlate with those expected for carbohydrates due to C-H deformation and O-H vibration which occurs between 1460-1200 cm^{-1} (Campion and Kambhampati, 1998). The weak peak observed at 483 cm^{-1} in the case of fouled and cleaned membranes could possibly be due to DNA of microbial cells present in the foulant layer (Movasaghi, 2007).

7.5 Conclusion

This study employed surface enhanced Raman spectroscopy (SERS) for the first time to identify the functional groups of fouling causing organics on NF membrane used in drinking water treatment. Fouling detection efficiency of normal Raman spectroscopy was examined SEM was used for surface morphology characterization. A bench scale NF membrane fouling experiment was performed in a cross-flow unit using French River water, which is used for drinking water production in Nova Scotia, Canada. Small pieces of virgin and fouled membranes were analyzed using SEM, normal Raman spectroscopy and SERS. The fouled membrane was hydraulically cleaned to understand the nature of reversible and irreversible fouling caused by organics.

Surface morphology of SEM images of virgin and fouled membranes indicates the development of foulant on the membrane surface by natural organics and microorganisms. Normal Raman spectroscopy showed identical peaks for virgin, fouled and cleaned membranes indicating that only the polyamide membrane itself, not the foulant layer, could be characterized. When SERS was employed, the three membrane samples exhibited markedly different spectra, an indication that the foulant layer could now be monitored. The SERS band at 1544 cm^{-1} indicates the possible presence of proteinaceous substances and bands at 1444 cm^{-1}, 1305 cm^{-1}, and 1239 cm^{-1} suggest the presence of carbohydrate. In addition, the band at 483 cm^{-1} is indicative of nucleic acids. SERS has not been used here to identify the sources of these functional groups. This study suggests that SERS can be a useful technique for the characterization of fouling causing components in drinking water treatment, an understanding of which may eventually lead to more efficient and cost effective water treatment strategies.

CHAPTER 8 ADVANCED OXIDATION PROCESSES AS A PRETREATMENT FOR NANOFILTRATION MEMBRANE: EFFECT ON PERMEATE FLUX AND PERMEATE QUALITY

8.1 Abstract

This chapter investigated the application of H_2O_2/O_3, H_2O_2/UV, and O_3/UV AOPs as a pretreatment for NF membrane for treating surface water. The efficiency of each AOP for removing organic matter and changes in molecular weight distribution were evaluated in order to determine potential impacts to membrane permeate flux and quality. The nature and mechanism of organic fouling onto the membrane surface were examined by using different surface characterization techniques including SEM, AFM and SERS. All AOP pretreatment showed higher fouling reduction compared to UF pretreatment under the evaluated conditions. H_2O_2/UV pretreatment resulted in the highest NF permeate flux and permeated quality among the AOPs studied. This study revealed that the application of lower MWCO ($\leq$ 200 Da) NF membrane after AOP pretreatment would be better in order to balance mitigating fouling and improving permeate quality.

8.2 Introduction

Stringent regulations in the drinking water and wastewater industries have increased the demand for membrane filtration technology over conventional treatment processes due to the ability of this technology to remove broad ranges of organic and inorganic contaminants and pathogenic microorganisms. High pressure membranes such as NF and RO have shown superior removal of colour and odour causing organics and DBP precursors from the source water (Bond et al., 2010; Nilson and DiGiano, 1996; Siddiqui et al., 2000; Taylor et al., 1990). NF membranes, which operate at much lower pressures than RO systems, are predominant choice in water industries. The United States Environmental Protection Agency (USEPA) has included NF systems among the best available technologies (BAT) for compliance with Stage 1 and Stage 2 DBP precursors.

The key constraint to further application of NF membranes in drinking water and wastewater applications is membrane fouling. Membrane fouling is the accumulation or deposition of particles, inorganic and organic solids present in source waters on the membrane surface or within its pore which causes a reduction of finished water productivity, increase in TMP, and deteriorates finished water quality. Several strategies have been suggested to control and minimize membrane fouling. These include (i) selecting a membrane material that minimizes attractive interactions between foulants and membrane surface (Childress and Elimelech, 1996; Jucker and Clark, 1994; Lee et al., 2004), (ii) enhanced operating conditions that reduce fouling through more effective hydrodynamics (Chellam et al., 1997; Tang et al., 2007a), and (iii) chemical cleaning of membrane units (Li and Elimelech, 2004). However, foulant is continuous as long as it exists in membrane feed water. Therefore, pretreatment of source water is the best practice to improve membrane performance.

In drinking water treatment, the most common types of pretreatment before membrane filtration operations to reduce NOM include: oxidation (Brown et al., 2008; Kim et al., 2008), coagulation (Kim et al., 2007), and adsorption with powdered activated carbon (PAC) (Lee and Lee, 2007). Crozes et al. (1993) compared ozone and powdered activated carbon (PAC) adsorption pretreatment for UF membranes and observed that ozone was more effective than PAC adsorption in minimizing flux decline. Low pressure membranes (MF and UF) are the most common pretreatment technologies prior to NF and RO membranes for the removal of bacteria and large molecular weight organic compounds (Bonnèlye et al., 2008; Van der Bruggen et al., 2004). Removal of foulant material by the MF and UF membranes is dependent on MWCO of the membrane. MWCO is a measure of the removal characteristics of a membrane in terms of atomic weight or mass which is typically measured in terms of Daltons (USEPA, 2003). Membranes having lower MWCO can remove smaller molecular weight NOM present in water than membranes having higher MWCO. Previous studies have suggested that removal of DOM by low pressure membranes is limited due to the higher MWCO (Bonnèlye et al., 2008; Laine et al., 1990). However, DOM present in water has been shown to be a major foulant source for NF and RO membranes (Her et al., 2008a).

Among the various membrane fouling components in source water, NOM comprised of primarily humic substances, polysaccharides, and proteins have been shown to be the major components responsible for flux decline (K.L.Jones and O'Melia, 2000; Lin et al., 2000; Nilson and DiGiano, 1996; Speth et al., 1998). Several studies have shown that AOPs such as H_2O_2/UV (Goslan et al., 2006; Lamsal et al., 2011; Sarathy and Mohseni, 2007), H_2O_2/O_3 (Irabelli et al., 2008) and O_3/UV (Chin and Bérubé, 2005; Amirsardari and Williams, 2001) can remove significant amount of NOM including DOM and/or change humic or hydrophobic fractions of NOM into non-humic or hydrophilic fractions. Previous studies have shown that ozone pretreatment decreased the fouling rate of high pressure membranes due to the transformation of NOM components (Geluwe et al., 2011). AOPs which have shown higher removal rates of NOM than that of ozone treatment alone would be potentially a more effective membrane pretreatment choice to reduce fouling and maintain permeate flux by removing significant NOM from the feed water. Song et al. (2004) found that pretreatment of source water with H_2O_2/UV AOP was able to completely destroy synthetic organic chemicals (SOCs) and transform humic or hydrophobic substances into non-humic or less hydrophobic components and mitigate NF fouling. Pretreatment with TiO_2/UV for MF and UF membranes has been shown to be effective in controlling membrane fouling by changing MW distribution and SUVA of NOM due to preferential removal and transformation of large, hydrophobic NOM compounds (Huang et al., 2008). However, the effect of other AOPs (e.g. H_2O_2/O_3 and O_3/UV) as pretreatment for NF membranes has not yet been evaluated.

The objective of this research was to evaluate the impact of H_2O_2/UV, H_2O_2/O_3 and O_3/UV AOPs evaluated in Chapter 6 as a pretreatment on the permeate flux and quality of a polyamide NF membrane treating surface source water. In addition, the efficiency of the AOP pretreatments was compared with existing full-scale pretreatment approach (i.e. UF membrane) in terms of fouling reduction in the NF membrane. Full-scale UF permeate collected from the Tatamagouche WTP, was used for bench-scale NF fouling studies. Raw water was used during bench-scale NF and AOP+NF filtration experiments. HPSEC analysis was performed on the raw and preoxidized water samples in order to determine the effect of changes in MW distributions of NOM after AOP treatment on fouling reduction in the NF membrane. Different surface characterization techniques such as SEM, AFM, and SERS were also employed for virgin and fouled membranes with raw and peroxidized waters to provide insight into the mechanistic features associated with NF fouling due to NOM containing raw and AOPs pretreated waters.

8.3 Materials and Methods

8.3.1 Source Water Characterization

This bench-scale AOPs and NF filtration study was conducted with the raw water samples collected from the French River and UF permeate samples collected from the Tatamagouche WTP. Table 8.1 outlines the source water characteristics during these experiments.

Table 8.1 Raw and UF Permeate Water Characteristics from Tatamagouche WTP

Analyte	**Units**	**Raw Water**	**UF Permeate**
pH		6.9 ± 0.04	6.68 ± 0.04
UV_{254}	cm^{-1}	0.109 ± 0.007	0.092 ± 0.003
Turbidity	NTU	0.92 ± 0.5	0.51 ± 0.3
Colour	Pt-Co	28. ± 2.0	25.0 ± 1.0
Conductivity	µS/cm	79.8 ± 9.0	72.0 ± 3.4
TOC	mg/L	4.09 ± 0.035	
DOC	mg/L	3.45 ± 0.048	3.31 ± 0.095
SUVA	L/m.mg	3.16	2.78

8.3.2 Bench-Scale AOP Pretreatment

Bench-scale H_2O_2/O_3, H_2O_2/UV and O_3/UV experiments were conducted under the same conditions and methodologies as described in Chapter 6 in order to evaluate the effect of AOP pretreatments on NF membrane permeate flux and permeate quality. Raw water was first filtered through 0.45 µm pore size filter to remove colloids and particles. Dosages of H_2O_2, ozone and UV for those experiments are presented in Table 8.2, and reflect dosages that achieved the highest reduction of NOM as presented in Chapter 6.

Methodology for the preparation of AOP treated water as described in Chapter 6 was repeated in order to make a final volume of 15 L AOP treated water for the NF fouling

Table 8.2 Concentrations of H_2O_2, Ozone and UV Used in AOPs Pretreaments

AOPs	H_2O_2 Concentration	O_3Concentration and/or UV Dose	Residence Time (min)
H_2O_2/O_3	23 mg/L	4 mg/L	30
H_2O_2/UV	23 mg/L	1140 mJ/cm^2	15
O_3/UV		4 mg/L, 1140 mJ/cm^2	30

experiments. The residual H_2O_2 were quenched with 0.2 mg/L bovine liver catalase (Filtered aqueous solution, Code: CTR without thymol, $\geqslant$ 40,000 units per mg protein, Worthington, Biochemical Corporation) (Liu et al., 2003). Samples were taken after completion of each AOP treatment and analyzed for UV_{254}, TOC and MWD analysis.

8.3.3 NF Membrane and Operating Conditions

DK-NF (GE Osmonics, Minnetonka, CA) test sheet membranes were used in these experiments and characteristics of the membrane are presented in Table 5.3 in Chapter 5. The membrane was available in flat sheet pre-cut form (14.6 cm × 9.5 cm).

Raw, UF permeate and preoxidized waters were run through the bench-scale cross-flow NF filtration unit (SEPA II, GE-Osmonics, Minnetonka, MN, USA). Virgin test membrane sheets used in the experiments were soaked in milli-Q water for 24 hours prior to loading into the bench-scale NF module. The milli-Q water was refreshed four times during this membrane pre-soak procedure. The membrane test sheets were then pre-compacted with milli-Q water overnight in the test-unit prior to commencing the fouling experiments.

Feed water was pumped through the NF test unit at a flowrate of 800 mL/min (cross-flow velocity = 0.09 m/s) with a constant flow diaphragm pump (Hydracell, Wanner Engineering, Inc., Minneapolis, MN) equipped with variable speed motor and variable frequency drive (Baldor Electric Co., Forth Smith, AR). The bench-scale test unit was operated at constant pressure, variable flux mode, with a transmembrane pressure (TMP) of 72 psi maintained during the entire filtration cycle of each experiment. The temperature of the feed water was kept constant ($24 \pm 2^{o}C$) by passing concentrate line through a water refrigerated bath (Thermo Scientific NESLAB RTE Series, P/N U00694) before recycling into the feed tank. The experiments were performed in recycle mode with both the concentrate and permeate streams returned to the feed tank. The NF fouling experiments were conducted for four days (96 hours) for the raw, UF permeate and H_2O_2/O_3, H_2O_2/UV and O_3/UV AOP treated waters. NF fouling experiments were repeated two times for each trial to check for consistency of the experimental results.

8.3.4 Water Quality Analysis

Raw, UF permeate and the pretreated waters from the feed tank were taken before NF experiment to measure UV_{254}, TOC, DOC, conductivity and colour. Samples from feed, concentrate and permeate line were taken almost every two hours during 4 days of experiment to measure these parameters. The methods for measurement of the water quality parameters are described in Section 3.7 of Chapter 3.

8.3.5 Molecular Weight Distribution Analysis

HPSEC with UVA detector was used to determine the MW of NOM. Further details on the HPSEC analysis procedure used in this research is presented in Section 3.7 of Chapter 3.

8.3.6 Characterization of Membrane Surface and Foulant Layers

At the end of the fouling experiments (i.e. after 4 days), the membrane tests sheets were carefully removed from the SEPA-cell test unit and stored in a sterilized beaker and covered with aluminium foil in order to avoid potential contamination from air sources. Dry membrane coupons were cut into several pieces for SEM, AFM and SERS analysis.

SEM Analysis

SEM analysis was performed to characterize the surface morphologies of virgin and fouled membranes with different types of feed waters. The detail about SEM analysis is described in Section 5.4.4 of Chapter 5.

AFM Analysis

AFM analysis was performed to obtain three dimensional images and roughness of the membrane surfaces. AFM analysis was performed as described in Section 5.4.3 of Chapter 5.

Surface Enhanced Raman Spectroscopy Analysis

The SERS technique was used to investigate functional groups and molecular structures on the membrane surface and foulants. The detail about SERS analysis is provided in Section 7.3.5 of Chapter 7.

8.4 Results and Discussion

8.4.1 NOM Removal by AOPs

The average water quality parameters in H_2O_2/O_3, H_2O_2/UV, and O_3/UV pretreatment are presented in Table 8.3. H_2O_2/UV showed improved the greatest reduction of NOM as quantified by UV_{254} and DOC measurements compared to the H_2O_2/O_3 and O_3/UV treatment of the raw water. The UV_{254} measurements were reduced 46%, 67% and 61% in H_2O_2/O_3, H_2O_2/UV and O_3/UV, respectively. DOC was reduced after the H_2O_2/O_3, H_2O_2/UV and O_3/UV treatment by 26%, 30% and 28%, respectively. The relatively higher removal of UV_{254} compared to DOC can be explained by transformation of aromatic fractions into aliphatic fractions, without significant conversion of organic compounds to carbon dioxide.

Table 8.3 Average Water Quality Parameters of Raw and AOP Treated Water Samples

AOPs	**UV_{254} (cm^{-1})**	**Colour (Pt-Co)**	**TOC/DOC (mg/L)**
Raw	0.109 ± 0.0007	27.5 ± 2.3	4.09 ± 0.035
H_2O_2/O_3	0.059 ± 0.013	10.7 ± 1.2	3.04 ± 0.06
H_2O_2/UV	0.036 ± 0.005	11.0 ± 1.0	2.86 ± 0.14
O_3/UV	0.043 ± 0.009	9.7 ± 0.57	2.94 ± 0.12

8.4.2 Impact of AOPs on NOM MW

The raw and AOP treated waters were analyzed by HPSEC to evaluate the MWD of UV_{254} active DOC following AOP pretreatment. Since HPSEC analysis was performed with only UV detector, the identified MW ranges presented here are representative of only UV_{254} active DOC. Allpike et al (2005) and Ates et al. (2007) have suggested that although HPSEC analysis with UV detector does not provides a means of assessing the MWD of the total mass of DOC, it provides analysis of the relative removals of UV active DOC within identified MW ranges.

Figure 8.1 shows the elution pattern of the different organic fractions in the raw and AOP treated waters. Each peak was numbered for organic fraction identification and analysis. The elution times and MW of these fractions associated with Peaks 1 to 9 are provided in appendix D Table D. Nine general MW peaks in the raw water were found in i) 60,000 to 50,000 Da , ii) 2,000 to 1,900 Da, iii) 1208 Da, iv) 912 Da, v) 650 to 550 Da, vi) 404 Da, vii) 290 Da, and viii) < 250 Da. The compounds in the range of 60, 000 to 50,000 Da are biopolymers (protein); 2,000 to 912 are humic substances; 650 to 404 are building blocks (hydroxylates of humic acids), 404 to 290 Da are acids and less than 200 Da are low MW neutrals (amino acids, sugars, aldehydes and ketones) (Huber, 1998).

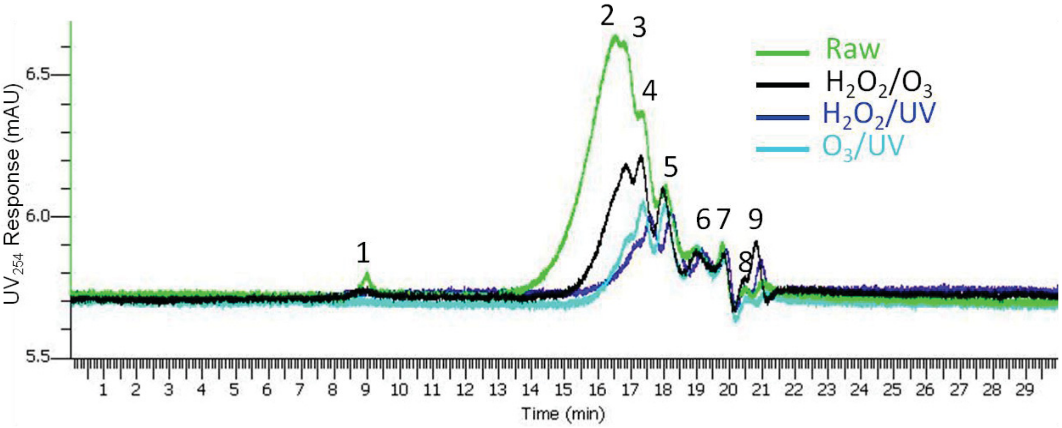

Figure 8.1 HPSEC Chromatogram of Raw and Oxidized Waters.

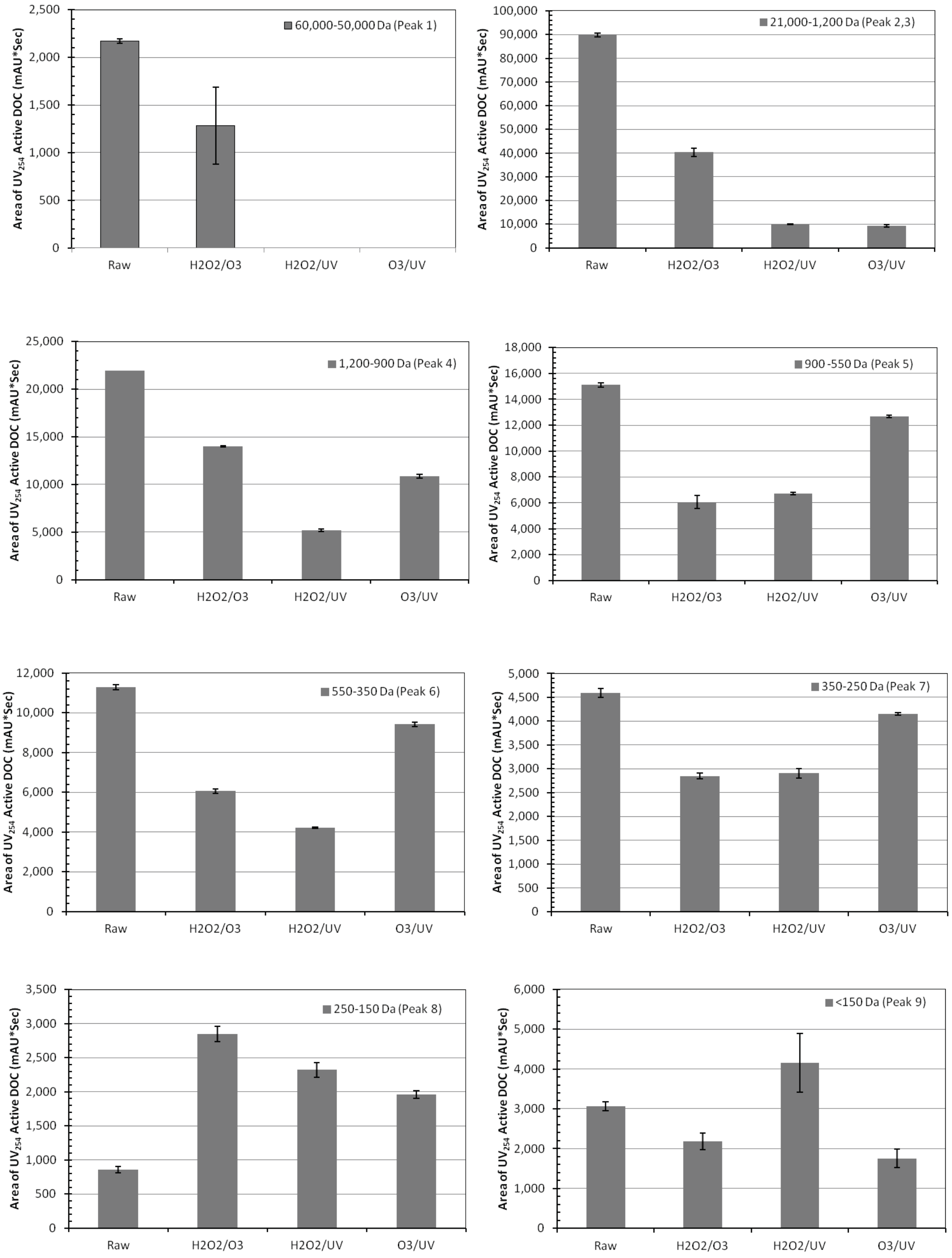

Figure 8.2 Area of UV_{254} Active DOC with Different MW for Evaluating Changes in MW of Organics during Different AOPs Pretreatment.

A relative comparison of the area of UV_{254} active DOC for each fraction was made to compare the performance of each AOP pretreatment evaluated in this study (Figure 8.2). The elution pattern of UV_{254} response versus retention times (Figure 8.1) and the relative comparisons of the area of UV_{254} active DOC (Figure 8.2) revealed that the reduction or oxidation of UV_{254} active DOC (aromatic DOC) was significantly different between these three AOPs pretreatment. In general, higher MW organics were removed or transformed into smaller MW organics after AOP pretreatment.

Organics fractions with MW 60,000 to 50,000 Da were removed completely with the H_2O_2/UV and O_3/UV pretreatment. H_2O_2/UV AOP showed the highest removal of UV_{254} active organic fractions with MW 60,000 to 900 Da followed by O_3/UV and H_2O_2/O_3. However, organic fractions with the MW 900 to 250 Da were reduced greatly by H_2O_2/O_3 compared to by O_3/UV AOP. All of the AOPs resulted in increased formation of lower MW organics (i.e. 250 to 100 Da) when compared to the raw water. Similar to the UV_{254} and TOC water quality analysis, MW distribution results suggested that H_2O_2/UV showed improved transformation of NOM compared to the other two AOPs evaluated. Although the H_2O_2/UV formed the lower MW organic fractions (25 to 100 Da) as other two AOPs, the formation of lower MW organics were minimal compared to the reduction of higher MW organics. Overall, the MWD analysis suggested that AOPs treatment transformed higher MW organic fractions into lower MW organic fractions which are consistent with the finding reported in previous studies (Sarathy and Mohseni, 2007; Thomson et al., 2004; Westerhoff et al., 1999). The reduction of the larger MW organic fraction was higher than that of the lower MW organic fractions. The preferential reduction of larger MW organic fractions, in comparison to lower MW organic fractions, could be a result of the higher reaction rate constant between HO• radicals and the larger MW organic fractions (Thomson et al., 2004).

8.4.3 NOM Removal by NF Membrane Alone

The feed, concentrate and permeate waters were analyzed during NF filtration tests with raw and AOP treated waters. NOM rejection by the NF membrane and permeate quality were investigated in terms of UV_{254}, colour, conductivity and TOC. The average reduction of these parameters is given in the Table 8.4. The average rejection of UV_{254}, colour and conductivity were found to be 99.8, 98 and 95% respectively with NF membrane alone. However, the TOC rejection of the NF membrane was comparatively lower (87%) than UV_{254}. These results suggest that NF membrane alone can remove almost all the humic or aromatic fraction of the NOM.

Table 8.4 Average Water Quality Parameters during NF Experiments

	Units	**Types of Waters**	**Raw**	**H_2O_2/UV**	**H_2O_2/O_3**	**O_3/UV**
Permeate flux	$Lm^{-2}hr^{-1}$		39.11	41.71	41.89	42.08
UV_{254}	cm^{-1}	Feed	0.114 ± 0.004	0.042 ± 0.006	0.069 ± 0.005	0.041 ± 0.004
		Permeate	0.0002	0	0	0
DOC	mg/L	Feed	3.72 ± 0.16	2.1 ± 0.19	3.05 ± 0.17	2.54 ± 0.31
		Permeate	0.48 ± 0.11	0.43 ± 0.04	0.88 ± 0.07	0.71 ± 0.17
Conductivity	µS/cm	Feed	78.37 ± 5.16	65.31 ± 17.39	73.14 ± 32.81	75.66 ± 33.49
		Permeate	4.14 ± 2.97	2.69 ± 1.25	2.69 ±1.08	2.92 ± 0.85
Colour	Pt-Co	Feed	24.23 ± 3.28	13.29 ± 4.14	13.8 ± 6.53	12.36 ± 6.35
		Permeate	0.59 ± 0.97	0	0	0

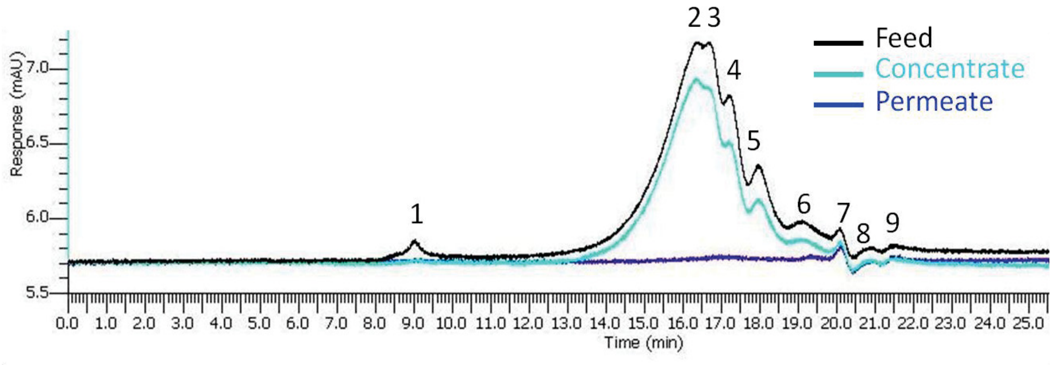

Figure 8.3 HPSEC Chromatograms of the Feed, Concentrate and Permeate Water after 2 hours of NF Filtration.

The HPSEC chromatogram of the feed, concentrate and permeate waters after 2 hours of NF filtration is shown in Figure 8.3. Different fractions in the chromatogram are numbered for average MW identification. The lower intensity of the concentrate water than that of the feed water and absence of higher MW organic fraction (Peak1) indicates that organic macromoleucles started collecting on the membrane surface. Organic fractions associated with Peaks 1 to 6 are removed by the NF membrane since those fractions were not observed in the NF permeate. The elution times and molecular weights associated with all peaks observed in Figure 8.3 are presented in Appendix D, Table D1.

The relative areas of each organics fractions and their average MW are presented in Figure 8.4. The number above the bars represents peaks shown in the Figure 8.3. The NF membrane was not able to remove the organics fractions with MW 290, 215 and 162 Da.

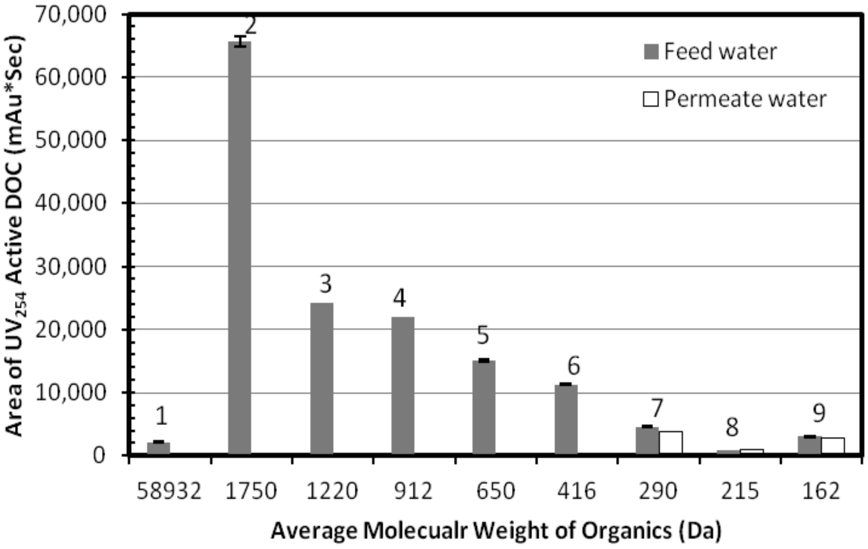

Figure 8.4 Area of UV_{254} Active DOC with Different MW of Organics in the Feed and Permeate Waters during NF Experiment.

This is due to the fact that MWCO of the test NF membrane (i.e. DK-NF) is 400 Da (Li et al., 2008), therefore, it rejects organic fractions larger than its MWCO.

8.4.4 Effect of AOPs on NF Membrane Permeate Flux

Figure 8.5 shows the permeate flux performance of the DK-NF test membranes over 96 hours fouling tests with raw and peroxidized waters.

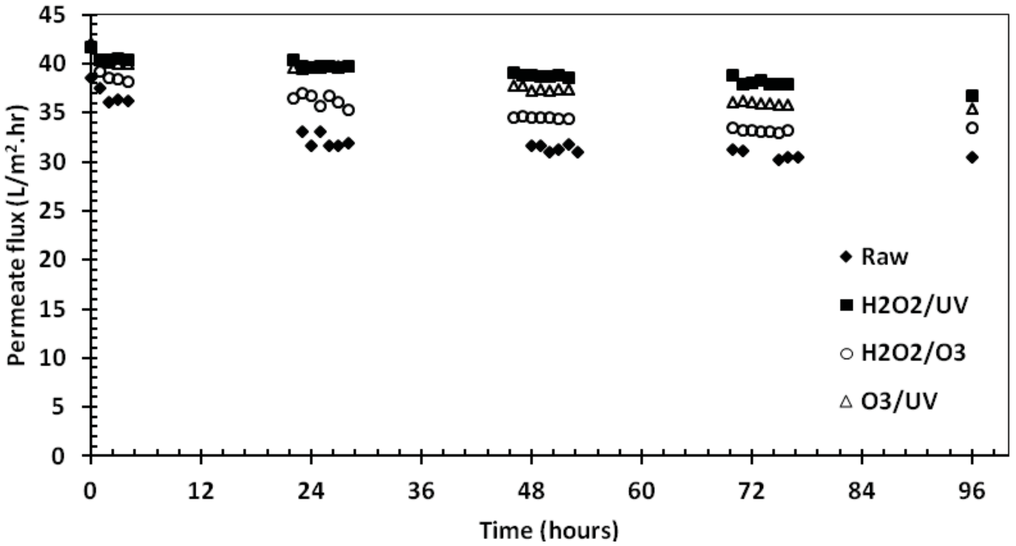

Figure 8.5 NF Permeate Fluxes for Raw and Oxidized Waters.

The preoxidized waters exhibited significantly lower flux declines than the raw water. Decrease in NOM molecular characteristics such as hydrophobicity or aromaticity, and molecular weight in the AOP treated water, as measured by UV_{254} values (Table 8.4) and molecular weights (Figures 8.1 and 8.2) are important reason for decrease in membrane fouling. This may be due to a decrease in adsorption of NOM by hydrophobic interactions. Aromatic and hydrophobic fractions of NOM have been shown to cause severe fouling in NF membranes compared to less aromatic or aliphatic or hydrophilic fractions of NOM (Nilson and DiGiano, 1996; Cho et al., 2000). Increases in carboxylic functional groups in oxidized waters have also been shown to result in great repulsion with negative membrane surface that results in less fouling on/into membrane surface (Van Geluwe et al., 2011). Van Geluwe et al. (2011) suggested that these repulsive forces have a comparable strength as the hydrogen bridges that carboxylic groups can form with the membrane surface. During oxidation, the phenolic groups are replaced by the quinodial groups in the aromatic moieties of the humic acids, therefore, quinodial groups can form hydrogen bond with water molecules instead of membrane (Song et al., 2004). The reduced fouling with preoxidized water may be also associated with a decrease in biofouling due to destruction of microorganism in preoxidation processes. Several studies have observed decrease in MF and UF membrane fouling with ozonated water due to changes in the NOM characteristics (Karnik et al., 2005b; Kim et al., 2008; Song et al., 2010). Kim et al. (2008) observed increase in permeate flux of ceramic UF membrane with ozone pretreatment and increase in permeate flux was proportional with ozone dose or availability of dissolved ozone. Huang et al. (2008) found decrease in UF membrane fouling with TiO_2/UV pretreatment.

Among the different AOP treated waters evaluated in this study, H_2O_2/UV preoxidation exhibited the highest permeate flux. Increases in the permeate flux of the NF membrane with the AOP treated waters followed the same trend with removal of DOC. H_2O_2/UV preoxidation resulted in the highest removal of DOC and the highest transformation of aromatic compounds into less aromatic compounds as measured by UV_{254} and MWD analysis (Table 8.2 and Figures 8.1 and 8.2).

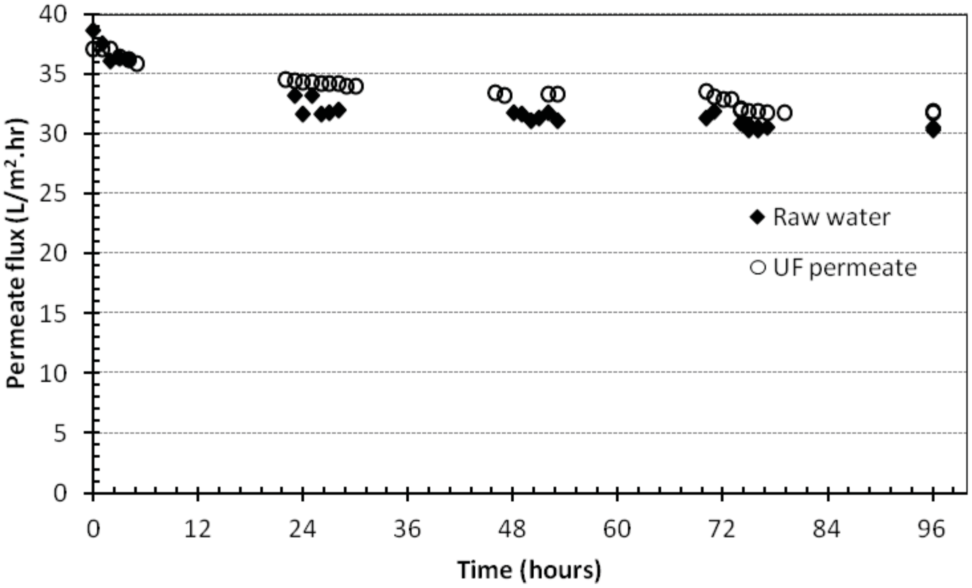

Figure 8.6 NF Permeate Fluxes with Raw and UF Permeate Feeds.

Figure 8.6 shows the permeate flux of the NF membrane with the raw and full-scale UF permeate water used as the NF feed. As described earlier, overall the raw water reduced permeate flux by 22% compared to initial flux.UF pretreatment was found to improve the NF permeate flux decline from 22% to 14%. This may be associated with the removal of particles and large size organic material (i.e., > 0.45 µm) achieved with UF pretreatement. As presented in Table 8.1, UF membrane basically removed particles. UV_{254} and DOC data of the raw and UF permeate water suggested that UF membrane removed limited organic compounds.

The UF permeate feed to the NF membrane did not improve the permeate flux of the NF membrane to the same level as the feed water that had been treated with the AOPs evaluated in this study. This is likely due to the higher removal of DOC (approximately 31%) in AOPs pretreatment compared to that achieved with the full-scale UF membrane where only 19% of DOC removal was observed. The transformation of higher MW organics into lower MW organics with AOP treatment is another important reason for the improved permeate flux of the NF membrane with preoxidized waters compared to that achieved with UF pretreated water.

8.4.5 Effect of AOPs on Permeate Quality

NOM Removal by Nanofiltration Membrane with AOPs Pretreatment

UV_{254} measurements taken during the NF filtration experiments with the raw and AOPs preoxidized waters are presented in Figure 8.7. The average values are presented in Table 8.4. UV_{254} values of the permeate waters are not included in Figure 8.7 since those values were zero most of the time during NF filtration experiments. This is due to almost complete reduction of humic or aromatic fraction of NOM in AOPs and NF membrane combined process. The removal of aromatic fraction of NOM is almost same with H_2O_2/UV and O_3/UV preoxidation.

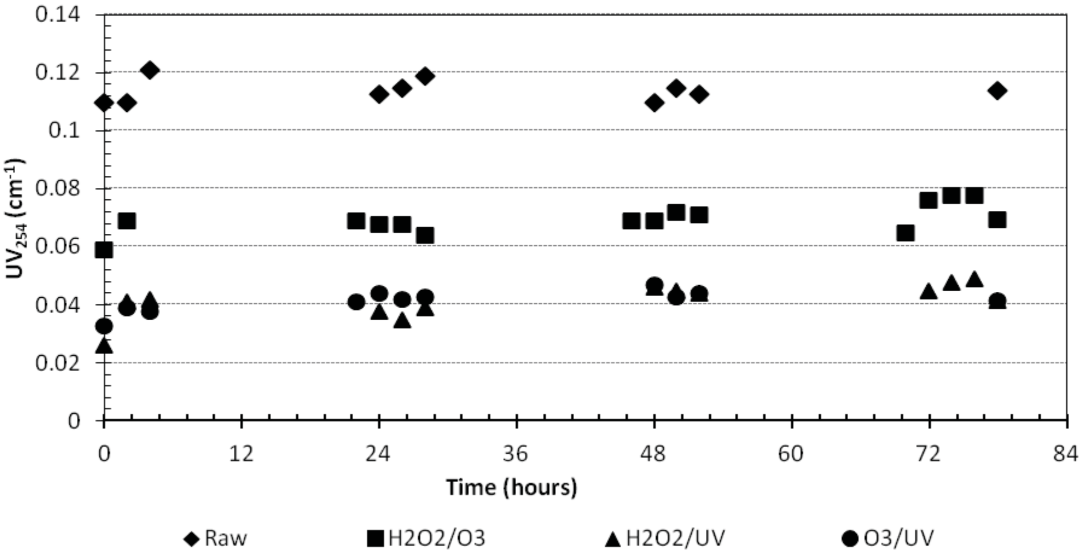

Figure 8.7 UV_{254} Measurments of Feedwaters during NF Fouling Experiments.

DOC measurements taken on both the feed and permeate water samples during the NF filtration experiments with the raw and AOPs preoxidized waters are presented in Figures 8.8. Overall, the DOC rejections with preoxidized waters feeds to the NF membrane were found to be lower than with the raw water feed through the 4-day fouling experiments. As previously presented, DOC rejection with the raw water was 87% whereas DOC removal after NF filtration with H_2O_2/O_3, H_2O_2/UV and O_3/UV oxidized water were 71%, 80% and 72% respectively. The lower DOC rejection with the preoxidized water is likely due to a decreased capability for membrane removal by size exclusion as a result of transformation of higher MW organics into lower MW organics (Figures 8.1 and 8.2). All of the AOP resulted in an increase in the organic fractions with MW ranges of 250 to 100 Da. Since these organic fractions have lower MW than MWCO of the NF membrane (i.e. 400 Da) used in this study, these organics would

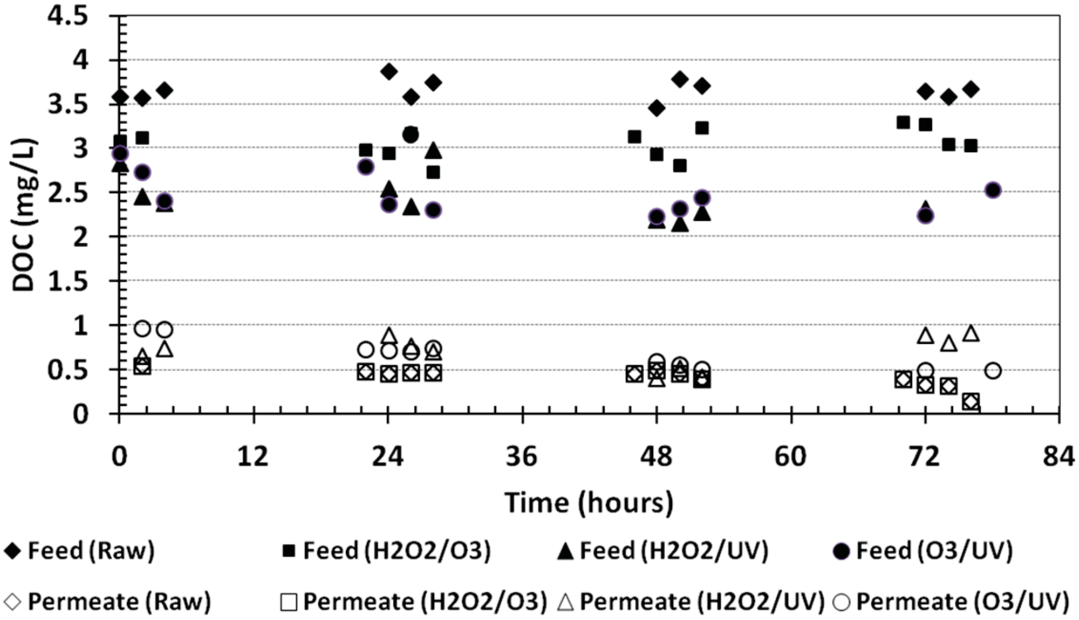

Figure 8.8 DOC Concentrations of Feed and Permeate Water in NF Filtration Experiment.

expected to be poorly rejected by the test membrane. Another possible reason for the reduced DOC removal capacity with the AOP treated waters could be related to a decrease in electrostatic exclusion as a result of preoxidation that results in a decrease in the negative charge of NOM. However, further study would be required to determine this. The higher NF permeate quality observed with H_2O_2/UV pretreatment compared to the H_2O_2/O_3 and O_3/UV pretreatments is likely associated to an increased reduction of the aromatic organics fractions measured by UV_{254} and MW and an increased reduction of both aromatic and aliphatic organics as measured by DOC. MWD analysis showed that H_2O_2/UV prexidation caused the lowest formation of lower MW organic fractions which is poorly rejected during subsequent NF membrane filtration.

Collectively, the permeate flux and permeate quality experimental results showed that the H_2O_2/UV AOP would be the better pretreatment process for the NF membrane under the treatment conditions considered in this study. Since AOP treatment results in the transformation of macromolecules into lower MW organics which may be poorly reject in subsequent membrane filtration, selection of proper AOP and the oxidation conditions are important before membrane filtration in order to balance membrane fouling reduction and NOM rejection. If AOPs pretreatment were followed by a membrane with a relatively higher MWCO, the oxidation could results in decreased cake formation and potential fouling mitigation due to transformation of macromolecules into smaller MW organics. However, permeate quality could deteriorate due to reduced rejection of these lower MW organics. Therefore, membranes with relatively lower MWCO would be effective in order to remove low molecular weight organics which are present in the source water and formed during AOPs pretreatment.

8.4.6 Characterization of Membrane Surface and Foulant Layers

A virgin membrane (as a control) and NF membrane test sheets after filtering raw and preoxidized waters were characterized by SEM, AFM and SERS analysis.

SEM Analysis

SEM analysis was performed for multiple samples (cut same membrane in 4 small pieces) of the same type of membrane. The representative samples were presented which had

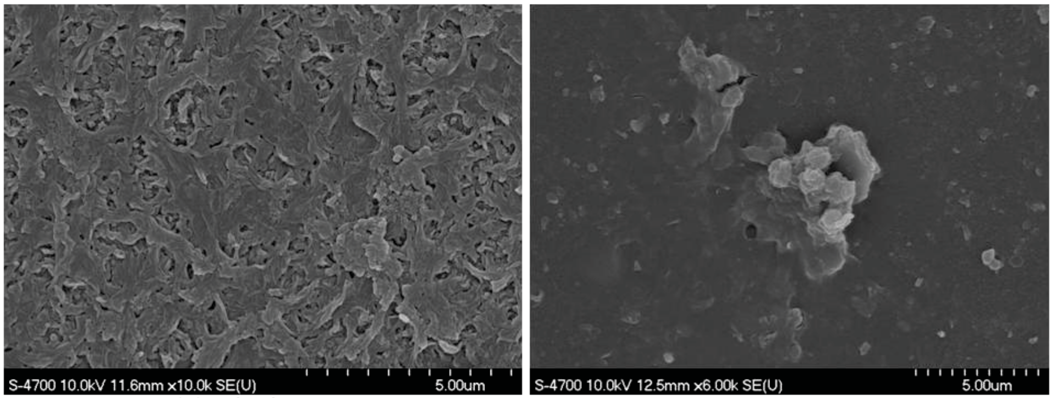

(a) Virgin (b) Fouled with Raw water

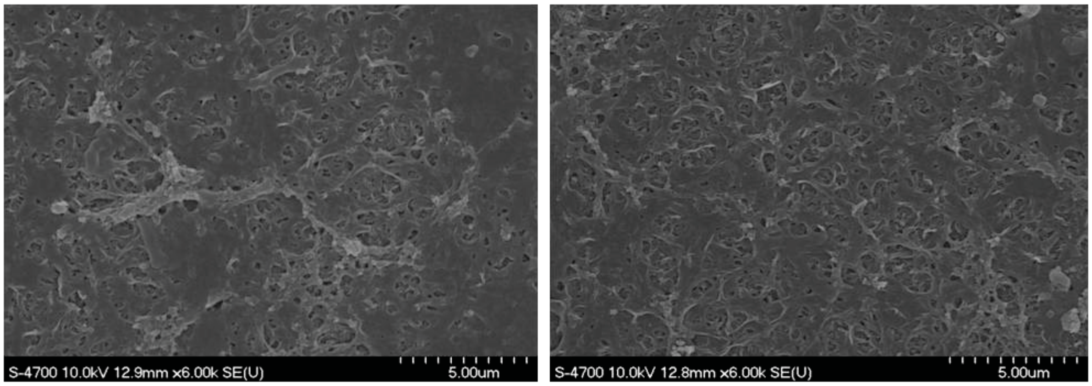

(c) H_2O_2/O_3 pretreated water (d) H_2O_2/UV pretreated water

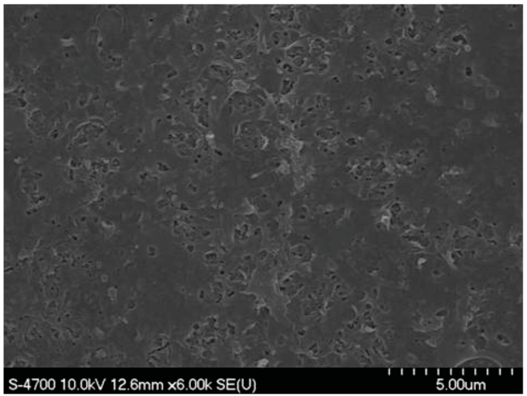

(e) O_3/UV pretreated water

Figure 8.9 SEM Images: (a) Virgin Membrane and Fouled Membranes after NF Filtration of (b) Raw Water, (c) H_2O_2/O_3 Preoxidized Water, (d) H_2O_2/UV Oxidized Water, and (e) O_3/UV Oxidized Water.

similar type of foulant nature after visual observation of SEM images. Figures 8.9 a-e present the SEM images of the virgin and fouled membranes with raw and preoxidized waters (H_2O_2/O_3, H_2O_2/UV and O_3/UV). The SEM micrograph of the virgin DK-NF membrane (Figure 8.9a) exhibits the network like structure typical of a polyamide barrier layer, showing ridge and valley network structure as described by Mukherjee et al. (1996). The SEM images of the fouled membranes with raw and oxidized waters exhibited different morphologies. The NF membrane surface with raw water used as the feed water was shown to be covered with foulants material. The visual observations obtained from a virgin membrane (Figure 8.9a) and a fouled membrane with the raw water (Figure 8.9b) suggested that surface adsorption was the dominant fouling mechanism (Li and Elimelech, 2004; Braghetta et al., 1998).

SEM images of the membranes fouled with preoxidized waters exhibited sparse and thin layers of foulants compared to the membrane fouled with raw water used as the feed water. This could be due to deposition of lower MW organics that were formed in preoxidation processes. There was also significant morphological difference observed among fouled membrane surfaces with different preoxidized waters.

AFM Analysis

The AFM images of the virgin and fouled membranes with different types of feed waters are presented in Figures 8.10 a-e. A significant difference was observed between the surface morphologies of the virgin and fouled membranes. These differences were

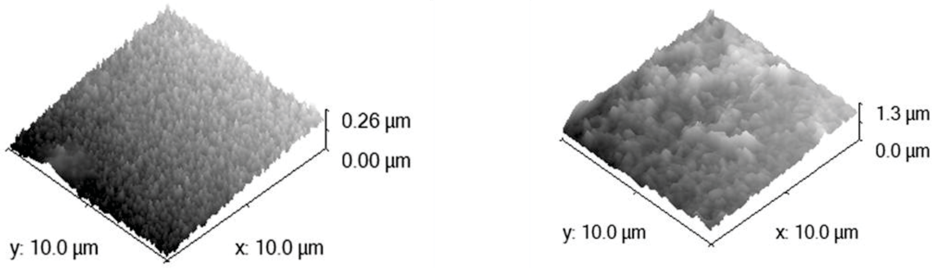

(a) Virgin (b) Fouled with Raw water

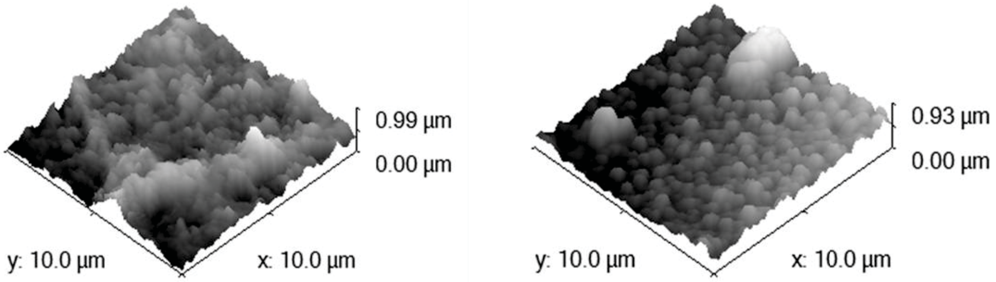

(c) H_2O_2/O_3 pretreated water (d) H_2O_2/UV pretreated water

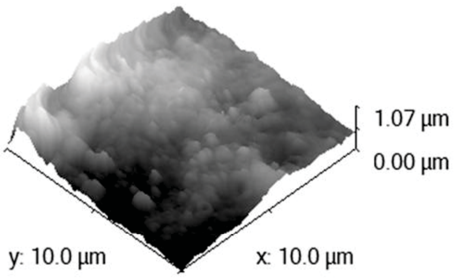

(e) O_3/UV pretreated water

Figure 8.10 AFM Images: (a) Virgin Membrane and Fouled Membranes after NF Filtration of (b) Raw Water, (c) H_2O_2/O_3 Preoxidized Water, (d) H_2O_2/UV Oxidized Water, and (e) O_3/UV Oxidized Water.

quantified by quantification of the average roughness parameter of the membrane surfaces (Khulbe et al., 1996, 2000) using Gwyddion software. The virgin membrane exhibited an average surface roughness of 46 nm (Figure 8.10a) which is significantly lower than the fouled membranes. The average roughness of the fouled membranes with the raw water used as the feed water (Figure 8.10b) was found to be 178 nm. The increase in roughness of the membrane surface compared to the virgin membrane surface was most likely due to adsorption of NOM macromolecules onto the membrane surface. Membranes fouled with H_2O_2/O_3, H_2O_2/UV, and O_3/UV prexidized waters had surface roughness 111, 127 and 158 nm respectively. These roughness values are higher than the average roughness values of the virgin membrane and lower than the roughness of the fouled membrane with the raw water.

SERS Analysis

Figures 8.11a and b show SERS spectra of the virgin NF membrane and the fouled membranes after filtration with the different types of the feed waters. SERS analyses were carried out two times in each sample and similar results were obtained in each case. The representative spectra are shown in Figure 8.11. The virgin membrane showed a typical band pattern of polyamide membrane. The principle bands consists of wave numbers associated with these characteristics: N-H and C-N stretching vibrations of amide group at 1627 cm^{-1}, C-H and O-H deformation vibrations at 1345 and 1272 cm^{-1}, NH_3 rocking vibration of free amino acid between 1295-1090 cm^{-1} or C-O stretch between 1200-1030 cm^{-1}. The spectrum at 1168 cm^{-1} was due to NH_3 rocking vibration of free amino acid. The spectra at 797 and 737 cm^{-1} are due to the C-H deformation vibration occurring in 960-730 cm^{-1}. Spectra at 1405 and 959 cm^{-1} are as a result of citrate.

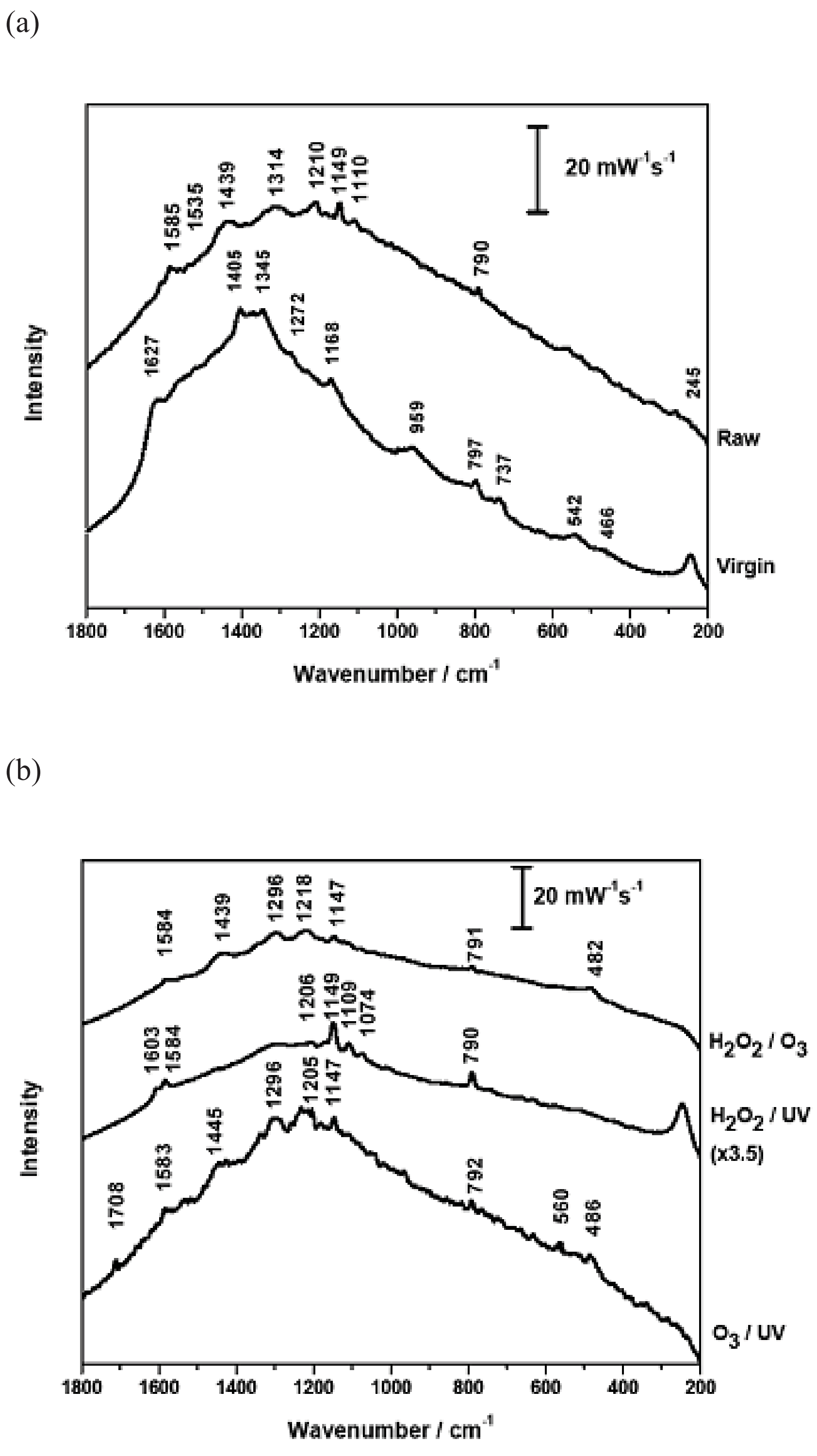

Figure 8.11 SERS Spectra a) Virgin and Fouled Membrane with Raw Water b) Fouled Membranes with H_2O_2/O_3, H_2O_2/UV, and O_3/UV Preoxidized Waters.

The spectra at 1585 cm^{-1} in all the fouled membranes indicated the presence of protein like substances (Kateinen et al., 2007). The peak at 1535 cm^{-1} is attributed to the amide vibration and indicates the presence of proteinaceous like substance in the fouled membrane with the raw water (Barber et al., 2001b). The SERS band at 1439 or 1445 cm^{-1} suggested the existence of carbohydrates and possible band assignment can be made due to C-H and O-H deformation vibration. These bands were not detected in the fouled membrane with H_2O_2/UV preoxidized water. This might be due to oxidation of this compound in H_2O_2/UV process. The SERS band at 1314 cm^{-1} was due to aromatic amine which occurs between 1380 -1260 cm^{-1}. This aromatic amine was oxidized during preoxidation processes therefore was not observed in the membrane fouled with preoxidized waters. These findings demonstrate that the fouling causing organics (proteins and carbohydrates) were transformed into organic material with less fouling potential in AOP prexidation. These results support the lower fouling potential with waters observed in Figure 8.5.

8.5 Conclusion

This study investigated the effects of three AOPs, namely H_2O_2/O_3, H_2O_2/UV, and O_3/UV on permeate flux and permeate quality during filtration with a NF membrane. Raw and UF permeate waters collected from the Tatamagouche WTP were used for experiments with a bench-scale cross flow NF membrane unit. HPSEC analysis was performed on raw and preoxidized waters to determine the changes in MW characteristics of NOM due to oxidation, and therefore their effect on membrane permeate flux and permeate qualities. In addition, membrane surface characterization techniques including SEM, AFM, and SERS were used to determine the fouling mechanism and major fouling causing organics in the source waters for virgin as well as fouled membranes.

Parameters including DOC, UV_{254}, and MWD showed that all preoxidized waters improved permeate flux of NF membrane by removing NOM and transforming hydrophobic fractions of NOM into hydrophilic fractions measured. All preoxidation processes showed higher permeate flux than the UF pretreatment. This is due to a higher reduction of DOC (up to 31%) and the transformation of organic compounds during preoxidation compared to UF pretreatment (19%). NOM rejection efficiency of the NF membrane was lower with preoxidized waters, likely due to transformation of higher MW organics into lower MW organics that resulted in a decrease in size exclusion.

Among the three AOP treatments evaluated in this study, H_2O_2/UV treatment showed the greatest increase in NF permeate flux and the highest permeate water quality. This is likely due to higher reduction of NOM, measured as DOC, UV_{254} and MWD. SEM analysis showed that the virgin membrane exhibited a ridge and valley network like structure. Membrane fouling caused by preoxidized waters created sparse and thin layers of foulants compared to membrane fouling due to raw water. SERS analysis demonstrated that proteins and carbohydrates were the major fouling causing organics of the surface water.

CHAPTER 9 SUMMARY AND CONCLUSIONS

9.1 Summary

The overall objective of this research was to characterize fouling of NF membranes used in drinking water treatment and to evaluate AOP pretreatment alternatives for reducing NF fouling with low alkalinity source water. A bench-scale membrane filtration system was utilized in the study and a series of bench-scale experiments were performed. In addition, a direct comparison of bench and full-scale data was conducted to examine the impact of source water quality on NF membrane fouling. Overall, the following research questions and tasks were addressed in these studies.

1) What is the composition of NOM in the source water of the Tatamagouche water treatment plant? Which NOM fractions are removed by the UF membrane?

   NOM fractions and their relationship with disinfection by-products formation in the IMS plant employing the UF and NF membranes was investigated in Chapter 4. Raw water and UF permeate were fractionated into six fractions: hydrophobic acid (HOA), base (HOB) and neutral (HON) and hydrophilic acid (HIA), base (HIB) and neutral (HIN). The THMFP and HAAFP of each NOM fraction were determined for both waters to understand which fraction of the NOM was responsible for THMFP and HAAFP.

2) What is the impact of source water quality on NF membrane fouling?

   To examine the impact of source water quality on NF membrane fouling, feed water properties and fouling behaviour of two IMS water treatment plants, Tatamagouche and Collins Park, were compared in Chapter 5. Bench-scale NF fouling experiments were conducted using a cross-flow membrane fouling unit for source waters from the two plants. To understand the characteristics and composition of foulant material present in the two source waters, membrane autopsies were conducted on virgin and fouled membranes using the SEM, AFM and SERS techniques. In addition, full-scale NF fouling data were analyzed for both plants in order to understand the actual fouling behaviour at the full-scale.

3) Which is the most effective AOP for removal of NOM and DBPs from the surface source water?

   In Chapter 6, ozone and UV oxidation and the H_2O_2/O_3, H_2O_2/UV, and O_3/UV AOPs experiments were conducted in bench-scale to study the impact of those processes in reducing NOM and DBPFP from low alkalinity surface source water. The treatment efficiency of each process was compared under optimum conditions in terms of UV_{254} and TOC reduction. The impact of AOP treatment on the MWD of NOM was examined using the HPSEC technique.

4) Can SERS be used as a novel technique to detect functional groups of foulant in natural source water?

Chapter 7 explored an alternative technique for a better characterization of membrane materials and fouling causing organics. SERS has been used for the first time to examine fouling on polymeric NF membrane by naturally occurring organics. Comparison of normal Raman spectroscopy versus SERS was made for the characterization of membrane materials and the foulant layers.

5) How do AOP pretreatments affect permeate flux and permeate quality of the NF membranes?

The fifth question is addressed in Chapter 8. The H_2O_2/O_3, H_2O_2/UV, and O_3/UV AOPs evaluated in Chapter 6 were examined as a pretreatment alternative for reducing downstream NF membrane fouling. The impacts of AOP pretreatment on the MWD of NOM and the effect on permeate flux and permeate quality of the NF membrane were evaluated. The efficiency of AOPs for removing NF fouling was compared with the existing UF pretreatment process. In addition, the nature and mechanisms of organic fouling onto the membrane surface were examined by using surface characterization techniques including SEM, AFM, and SERS.

9.2 Conclusions

NOM Characterization in IMS Plant

The characterization of NOM in source water is crucial for better understanding the removal efficiency of the treatment process for specific organic fractions. Organic fractionation results showed that the French River water is mostly comprised of the HIN (50%) and HOA (35%) fractions. The HOA fraction was found to be responsible for DBPFP, and most of this fraction was removed in the UF treatment. The effect of the HIN fraction on both THMFP and HAAFP was high in the UF permeate. Compared to other studies, the overall removal of DOC by the UF membrane was quite high at 66%, while only 20-30% reduction of DOC by UF membranes have been reported (Bonnèlye et al., 2008; Siddiqui et al., 2000). The MWD results also suggested a high removal of NOM with MW 1,700 to 60,000 Da despite the fact that the MWCO of the membrane is ~ 40,000 Da. The removal of NOM with MW lower than the MWCO of the UF membrane is likely due to the formation of foulant on the membrane that may have resulted in a reduction in the effective pore size of the membrane as observed in a previous study by Schäfer et al. (2000).

Comparison of NF Fouling Behaviour in Two IMS Plants

Identification of fouling causing components in an actual membrane filtration plant provides insights on the actual mechanisms of membrane fouling, improves operational strategies, and if necessary, identifies where updates are required in the treatment process.

Bench-scale NF fouling results showed that Collins Park source water caused higher fouling than the Tatamagouche source water. The increase in flux decline with the Collins Park source water was due to the higher concentration of DOC and ionic species and higher conductivity. Both source waters contained higher percentage of organics with MW less than 4,500 Da. Uniform formation conditions showed that the NF membrane was able to reduce THMFP and HAAFP by more than 90% for both source waters.

The full-scale NF fouling analyses suggested that the Collins Park NF membrane appears to have fouling, consistent with the bench-scale observations. Although the bench-scale analysis showed permeate flux decline with the Tatmagouche source water, the full-scale data indicated that there was in fact no real NF fouling during the study period. Both the bench- and full- scale NF fouling studies suggested that the Collins Park WTP had more NF fouling than the Tatamagouche WTP. These observations support the current practices of regular membrane cleaning almost every month in the Collins Park WTP. The NF membrane in Tatamagouche was cleaned only once after 2 years of operation. The higher values of all water quality parameters (DOC, SUVA, conductivity, concentration of ions, and the number of heterotrophic bacteria) suggested that water quality might be playing a major role for the higher NF fouling rate at the Collins Park WTP.

Oxidation and AOPs for NOM and DBPs Reduction

Determination of effective AOPs for the maximum reduction of NOM from low alkalinity source water would help the water utilities that are investigating the alternative advanced oxidation processes currently available. Among those available including the ozone, UV, H_2O_2/O_3, H_2O_2/UV and O_3/UV processes, the O_3/UV process showed higher reduction of NOM with 88% UV_{254} and 31% TOC reduction. The H_2O_2/UV process reduced UV_{254} by 60% and TOC by 23%, achieving somewhat lower reductions than the O_3/UV process. However, H_2O_2/UV process was found most effective for the reduction of THMFP and HAAFP. The MWD analysis indicated that high MW aromatic organic constituents were readily removed unlike lower MW organic constituents, and higher MW organic fractions were transformed into lower MW organic fractions in all AOPs. These results are consistent with the findings of other researchers (Huang et al., 2008; Sarathy and Mohseni, 2007; Wang et al., 2006). Overall, the O_3/UV and H_2O_2/UV processes are viable treatment options for the maximum reduction of NOM from low alkalinity drinking water sources.

SERS for Functional Group Identification of Fouling Causing Organics

A better characterization of membrane material and foulant layer would provide a better understanding of membrane fouling processes. SEM analysis of virgin and fouled membranes indicated a development of fouling onto the membrane surface mostly caused by natural organics and microorganisms. Analysis of virgin, fouled and cleaned membranes by normal Raman spectroscopy showed identical peaks indicating that only the polyamide membrane itself, not the foulant materials, could be characterized by normal Raman spectroscopy. The SERS analysis of virgin and fouled membrane exhibited markedly different spectra which indicate that the foulant layer could be monitored. The observed band at 1544 cm^{-1} in case of fouled and cleaned membranes indicated the presence of proteins like substances whereas the bands at 1444 cm^{-1}, 1305 cm^{-1}, and 1239 cm^{-1} suggested the presence of carbohydrates. The band at 483 cm^{-1} is indicative of nucleic acids.

The SERS peaks for fouled and cleaned membranes were almost identical indicating that hydraulic cleaning did not remove foulant materials observed in the SERS analysis. On the other hand, results also suggested that SERS is capable of detecting both reversible and irreversible membrane foulants. The work presented in Chapter 7 demonstrated that SERS can be a useful technique for the characterization of fouling causing components in water treatment.

AOPs Pretreatment to Control Fouling on NF Membrane

Integration of advanced oxidation processes with membrane filtrations can provide a multiple barrier water system by removing a broad range of chemicals and microorganisms. Bench-scale AOP pretreatments of source waters showed mitigation of NF membrane fouling by reducing NOM. The changes in NOM molecular characteristics and decreases in MW in preoxidized water lead to the decrease in membrane fouling with preoxidized waters. Among the three AOP treatments evaluated in this study, H_2O_2/UV resulted in an improved NF permeate flux and permeate water quality. This is due to higher reduction of TOC, UV_{254} and MWD by H_2O_2/UV as compared to the H_2O_2/O_3 and O_3/UV preoxidation processes. The SEM measurements showed that membranes fouled with preoxidized waters exhibited sparse and thin foulant layers as compared to membranes fouled with the raw water. Average roughness values measured by AFM were lower for the fouled membranes with preoxidized waters as compared to the fouled membrane with raw water. The SERS band observed at 1314 cm^{-1} due to aromatic amine in the membrane fouled with the raw water was not observed in the membrane fouled with the preoxidized waters. This finding suggests that the fouling causing organics, such as proteins and carbohydrates, were transformed into organic materials by AOP preoxidation and had less fouling potential.

Table 9.1 summarizes overall conclusion and outcome of the thesis. NOM fractionation analyses presented in chapter 4 suggested that hydrophilic neutral is the dominant fraction in the Tatamagouche source water. These observations were supported by identification of proteins and carbohydrates as major fouling causing organics by surface enhanced Raman spectroscopy discussed in chapter 7. Chapter 5 presented NF fouling studies performed at both bench- and full- scale levels with two surface source waters which suggested that water quality plays major role in the NF membrane fouling. Comparison of oxidation and advanced oxidation processes for NOM removal presented in chapter 6 suggested O_3/UV as the most effective process. However, difference in removal efficiency of the H_2O_2/UV and O_3/UV pretreatments (chapter 8) for organics is statistically insignificant. All pretreatment processes improved the permeate flux of the NF membrane but did not improve the permeate quality since higher molecular weight organics are converted to lower molecular weight organic by preoxidation processes.

Table 9.1 Overall Conclusions and Outcome of Thesis

Chapters	Aim/Scope	Main Findings	Overall Outcome
4	NOM characterization by resin fractionation	1) Hydrophilic neutral and hydrophobic acid comprised 50% and 35%, respectively of the NOM in the source water 2) UF membrane removed most of the hydrophobic acid fraction	Hydrophilic neutral organics were the dominant fraction in the surface source water
5	NF fouling studies	Collins Park source water caused more NF membrane fouling than the Tatamagouche source water	Water quality played important role in NF membrane fouling
6	Comparison of oxidation and advanced oxidation process for NOM removal	O_3/UV showed higher NOM removal than other oxidation processes	O_3/UV and H_2O_2/UV are viable AOPs for NOM and DBP precursor removal
7	Characterization of functional groups of fouling causing organics	Surface enhanced Raman spectroscopy can characterize the functional groups of	Proteins and carbohydrates were observed as major foulants in the surface

Chapters	Aim/Scope	Main Findings	Overall Outcome
		of fouling causing organics in the natural source water.	surface source water
8	AOP pretreatments for NF membrane process	The removal performance of NOM in H_2O_2/UV and O_3/UV preoxidation processes are statistically similar	All AOP pretreatments improved permeate flux of NF membrane but permeate qualities with preoxidized waters were lower than with the raw water.

CHAPTER 10 RECOMMENDATIONS

The research objectives completed in this dissertation has contributed to the body of knowledge regarding the application of advanced technologies in drinking water treatment. Further insights and recommendations are discussed in the following section.

Comparison among Oxidation and AOPs

Although the O_3/UV and H_2O_2/UV AOPs are presented in Chapter 6 as viable options for maximum reduction of NOM and DBPFP from low alkalinity, low turbidity drinking water source, measurement of HO• radicals yields, not considered in this work, could have provided more quantitative information for evaluating the effectiveness of the AOP treatments. *Para*-chlorobenzoic acid (*p*CBA) is a commonly used probe compound for the detection of HO• radicals in water. Preliminary experiments performed to compare HO• radical production in oxidation and AOPs using *p*CBA were promising, but have not been thoroughly evaluated. Future work in this area should consider measuring HO• radical yields in each AOP to aid in selecting the appropriate AOPs. In addition, any specific selection of AOPs should evaluate the chemical and energy costs.

Integration of MF/UF and AOP Pretreatment for NF/RO Membrane

The UF pretreatment process was effective for the NF fouling reduction in the Tatamagouche WTP whereas the UF membrane at the Collins Park WTP showed limited reduction of NOM where organic- and bio-fouling were found to be dominant NF fouling mechanisms from both bench- and full-scale studies. Therefore, evaluation of alternative pretreatment options that can reduce the organic load and inactivate (disinfect) microbial organisms in the NF feed stream is important to improve finished water quality and membrane sustainability.

The existing water treatment processes in the Collins Park WTP employs the UF+NF membrane and UV treatment is used as the primary disinfectant to ensure regulatory compliance with the provincial drinking water regulations. Chlorine is used as a final disinfectant. Future research should consider evaluating the UF+AOP pretreatment option for source waters with particles and high organic and microbial loads to reduce NF membrane fouling. The application of UF+AOP upstream of a NF or RO membrane (UF+AOP+NF/RO) could have three main benefits: 1) removal of particles and colloidal materials in UF pretreatment thereby reducing colloidal fouling in the NF system, 2) oxidation or reduction of organic load during the AOP treatment which will decrease organic fouling in the NF system, and 3) a high level of disinfection and therefore decrease in biofouling in the NF system by AOP. Such an integrated system may have higher capital and energy costs. However, the operational cost may be balanced by lower chemical cleaning of the NF unit and enhanced NF membrane life.

The combined AOP+NF experiments were performed under optimum AOP treatment conditions determined in this study. Such optimum conditions may not be necessary for a

AOPs+NF integration system since residual NOM would be removed by the NF membrane. Choosing the lowest possible concentrations of ozone and H_2O_2 and UV dose in each AOP may be beneficial from an energy consumption perspective and from potentially reducing cleaning and lifecycle costs of the NF/RO membranes. Therefore, future investigations should examine AOP pretreatments at lower oxidation conditions.

Measurements of assimilable organic carbon (AOC)/biodegradable organic carbon (BDOC) after AOP pretreatment and removal efficiency of AOC/BDOC by the NF/RO membrane provide insights into the implication of AOP+NF/RO integration processes on the water quality in distribution systems. Examination of other AOP pretreatment alternatives (e.g. TiO_2/UV) for performance and fouling mitigation of NF/RO membrane system is recommended.

REFERENCES

Aiken, G.R., McKnight, D.M., Thorn, K.A., Thurman, E.M., 1992. Isolation of hydrophilic organic acids from water using nonionic macroporous resins. Organic Geochemistry, 18(4): 567-573.

Al-Amoudi, A., William, P., Mandale, S., Lovitta, R.W., 2007. Cleaning results of new and fouled nanofiltration membrane characterized by zeta potential and permeability. Separation Science and Technology, 54: 234-240.

Albrecht, M.G., Creighton, J.A., 1977. Anomalously intense Raman spectra of pyridine at a silver electrode. Journal of American Chemical Society, 99: 3215-5217.

Allpike, B.P., Heitz, A., Joll, C.A., Kagi, R.I., 2005. Size exclusion chromatography to characterize DOC removal in drinking water treatment. Environmental Science and Technology, 39: 2334-2342.

Alvarez-Puebla, R.A., Santos, D.S.D., R.F. Aroca, Analyst, 132 (2007) 1210–1214., 2007. SERS detection of environmental pollutants in humic acid-gold nanoparticle composite materials. Analyst., 132: 1210-1214.

Amirsardari, Y., Yu, Q., Williams, P., 2001. Effect of ozonation and UV irradiation with direct filtration and disinfection byproduct precursors in drinking water treatment. Environmental Technology, 22: 1015-1023.

Amy, G., 1990. Removal of dissolved organic matter by nanofiltration. Journal of Environmental Engineering-ASCE, 116: 1046-1062.

Amy, G.L., Chadik, P.A., Chowdhury, Z.K., 1987a. Developing models for predicting trihalomethane formation potential and kinetics. Journal of American Water Works Association, 79: 89-97.

Amy, G.L., Collins, M.R., Kuo, C.J., King, P.H., 1987b. Comparing gel permeation chromatography and ultrafiltration for the molecular weight characterization of aquatic organic matter. Journal of American Water Works Association, 79(1): 43-49.

Ang, W.S., Elimelech, M., 2008. Fatty acid fouling of reverse osmosis membranes: Implications for wastewater reclamation. Water Research, 42(16): 4393-4403.

Anselme, C., Mandra, V., Baudin, I., Jacangelo, J.G., Mallevialle, J., 1993. Removal of total organic matters and micropollutants by membrane processes in drinking water treatment Water Supply, 11(3-4): 249-258.

APHA, A., WPCF, 1995. Standard methods for the examination of water and wastewater. 19th ed.

Ates, N., Kitis, M., U.Yetis, 2007. Formation of Chlorination Byproducts in Waters with Low SUVA – Correlations with SUVA and differential UV Spectroscopy. Water Research, 41(18): 4139-4148.

Ates, N., Yilmaz, L., Kitis, M., Yetis, U., 2009. Removal of disinfection by-product precursors by UF and NF membranes in low-SUVA waters. Journal of Membrane Science, 328(1-2): 104-112.

Backlund, P., 1994. Destruction of natural mutagen and trihalomethane precursors in water by ozonation, UV-irradiation, and photolytic ozonation. Environment International, 20(1): 113-120.

Baker, G.A., Moore, D.S., 2005. Progress in plasmonic engineering of surface-enhanced Raman-scattering substrates toward ultratrace analysis. Analytical and Bioanalytical Chemistry, 382: 1751-1770.

Baker, J.S., Dudley, L.Y., 1998. Biofouling in membrane systems –A review. Desalination, 118: 81-89.

Bao, L., Mahurin, S.M., Haire, R.G., Dai, S., 2003. Silver-doped sol-gel film as a surface-enhanced Raman scattering substrate for detection of uranyl and neptunyl ions. Analytical Chemistry, 75: 6614-6620.

Barber, L.B., Leenheer, J.A., Noyes, T.I., Stiles, E.A., 2001a. Nature and transformation of dissolved organic matter in treatment wetlands. Environmental Science and Technology, 35(24): 4805-4816.

Barber, L.B., Leenheer, J.A., Noyes, T.I., Stiles, E.A., 2001b. Nature and transformation of dissolved organic matter in treatment wetlands. Environmental Science and Technology, 35: 4805-4816.

Bellona, C. et al., 2008. Comparing nanofiltration and reverse osmosis for drinking water augmentation. Journal of American Water Works Association, 1000: 102-116.

Bellona, C., Marts, M., Drewes, J.E., 2010. The effect of organic membrane fouling on the properties and rejection characteristics of nanofiltration membranes Separation and Purification Technology, 74: 44-54.

Birke, R.L., Lombardi, J.R., 1988. Surface Enhanced Raman Scattering. In Spectroelectrochemistry: Theory and Practice, R. J., Ed.; Plenum: New York.

Bond, T., Goslan, E.H., Parsons, S.A., B.Jefferson, 2010. Disinfection by-products formation of natural organic matter surrogates and treatment by coagulation, MIEX and nanofiltration. Water Research, 44: 1645-1653.

Bond, T., Henriet, O., Goslan, E., Parsons, S.A., Jefferson, B., 2009. Disinfection By-Product Formation and Fractionation Behaviour of Natural Organic Matter Surrogates. Environmental Science and Technology, 43(15): 5982–5989.

Bonnèlye, V., Guey, L., Castillo, J.D., 2008. UF/MF as RO pretreatment: the real benefit. Desalination, 222: 59-65.

Boussu, K., Vadecasteele, C., Van der Bruggen, B., 2008. Relation between membrane characteristics and performance in nanofiltration Journal of Membrane Science, 310: 51-65.

Bowen, W.R., Doneva, T.A., 2000. Atomic force microscopy studies of membranes: effect of surface roughness on double-layer interactions and particle adhesion. Journal of Colloid Interficial Science, 229: 544-549.

Bowen, W.R., Mohammad, A.W., Hilal, N., 1997. Characterisation of nanofiltration membranes for predictive purposes — use of salts, uncharged solutes and atomic force microscopy. Journal of Membrane Science, 126(1): 91-105.

Braghetta, A., 1995. The influence of solution chemistry operating conditions on nanofiltration of charged and uncharged organic macromolecules. Ph.D Dissertation.University of North Carolina, Chapel Hill.

Braghetta, A., DiGiano, F.A., Ball, W.P., 1997. Nanofiltration of natural organic matter:pH and ionic strength effects. Journal of Environmental Engineering-ASCE, 123(7): 628-641.

Braghetta, A., DiGiano, F.A., Ball, W.P., 1998. NOM accumulation at NF membrane surface: impact of chemistry and shear. Journal of Environmental Engineering, 124(11): 1087-1098.

Brosseau, C.L. Gambardella, A., Casadio, F., Grzywacz, C.M., Wouthers, J., Van Duyne, R.P. 2009b. Ad-hoc Surface-Enhanced Raman Spectroscopy Methodologies for the Detection of Artist Dyestuffs: Thin Layer Chromatography-Surface Enhanced Raman Spectroscopy and in Situ on the Fiber Analysis,. Analytical Chemistry, 81: 3056-3062.

Brosseau, C.L., Rayner, K.S., Casadio, F., Grzywacz, C.M., Van Duyne, R.P., 2009a. Surface-Enhanced Raman Spectroscopy: A Direct Method to Identify Colorants in Various Artist Media. Analytical Chemistry, 81: 7443-7447.

Brown, S.L., Leonard, K.M., Messimer, S.L., 2008. Evaulation of ozone pretreatment on flux parameters of reverse osmosis for surface water treatment. Ozone Science and Engineering, 30: 152-164.

Cabaniss, S.E., Zhou, Q., Maurice, P.A., Chin, Y.-P., Aiken, G.R., 2000. A log-normal distribution of model for the molecular weight of aquatic fulvic acids. Environmental Science and Technology, 34: 1103-1109.

Calvo, J.I. et al., 1997. Bulk and surface characterization of composite UF membranes Atomic force microscopy, gas adsorption-desorption and liquid displacement techniques. Journal of Membrane Science, 128(1): 7-21.

Campion, A., Kambhampati, P., 1998. Surface-enhanced Raman scattering. Chem Soc Rev, 27: 241-250.

Carroll, T., King, S., S.R.Gray, Bolto, B.A., Booker, N.A., 2000. The fouling of microfiltration membranes by NOM after coagulation treatment. Water Research, 34: 2861-2868.

Chellam, S., Jancangelo, J.G., Bonacquisti, T.P., Schaur, B.A., 1997. Effect of pretreatmen on surface water nanofiltration. Journal of American Water Works Association, 89(10): 77-89.

Childress, A.E., Deshmukh, S.S., 1998. Effect of humic substances and anionic surfactants on the surface charge and performance of reverse osmosis membranes. Desalination, 118(1-3): 167-174.

Childress, A.E., Elimelech, M., 1996. Effect of solution chemistry on the surface charge of polymeric reverse osmosis and nanofiltration membranes. Journal of Membrane Science, 119(2): 253-268.

Chin, A., Bérubé, P.R., 2005. Removal of disinfection by-product precursors with ozone-UV advanced oxidation process. Water Research, 39(10): 2136-2144.

Chin, Y.P., Alken, G., Loughlln, E.O., 1994. Molecular weight, polydispersity, and spectroscopic properties of aquatic humic substances. Environmental Science and Technology, 28: 1853-1858.

Cho, J., Amy, G., Pellegrino, J., 1999. Membrane filtration of natural organic matter: initial comparison of rejection and flux decline characteristics with ultrafiltration and nanofiltration membranes. Water Research, 33(11): 2517-2526.

Cho, J., Amy, G., Pellegrino, J., 2000. Membrane filtration of natural organic matter: factors and mechanisms affecting rejection and flux decline with charged ultrafiltration (UF) membrane. Journal of Membrane Science, 164(1-2): 89-110.

Cho, J., Amy, G., Pellegrino, J., Yoon, Y., 1998a. Characterization of clean and natural organic matter (NOM) fouled NF and UF membranes, and foulants characterization. Desalination, 118: 101-108.

Cho, J., Pellegrino, G.A.J., Yoon, Y., 1998b. Characterization of clean and natural organic matter (NOM) fouled NF and UF membranes, and foulants characterization. Desalination, 118: 101-108.

Cho, J., Sohn, J., Choi, H., Kim, L.S., Amy, G., 2002. Effects of molecular weight cutoff, f/k ratio (a hydrodynamic condition), and hydrodynamic interactions on natural organic matter rejection and fouling in membranes. Journal of Water Supply: Research and Technology-AQUA, 51(2): 109-123.

Combe, C., Molis, E., Lucas, P., R., R., Clark, M., 1999. The effect of CA membrane properties on adsorptive fouling by humic acid. Journal of Membrane Science, 154: 73-87.

Conlon, W.J., MCClellan, S.A., 1989. Membrane softening: A treatment process comes of age. Journal of American Water Works Association, 81(11): 47-51.

Crittenden, J.C., Hu, S., Hand, D.W., Green, S.A., 1999. A kinetic model for H2O2/UV process in a completely mixed batch reactor. Water Research, 33: 2315-2328.

Croue, J.P., Korshin, G.V., M.Benjamin, 2000. Characterization of Natural Organic Matter in Drinking Water. AWWA Research Foundation and AWWA Association.

Crozes, G.F., Jacangelo, J.G., Anselme, C., Laine, J.M., 1997. Impact of ultrafiltration operating conditions on membrane irreversible fouling. Journal of Membrane Science, 124: 63-76.

Cui, L., Yao, M., Ren, B., Zhang, K.S., 2011. Sensitive and Versatile Detection of the Fouling Process and Fouling Propensity of Proteins on Polyvinylidene Fluoride Membranes via Surface-Enhanced Raman Spectroscopy. Analytical Chemistry, 83: 1709-1716.

Dickenson, E.R.V., Drewes, J.E., Sedlak, D.L., Wert, E.C., Snyder, S.A., 2009. Applying Surrogates and Indicators to Assess Removal Efficiency of Trace Organic Chemicals during Chemical Oxidation of Wastewaters. Environmental Science and Technology, 43(16): 6242-6247.

Dotson, A., Westerhoff, P., Krasner, S.W., 2009. Nitrogen enriched dissolved organic matter (DOM) isolates and their affinity to form emerging disinfection by products. Water Science and Technology, 60(1): 135-143.

Edwards E., et. al. 1988. THM control using membrane technology. In Proceedings, Joint FS/AWWA, FPCA, and FW&PCOA, Fort Lauderdale, FL.

Edwards, G.A., Amirtharajah, A., 1985. Removing color caused by humic acids. Journal of Ammerican Water Works Association, 77(3): 50-57.

Edwards, M., Benjamin, M.M., 1992. Transformation of NOM by ozone and its effect on iron and aluminum solubility. Journal of American Water Works Association, 84(6): 56-66.

Edzwald, J.K., Becker, W.C., Wattier, K.L., 1985. Surrogate parameters for monitoring organic matter and trihalomethane precursors. Journal of American Water Works Association, 4: 122.

Escobar, I.C., Hong, S., Randall, A.A., 2000. Removal of assimilable organic carbon and biodegradable dissolved organic carbon by reverse osmosis and nanofiltration membranes. Journal of Membrane Science, 175: 1-17.

Escobar, I.C., Randall, A.A., Hong, S.K., Taylor, J.S., 2002. Effect of solution chemistry on assimilable organic carbon removal by nanofiltration: full and bench scale evaulation. Journal of Water Supply: Research and Technology-AQUA, 51.2: 67-76.

Fan, L., Harris, J.L., Roddick, F.A., Booker, N.A., (2001). Water Res. 35(18), -. 2001. Influence of the characteristics of natural organic matter on the fouling of microfiltration membranes. Water Reserch, 35(18): 4455-4463.

Flemming, H.C., Schaule, G., Griebe, T., Schmitt, J., Tamachkiarowa, A., 1997. Biofouling –the Achilles heel of membrane processes. Desalination, 113: 215-225.

G.Crozes, C.Anselme, Mallevialle, J., 1993. Effect of adsorption of organic matter on fouling of ultrafiltration membranes. Journal of Membrane Science, 84(1-2): 61-77.

Gagnon, G.A. et al., 1997. CArboxylic acids: Formation and removal in full-scale plants. Journal of American Water Works Association, 89: 88-97.

Ge, J.J. et al., 1998. Surface studies of polyimide thin films via surface-enhanced Raman scattering and second harmonic generation. Macromol. Rapid Commun. , 19: 619-623.

Glaze, W., Peyton, G., Lin, S., Huang, R., Burieson, J., 1982. Destruction of pollutants in water with ozone in combination with ultraviolet radiation. 2. Natural trihalomethane precursors. Environmental Science and Technology, 16: 454-458.

Goslan, E.H., Gurses, F., Banks, J., S.A. Parsons . Chemosphere. 65(7), -. 2006. An investigation into reservoir NOM reduction by UV photolysis and advanced oxidation processes. Chemosphere, 65(7): 1113-1119.

Gwon, E.-m., Yu, M.-j., Oh, H.-k., Ylee, Y.-h., 2003. Fouling characteristics of NF and RO operated for removal of dissolved matter from groundwater. Water Research, 37(12): 2989-2997.

Harris, G.D., Adams, V.D., Sorensen, D.L., Curtis, M.S., 1987. Ultraviolet inactivation of selected bacteria and viruses with photoreactivation of the bacteria. Water Research, 21(6): 687-692.

Harrison, C.J., Gouellec, Y.A.L., Cheng, R.C., Childress, A.C., 2007. Bench-scale testing of nanofiltration for seawater desalination. Journal of Environmental Engineering, 133(11): 1004-1014.

Her, N., Amy, G., Chung, J., Yoon, J., Yoon, Y., 2008a. Characterizing dissolved organic matter and evaluating associated nanofiltration membrane fouling. Chemosphere, 70(3): 495-502.

Her, N., Amy, G., Chung, J., Yoon, J., Yoon, Y., 2008b. Characterizing dissolved organic matter and evaluating associated nanofiltration membrane fouling. 70: 495-502.

Her, N. et al., 2002. Optimization of method for detecting and characterizing NOM by HPLC-size exclusion chromatography with UV and on-line DOC detection. Environmental Science and Technology, 36: 1069-1076.

Her, N., Amy, G., Jarusutthirak, C., 2000. Seasonal variations of nanofiltration (NF) foulants: identification and control,. Proceedings of the Conference in Membranes in Drinking and Industrial Water Production, 2: 257-274.

Her, N., Amy, G., Park, H.-R., Song, M., 2004. Characterizing algogenic organic matter (AOM) and evaluating associated NF membrane fouling. Water Research, 38(6): 1427-1438.

Her, N., Amy, G., Plottu-Pecheux, A., Yoon, Y., 2007. Identification of nanofiltration membrane foulants. Water Research, 41(17): 3936-3947.

Hobbs, C., Hong, S., Taylor, J., , 2006. Effect of surface roughness on fouling of RO and NF membrane during filtration of a high organic surfical groundwater. Journal of Water Supply: Research and Technology-AQUA, 55(7-8): 559-570.

Hong, S., Elimelech, M., 1997a. Chemical and physical aspects of natural organic matter (NOM) fouling of nanofiltration membranes. Journal of Membrane Science, 132: 159-181.

Hong, S., Elimelech, M., 1997b. Chemical and physical aspects of natural organic matter (NOM) fouling of nanofiltration membranes. Journal of Membrane Science, 132: 159-181.

Howe, K.J., Ishida, K.P., Clark, M.K., 2002. Use of ATR/FTIR spectroscopy to study fouling of microfiltration membranes by natural waters. Desalination, 147: 251-255.

Huang, X., Leal, M., Li, Q., 2008. Degradation of natural organic matter by TiO2 photocatalytic oxidation and its effect on fouling of low-pressure membranes. Water Research, 42(4-5): 1142-1150.

Hwang, C. et al., 2001. Polar NOM:Characterzation, DBPs, Treatment. AWWA Research Foundation.

Jacangelo, J.G., Aieta, E.M., Carns, K.E., Cummings, E.W., Mallevialle, J., 1995. Assessing hollow-fiber ultrafiltration for particulate removal. Journal of American Water Works Association, 87(11): 68-75.

Jagger, J.H., 1967. Introduction to research in UV photobiology. Prentice-Hall. Inc. Englewood Cliffs, NJ, United States.

Jarusutthirak, C., Amy, G., 2006. Role of Soluble Microbial Products (SMP) in Membrane Fouling and Flux Decline. Environmental Science and Technology, 40: 969-974.

Jarusutthirak, C., Amy, G., Croué, J.-P., 2002. Fouling characteristics of wastewater effluent organic matter (EfOM) isolates on NF and UF membranes. Desalination, 145(1-3): 247-255.

Jarusutthirak, C., Mattaraj, S., Jiraratananon, R., 2007. Influence of inorganic scalants and natural organic matter on naofiltration membrane fouling. Journal of Membrane Science, 287: 138-145.

Jones, K.L., O'Melia, C.R., 2000. Protein and humic acid adsorption onto hydrophilic membrane surfaces: effects of pH and ionic strength. Journal of Membrane Science, 165(1): 31-46.

Jucker, C., Clark, M.M., 1994. Adsorption of aquatic hnmic substances on hydrophobic ultrafiltration membranes. Journal of Membrane Science, 97: 37-52.

K.L.Jones, O'Melia, C.R., 2000. Protein and humic acid adsorption onto hydrophilic membrane surfaces: effects of pH and ionic strength. Journal of Membrane Science, 165(1): 31-46.

Kaiya, Y., Itoh, Y., Fujita, K., Takizawa, S., 1996. Study on fouling materials in the membrane treatment process for potable water. Desalination, 106: 71-77.

Kanokkantapong, V., Panyapinyophol, B., Wattanachira, S., Marhaba, T.F., Pavasant, P., 2005. Characterization of natural organic matter fractionation for Bangkok water source. Thai Environmental Journal, 19: 17-27.

Karimi, A.A., Redman, J.A., Glaze, W.H., Stolarik, G.F., 1997. Evaluating an AOP for TCE and PCE removal. Journal of American Water Works Association, 89(8): 41-53.

Karnik, B.S., Davies, S.H., Baumann, M.J., Masten, S.J., 2005a. The effects of combined ozonation and filtration on disinfection by-product formation. Water Research, 39(13): 2839-2850.

Karnik, B.S. et al., 2005b. Effects of ozonation on the permeate flux of nanocrystalline ceramic membranes. Water Research, 39: 728-734.

Kateinen, E. et al., 2007. Qualification of the amphetamine content in seized street samples by Raman spectroscopy. Journal of Forensic Science, 52(1): 88-92.

Khulbe, K.C., Gagné, S., Mohammadi, A.T., Matsuura, T., Lamarche, A.-M., 1995. Investigation of polymer morphology of integral-asymmetric membranes by ESR and Raman spectroscopy and its comparison with homogeneous films. Journal of Membrane Science, 98: 1917-1935.

Khulbe, K.C. et al., 1996. Characterization of membranes prepared from PPO by Raman scattering and atomic force microscopy. Journal of Membrane Science, 111(1): 57-70.

Khulbe, K.C., Matsuura, T., 2000. Characterization of synthetic membranes by Raman spectroscopy, electron spin resonance, and atomic force microscopy; a review. Polymer, 41(5): 1917-1935.

Khulbe, K.C., Matsuura, T., Lamarche, G., Kim, H.J., 1997. The morphology characterisation and performance of dense PPO membranes for gas separation. Journal of Membrane Science, 135(2): 211-223.

Kim, J., Davies, S.H.R., Baumannb, M.J., Tarabara, V.V., Masten, S.J., 2008. Effect of ozone dosages and hydrodynamic conditions on the permeate flux in a hybrid ozonation-ceramic ultrafiltration system treating natural waters. Journal of Membrane Science, 311: 165-172.

Kimura, K., Hane, Y., Watanabe, Y., Amy, G., Ohkuma, N., 2004. Irreversible membrane fouling during ultrafiltration of surface water. Water Research, 38: 3431-3441.

Kleiser, G., Frimmel, F.H., 2000. Removal of precursors for disinfection by-products (DBPs)-differences between ozone- and OH-radical-induced oxidation Science of Total Environment, 256(1): 1-9.

Koch, B., Gramith, J.T., Dale, M.S., Ferguson, D.W., 1992. Control of 2-methylisoborneol and geosmin by ozone and peroxone: a pilot study. Water Sicence and Technology, 25(2): 291-298.

Komulainen, H., 2004. Experimental cancer studies of chlorinated by-products. Toxicology, 198: 239-248.

Kusakabe, K., Aso, S., Hayashi, J., Isomura, K., Morooka, S., 1990. Decomposition of humic acid and reduction of trihalomethane formation potential in water by ozone with UV irradiation. Water Research, 24: 781-785.

L.Chang, P.B., Young, T.M., 2000. Kinetics of methyl tert-butyl ether degradation and by-product formation during UV/hydrogen peroxide water treatment. Water Research, 34: 2233-2240.

Laine, J.M., Clark, M.M., Mallevialle, J., 1990. Ultrafiltration of lake water: effect of retreatment on partitioning of organics, THMFP and flux. Journal of American Water Works Association, 82: 12-82.

Lamsal, R., K.R., M., Kent, F.C., Walsh, M.E., Gagnon, G.A., 2012. Characterization and removal of natural organic matter by an integrated membrane system. Desalination, In press.

Lamsal, R., Walsh, M.E., Gagnon, G.A., 2011. Comparison of advanced oxidation processes for the removal of natural organic matter. Water Research, 45: 3263-3269.

Lee, N., Amy, G., Croué, J.-P., Buisson, H., 2004. Identification and understanding of fouling in low-pressure membrane (MF/UF) filtration by natural organic matter (NOM). Water Research, 38(20): 4511-4523.

Lee, P.C., Meisel, D., 1982. Adsorption and surface-enhanced Raman of dyes on silver and gold sols. Journal of Physical Chemistry, 86(17): 3391-3395.

Lee, S., Ang, W.S., Elimelech, M., 2006. Fouling of reverse osmosis membranes by hydrophilic organic matter: Implications for water reuse. Desalination, 187(1): 313-321.

Lee, S., Cho, J., Elimelech, M., 2005. Combined influence of natural organic matter (NOM) and colloidal particles on nanofiltration membrane fouling. Journal of Membrane Science, 262: 27-41.

Lee, S., Lee, C., 2006. Microfiltration and ultrafiltration as a pretreatment for nanofiltration of surface water. Separation Science and Technology, 41(1): 1-23.

Lee, S., Lee, C.H., 2007. Effect of membrane properties and pretreatment on flux and NOM rejection in surface water nanofiltration. Separation Science and Technology, 56: 1-8.

Leenheer, J.A., 1981. Comprehensive approach to preparative isolation and fractionation of dissolved organic carbon from natural waters and wastewaters. Environmental Science and Technology, 15: 578-587.

Leenheer, J.A., P.Croue, J., 2003. Characterizing dissolved aquatic organic matter. Environmental Science and Technology, 37: 18A-26A.

Li, Q., Elimelech, M., 2004. Organic fouling and chemical cleaning of nanofiltration membranes: measurements and mechanisms. Environmental Science and Technology, 38: 4683-4693.

Li, Q., Xub, Z., Pinnau, I., 2007. Fouling of reverse osmosis membranes by biopolymers in wastewater secondary effulent role of membrane surface properties and inital permeate flux. Journal of Membrane Science, 290: 173-181.

Li, Y., Shahbazi, A., Williams, K., Wan, C., 2008. Separate and concentrate Lactic acid using combination of nanofiltration and reverse osmosis membranes. Applied Biochemistry and Biotechnology, 147: 1-9.

Liang, L., Singer, P.C., 2003. Factors Influencing Formation and Relative Distribution of Haloacetic Acids and Trihalomethanes in Drinking Water. Environmental Science and Technology, 37(13): 2920-2928.

Lin, C.F., Lin, T.Y., Hao, O.J., 2000. Effects of humic substances characteristics on UF performance. Water Research, 34(4): 1097-1106.

Lin, H.C., Wang, G.S., 2011. Effects of UV/H2O2 on NOM fractionation and corresponding DBP formation. Desalination, 270(1-3): 221-226.

Liu, F.M., Köllensperger, P.A., Green, M., Cass, A.E.G., Cohen, L.F., 2006. A note on distance dependence in surface enhanced Raman spectroscopy. Chemical Physics Letters, 430: 173-176.

Liu, S. et al., 2010. Comparison of photocatalytic degradation of natural organic matter in two Australian surface waters using multiple analytical techniques. Organic Geochemistry, 41: 124–129.

Liu, W. et al., 2002. Bench- scale investigations into comparative evaluation of DBP formation from different UV/H_2O_2 technologies. Proceedings, AWWA Water Quality Technology Conference. Seattle, WA.

Liu, W., Andrews, S.A., Stefan, M.I., Bolton, J.R., 2003. Optimal methods for quenching H_2O_2 residuals prior to UFC testing. Water Research, 37(15): 3697-3703.

Makdissy, G. et al., 2010. Investigating the fouling layer of polyamide nanofiltration membranes treating two different natural waters: internal heterogeneity yet converging surface properties. Journal of Water Supply: Research and Technology—AQUA 59(2-3): 164-178.

Mänttäri, M., Puro, L., Nuortila-Jokinen, J., Nyström, M., 2000. Fouling effects of polysaccharides and humic acid in nanofiltration. Journal of Membrane Science, 165: 1-17.

Marhaba, T.F., Pu, Y., Bengrain, K., 2003a. Modified dissolved organic matter fractionation technique for natural water. Journal of Hazardous Materials, B101: 43-53.

Marhaba, T.F., Pu, Y., Bengraine, K., 2003b. Modified dissolved organic matter fractionation technique for natural water. Journal of Hazardous Materials, 100(1-3): 179-195.

Marhaba, T.F., Van, D., 2000. The variation of mass and disinfection by-product formation potential of dissolved organic matter fractions along a conventional surface water treatment plant. Journal of Hazardous Materials, A74: 133-147.

Matilainen, A. et al., 2011. An overview of the methods used in the characterization of natural organic matter (NOM) in relation to drinking water treatment Chemosphere, 83: 1431-1442.

Matilainenm, A., Sillanpää, M., 2010. Removal of natural organic matter from drinking water by advanced oxidation processes. Chemosphere, 80(4): 351-365.

Moscovits, M., 1985. Surface-enhanced spectroscopy. Rev. Mod. Phys., 57: 783-826.

Moskovits, M., 2006. Surface-enhanced Raman spectroscopy: A brief perspective. In Surface-Enhanced Raman Scattering, Kneipp, K.; Moskovits, M.; Kneipp, H., Eds.; Springer: Berlin, Germany. 1-17.

Mosqueda-Jimenez, D.B., Huck, P.M., 2006. Characterization of membrane foulants in drinking water treatment. Desalination, 198: 173-182.

Mosteo, R., Miguel, N., Martin-Muniesa, S., Ormad, M.P., Ovelleiro, J.L., 2009. Evaluation of trihalomethane formation potential in function of oxidation processes used during the drinking water production process. Journal of Hazardous Materials 172(2-3): 661-666.

Movasaghi, Z., 2007. Raman spectroscopy of biological tissues. Applied Spectroscopy Reviews, 42: 493-541.

Mukherjee, D., Kulkarni, A., Gill, W., 1996. Chemical treatment for improved performance of reverse osmosis membranes. Desalination, 104(3): 239-249.

MWH, 2005. Water Treatment: Principles and Design, 2nd Edition, Crittenden, J.C., Trussell, R.R., Hand, D.W., Howe, K.J. and Tchobanoglous, G. eds, Wiley, New Jersey, USA.

Nilson, J.A., DiGiano, F.A., 1996. Influence of NOM composition on nanofiltration. Journal of American Water Works Association, 88(5): 53-66.

Nyström, M., Ruohomäki, K., Kaipia, L., 1996. Humic acid as a fouling agent in filtration. Desalination, 106(1-3): 79-87.

Oust, A. et al., 2006. Fourier Transform Infrared and Raman Spectroscopy for Characterization of Listeria monocystogenes Strains. Applied and Environmental Microbiology, 72: 228-232.

Owen, D.M. et al., 1995a. NOM characterization and treatability. Journal of American Water Works Association, 87: 46-63.

Owen, D.M. et al., 1995b. NOM characterization and treatibility. Journal of Ammerican Water Works Association(87): 46-63.

Panyapinyopol, B., Marhaba, T.F., Kanokkantapong, V., Pavasant, P., 2005. Characterization of precursors to trihalomethanes formation in Bangkok source water. Journal of Hazardous Materials, 120(1-3): 299-236.

Pelakani, C. et al., 1999. Characterization of natural organic matter using high performance size exclusion chromatography. Environmental Science and Technology, 33: 2807-2813.

Peuravuori, J., Pihlaja, K., ., N.V., Environ. Int., 453-464., 1997. Isolation and characterization of natural organic matter from lake water: two different adsorption chromatographic methods. Environmenal International, 23(4): 453-464.

Pressdee, J.R., Veerapaneni, S., -Darby, H.L.S., Clement, J.A., Hoek, J.P.V.d., 2006. Integration of Membrane Filtration into Water Treatment Systems. AWWA Research Foundation: 1-316.

Qian, X.M., Nie, S.M., 2008. Single-molecule and single-nanoparticle SERS: From fundamental mechanisms to biomedical applications. Chemical Society Review, 37: 912-920.

Rabiller-Baudry, M., Maux, M.L., Chaufer, B., Begoin, L., 2002. Characterisation of cleaned and fouled membrane by ATR-FTIR and EDX analysis coupled with SEM: application to UF of skimmed milk with a PES membrane. Desalination, 146: 123-128.

Ravichandran, M., Aiken, G.R., Reddy, M.M., Ryan, J.N., 1998. Enhanced dissolution of cinnabar (mercury sulfide) by dissolved organic matter isolated from the Florida Everglades. Environmental Science and Technology, 32: 3305-3311.

Richard Bowen, W., Hilal, N., Lovitt, R.W., Williams, P.M., 1996. Visualisation of an ultrafiltration membrane by non-contact atomic force microscopy at single pore resolution. Journal of Membrane Science, 110(2): 229-232.

Rittmann, B.E., Snoeylink, V.L., 1984. Achieving biologically stable drinking water. Journal of Ammerican Water Works Association, 76(10): 106-114.

Rule, K., Vikesland, P., 2009. Surface-enhanced resonance Raman spectroscopy for the rapid detection of Cryptosporidium parvum and Giardia lamblia. Environmental Science and Technology, 43: 1147-1152.

Sanly, M. et al., 2007. A study on the removal of humic acid using advanced oxidation processes. Separation Science and Technology, 42(7): 1391-1404.

Sarathy, S.R., Mohseni, M., 2007. The impact of UV/H2O2 advanced oxidation on molecular size distribution of chromophoric natural organic matter. Environmental Science and Technology, 41: 8815-8320.

Schäfer, A.I., Fan, A.G., Waite, T.D., 1998. Nanofiltration of natural organic matter: removal, fouling and the influence of multivalent ions. Desalination, 118(1-3): 109-122.

Schäfer, A.I., Fane, A.G., Waite, T.D., 2000. Fouling effects on rejection in the membrane filtration of natural waters. Desalination, 131(1-3): 215-224.

Schäfer, A.I., Fane, A.G., Waite, T.D., 2001. Cost factors and chemical pretreatment effects in the membrane filtration of waters containing natural organic matter. Water Research, 35: 1509-1517.

Schechter, D.S., Singer, P.C., 1995. Foration of aldehydes during ozonation. Ozone Science and Engineering, 17(1): 53-59.

Schmitt, D., Taylor, H.E., Aiken, G.R., Roth, D.A., Frimmel, F.H., 2002. Influence of Natural organic matter on the adsorption of metal ions onto clay minerals. Environmental Science and Technology, 36: 2932-2938.

Seidel, A., Elimelech, M., 2002. Coupling between chemical and physical interactions in natural organic matter (NOM) fouling of nanofiltration membranes: implicatins for fouling control. Journal of Membrane Science, 203: 245-255.

Sengupta, A., Mujacic, M., Davis, E., 2006. Detection of bacteria by surface-enhanced Raman spectroscopy. Analytical and Bioanalytical Chemistry 386: 1379-1386.

Sharma, R.R., Agrawal, R., Chellam, S., 2003. Temperature effects on sieving characteristics of thin-film composite nanofiltration membranes: pore size distributions and transport parameters. Journal of Membrane Science, 223: 69-87.

Siddiqui, M., Amy, G., Ryan, J., Oden, W., 2000. Membranes for the control of natural organic matter from surface waters. Water Research, 34(13): 3355-3370.

Sierka, R., Amy, G., 1985. Catalytic effects of UV light and/or ultrasound on the ozone oxidation of humic acid and THM precursors. Ozone Science and Engineering, 7: 47-62.

Singer, P.C., 1999. Humic substances as precursors for potentially harmful disinfection byproducts. Water Science and Technology, 40(9): 25-30.

Socrates, G., 1994. Infrared Characteristic Group Frequencies, Wiley-Interscience.

Sohn, J., Amy, G., Yoon, Y., 2007. Process-train profiles of NOM through a drinking water treatment plant. Journal of American Water Works Association, 99(6): 145-153.

Song, W., Ravindran, V., Koel, B.E., Pirbazari, M., 2004. Nanofiltration of natural organic matter with H2O2/UV pretreatment: fouling mitigation and membrane surface characterization. Journal of Membrane Science, 241(1): 143-160.

Song, Y., Dong, B., Gao, N., Xia, S., 2010. Huangpu River water treatment by microfiltration with ozone pretreatment. Desalination, 250(1): 71-75.

Speth, T.F., Summers, R.S., Gusses, A.M., 1998. Nanofiltration foulants from a treated surface water. Environmental Science and Technology, 32: 3612-3617.

Summers, R.S., Hooper, S.M., Solarik, G., Owen, D., 1996. Assessing DBP yield: uniform formation conditions. Journal of American Water Works Association, 81(7): 80-93.

Swietlik, J., Sikorska, E., 2005. Characterization of natural organic matter fractions by high pressure size-exclusion chromatography, specific UV absorbance and total luminescence spectroscopy. Polish Journal of Environmental Studies, 15: 145-153.

Tang, C.Y., Kwon, Y.-N., Leckie, J.O., 2007a. Fouling of reverse osmosis and nanofiltration membranes by humic acid—Effects of solution composition and hydrodynamic conditions. Journal of Membrane Science, 290(1-2): 86-94.

Tang, C.Y., Kwon, Y.-N., Leckie, J.O., 2009. Effect of membrane chemistry and coating layer on physiochemical properties of thin film composite polyamide RO and NF membranes. I. FTIR and XPS characterization of polyamide and coating layer chemistry. Desalination, 242: 149-167.

Tang, C.Y., Kwon, Y.N., Leckie, J.O., 2007b. Fouling of reverse osmosis and nanofitlration membraens by humic acid -effects of solution composition and hydrodynamic conditions. Journal of Membrane Science, 290: 86-94.

Taylor, J., Mulford, L.A., Barrett, W.M., Duranceau, S.J., Smith, D.K., 1990. Cost and performance of membranes for organic control in small systems: Flagler beach and Punta Gorda, Florida. USEPA, PB89-190367/AS(January).

Thomson, J., Parkinson, A., Roddick, F.A., 2004. Depolymerization of chromophoric natural organic matter. Environmental Science and Technology, 38: 3360-3369.

Thomson, J., Roddick, F., Dirkas, M., 2002. UV photooxidation facilitating biological treatment for the removal of NOM from drinking water. Journal of Water Supply: Research and Technology-AQUA, 51: 297-306.

Thurman, E.M., 1985. Organic Geochemistry of Natural Waters, Martinus Nijhoff/Dr W. Junk Publishers, Boston, MA.

Toor, R., Mohseni, M., 2007. UV/H_2O_2 based AOP and its integration with biological activated carbon treatment for DBP reduction in drinking water. Chemosphere, 66: 2087-2095.

USEPA, 1995a. Determination of chlorination disinfection byproducts, chlorinated solvents, and halogenated pesticides/herbicides in drinking water by liquid-liquid extraction and gas chromatography with electron-capture detection, method 551.1. 1-61.

USEPA, 1995b. Determination of haloacetic acids and dalapon in drinking water by liquid-liquid extraction, derivatization and gas chromatography with electron capture detection, method 552.2. 1-32.

USEPA, 2001. Low-pressure membrane filtration for pathogen removal:Application, implementation, and gegulatory issues. (EPA 815-C-01-001): 1-148.

USEPA, 2003. Membrane Filtration guidance manual, Proposal Draft, EPA, 815-D-03-008. 1-87.

USEPA, 2006a. Long Term 2 Enhanced Surface Water Treatment Rule (LT2ESWTR). 71(3).

USEPA, 2006b. Stage 2 Disinfectants and Disinfection Byproduct Rule (Stage 2 DBP rule). 71(2).

Van der Bruggen, B., Schaep, J., Wilms, D., Vandecasteele, C., 1999. Influence of molecular size, polarity and charge on the retention of organic molecules by nanofiltration. Journal of Membrane Science, 156(1): 29-41.

Van der Bruggen, B., Kim, J.H., DiGiango, F.A., Geens, J., Vandecasteele, C., 2004. Influence of MF pretreatment on NF performance for aqueous solutions containing particles and an organic foulant. Separation Science and Technology, 36: 203-213.

Van Geluwe, S., Braeken, L., Van der Bruggen, B., 2011. Ozone oxidation for the alleviation of membrane fouling by natural organic matter: A review. Water Research, 45(12): 3551-3570.

Violleau, D., Essis-Tome, H., Habarou, H., Croue´, J.P., Pontie´, M., 2005. Fouling studies of a polyamide nanofiltration membrane by selected natural organic matter: an analytical approach. Desalination, 173: 223-238.

Vrijenhoek, E.M., Hong, S., Elimelech, M., 2001. Influence of membrane surface properties on initial rate of colloidal fouling of reverse osmosis and nanofiltration membranes. Journal of Membrane Science, 188(1): 115-128.

Waller, D.H. et al., 1996. Characteristics of Nova Scotia surface waters and treatment options for removal of color and trihalomethane precursors. Canadian Journal of Civil Engineering, 23: 1316-1325.

Wang, G.S., Liao, C.H., Chen, H.W., Yang, H.C., 2006. Characteristics of natural organic matter degradation in water by UV/H_2O_2 treatment. Environmental Technology, 27(3): 277-287.

Wert, E.C., F. L. Rosario-Ortiz, Snyder, S.A., 2009. Effect of ozone exposure on the oxidation of traceorganiccontaminants in wastewater. Water Research, 43(4): 1005–1014.

Westerhoff, P., Debroux, J., Aiken, G., Amy, G., 1999. Ozone induced changes in natural organic matter (NOM) structure. Ozone Science and Engineering, 21: 551-570.

Westerhoff, P., Mezyk, S.P., Cooper, W.J., Minakata, D., 2007. Electron Pulse Radiolysis Determination of Hydroxyl Radical Rate Constants with Suwannee River Fulvic Acid and Other Dissolved Organic Matter Isolates. Environmental Science and Technology, 41(13): 4640-4646.

Wu, W.C., Evans, R.D., Dillon, P.J., Y.R. Cai Appl. Geochem. 22, 2007. Rapid quantification of humic and fulvic acids by HPLC in natural waters. Applied Geochemistry, 22: 1598-1605.

Xu, P., Drewes, J.E., Kim, T.-U., Bellona, C., Amy, G., 2006. Effect of membrane fouling on transport of organic contaminants in NF/RO membrane applications. Journal of Membrane Science, 279(1-2): 165-175.

Yuan, W., Zydney, A.L., 2000. Humic acid fouling during ultrafiltrqtion. Environmental Science and Technology, 34(23): 5043-5050.

Zhao, Y., Song, L., Ong, S.L., 2010. Fouling of RO membranes by effluent organic matter (EfOM): Relating major components of EfOM to their characteristic fouling behaviors. Journal of Membrane Science, 349(1): 75-82.

Zhou, H., Smith, D., 2001. Advanced technologies in water and wastewater treatment. Canadian Journal of Civil Engineering, 28.

Zhu, X., Elimelech, M., 1997. Collodial fouling of reverse osmosis membranes: measurements and fouling mechanisms. Environmental Science and Technology, 31: 3654-3662.

Appendix A - Chapter 4 Raw and Supplemental Data

Table A1 Total THM and HAA Formation Potentials of Raw and UF Permeate Waters of Tatamagouche WTP

	Total THMFP (µg/L)		**Total HAAfp (µg/L)**	
Water	Raw	UF permeate	Raw	UF permeate
HON	467.04	194.91	363.69	85.03
HOB	2.54	0.92	0.04	0.50
HOA	264.73	12.61	111.66	10.34
HIB	2.61	0.79	1.30	0.40
HIA	16.20	2.42	14.23	1.73
HIN	59.80	44.85	14.38	9.65

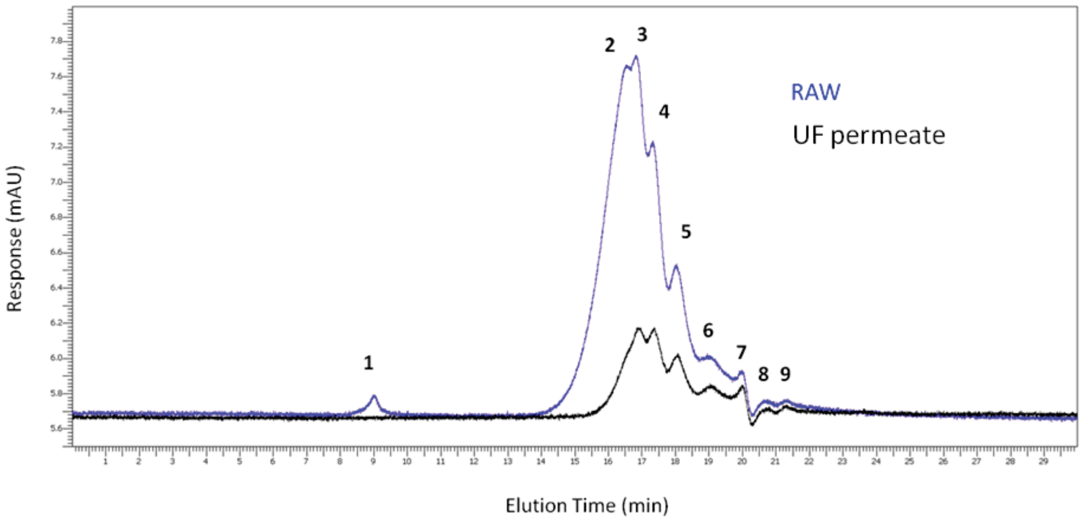

Figure A1 Size Exclusion Chromatogram of Raw and UF Permeate.

Appendix B – Chapter 5 Raw and Supplemental Data

Table B1 Detail Operating Conditions in Full-scale IMS Plants

NF Membrane and Design	Tatamagouche WTP	Collins Park WTP
NF Module	OSMO PRO 365	Hydranautics-ESPA4
Material		Composite Polyamide
Module Area	33.9 m^2 (365 ft^2)	37.1 m^2 (400 ft^2)
Diameter	8 inch	8 inch
Number of Skids	2	1
Number of Vessels	6	2
Number of Modules/Vessels	4	4
Total Modules (per skid)	24	8
Array	4-2	1-1
Permeate Flowrate	100 USgpm	29 USgpm
Recovery	75%	80%
Inlet Flowrate	133 USgpm	36.3 USgpm
Total Flowrate	170 USgpm	48.3 USgpm
Concentrate Flowrate	33 USgpm	7.3 USgpm
Recycle Flowrate	36 USgpm	12 USgpm
Average Design Flow per Module	4.17 Usgpm	3.63 USgpm
Flux per Module	16.5 gfd (27.9 lmh)	13.1 gfd (22.1 lmh)
Feed Flow per vessel (Stage 1)	42.5 USgpm	
Feed Flow per Vessel (Stage2)	16.64 USgpm	
Feed Flow (Stage 1)		48.3 USgpm
Feed Flow (Stage 2)		33.8 USgpm

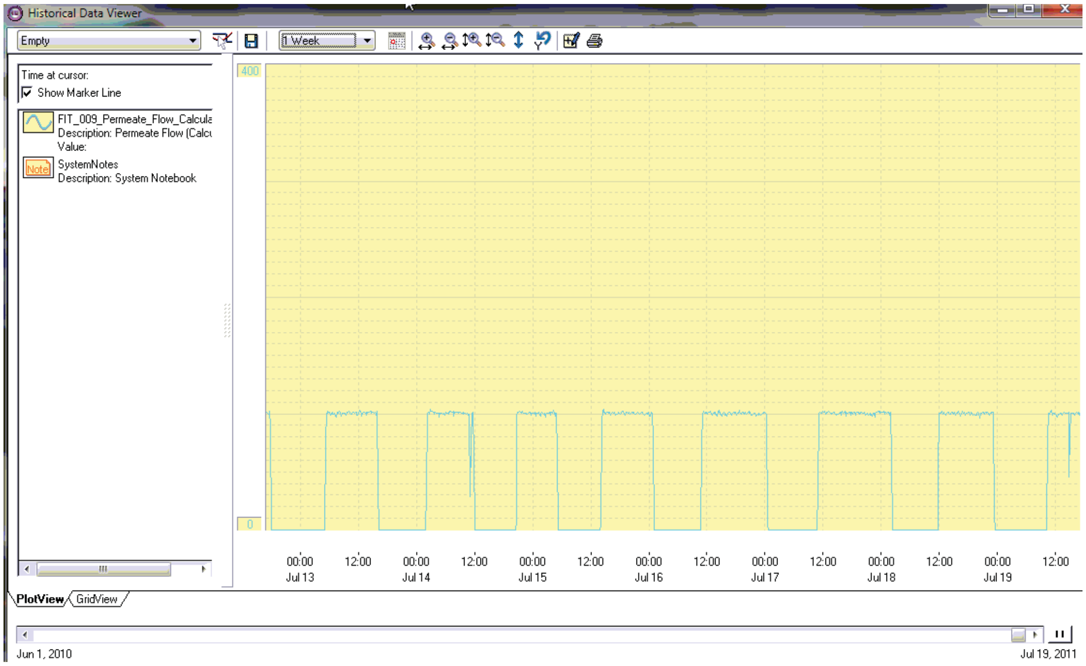

Time at cursor:
☑ Show Marker Line

FIT_009_Permeate_Flow_Calcula
Description: Permeate Flow (Calcu
Value:

SystemNotes
Description: System Notebook

Figure B1 Real-time Permeate Flow Rate of NF Membrane in Collins Park WTP in 13-19 July 2010.

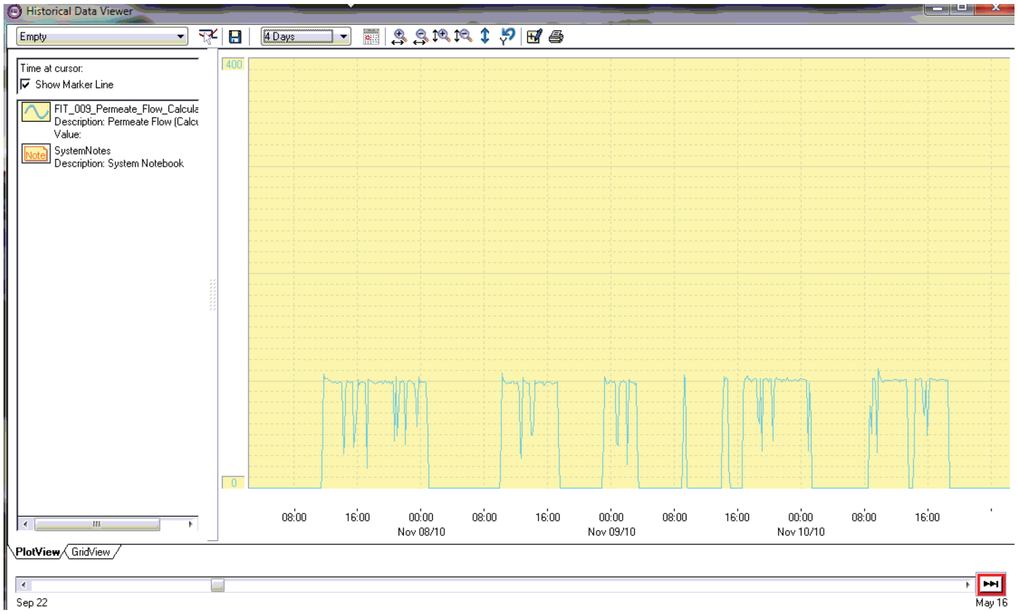

Time at cursor:
☑ Show Marker Line

FIT_009_Permeate_Flow_Calcula
Description: Permeate Flow (Calcu
Value:

SystemNotes
Description: System Notebook

Figure B2 Real-time Permeate Flow Rate of NF Membrane in Collins Park WTP in 08-10 Nov 2010.

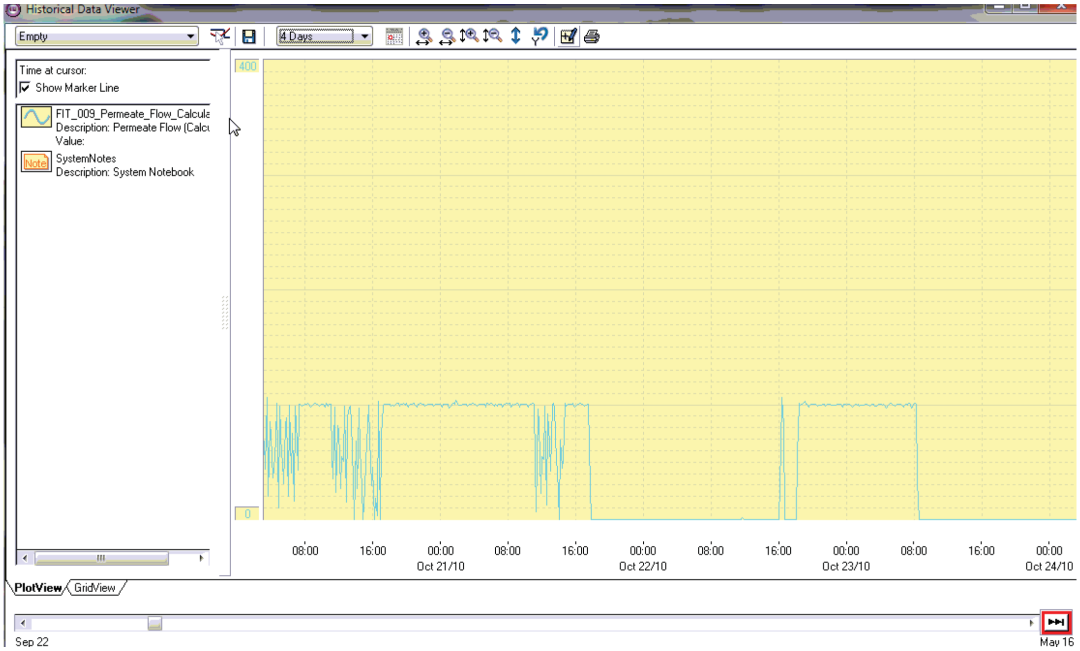

Figure B3 Real-time Permeate Flow Rate of NF Membrane in Collins Park WTP in 21-24 Oct.

Appendix C – Chapter 6 Raw and Supplemental Data

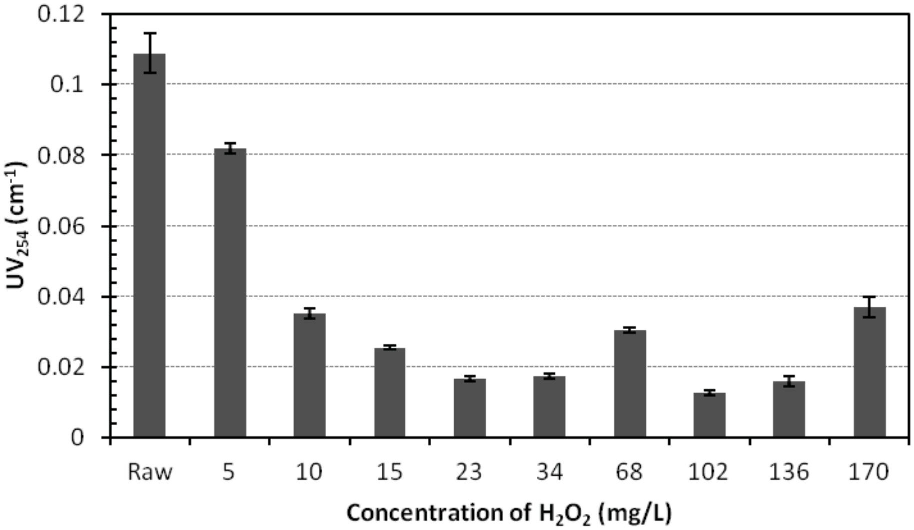

Figure C1 Impact of H_2O_2 Concentrations on UV_{254} Absorbance in H_2O_2/UV Process. Bars Represent the Average of Two Runs.

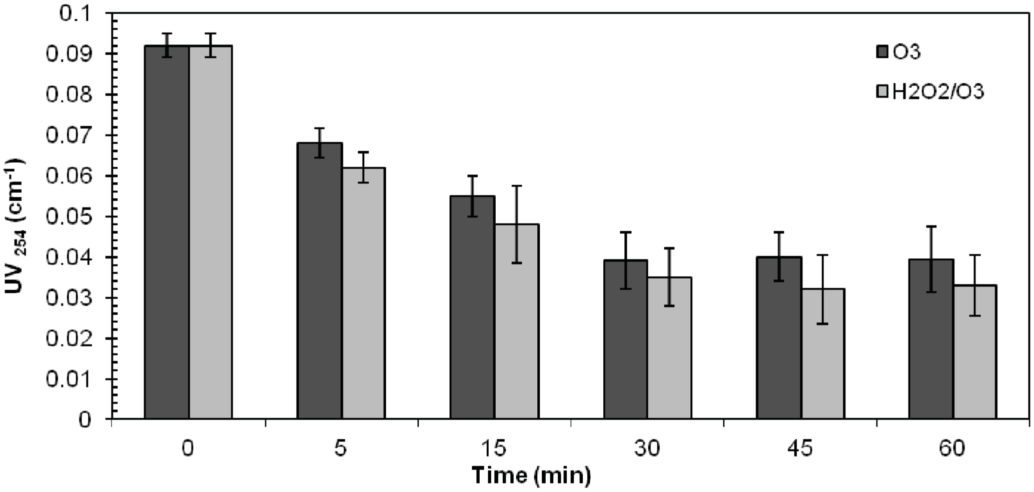

Figure C2 Changes in UV_{254} Values in Different Ozonation Times in Ozone and H_2O_2/O_3 Experiments. Bars Represent the Average of Two Runs.

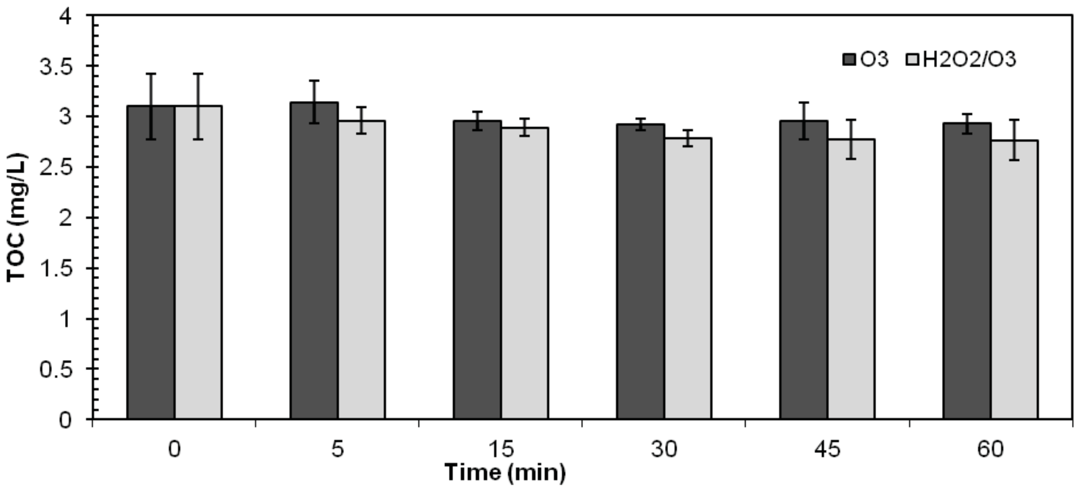

Figure C3 Changes in TOC Concentrations in Different Ozonation Times in Ozone and H_2O_2/O_3 Experiments. Bars Represent the Average of Two Runs.

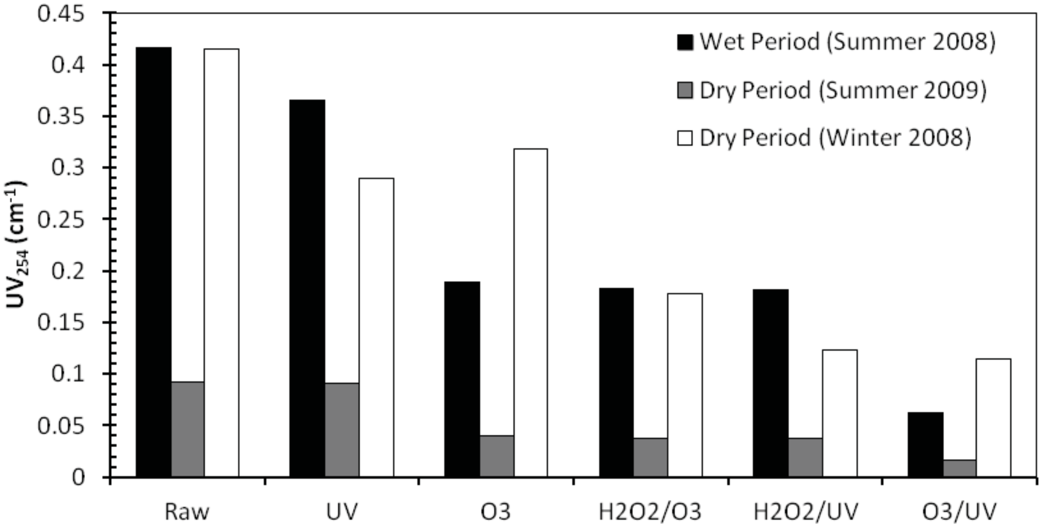

Figure C4 Observed UV_{254} Values for Raw and Oxidized Water Samples in Different Sampling Times. Bars Represent the Average of Three Runs.

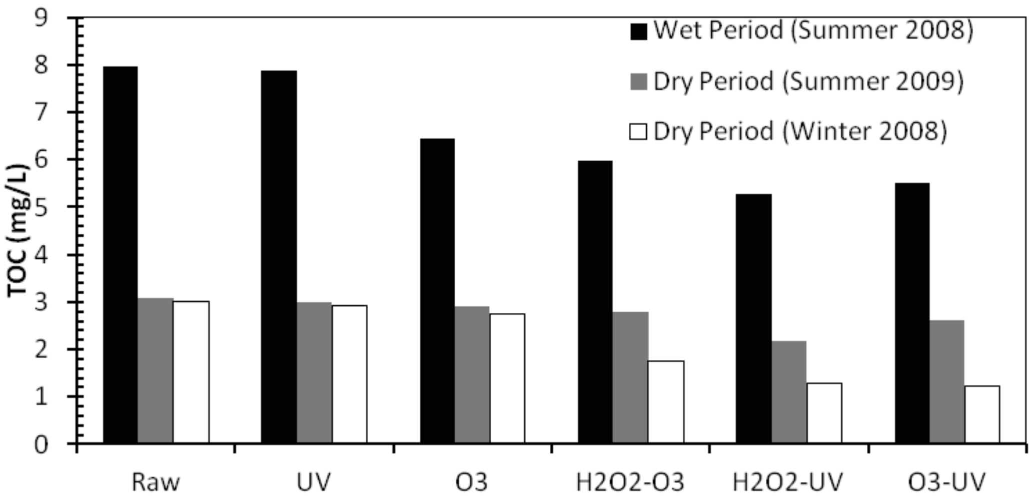

Figure C5 Observed TOC Concentrations for Raw and Oxidized Water Samples in Different Sampling Times. Bars Represent the Average of Three Runs.

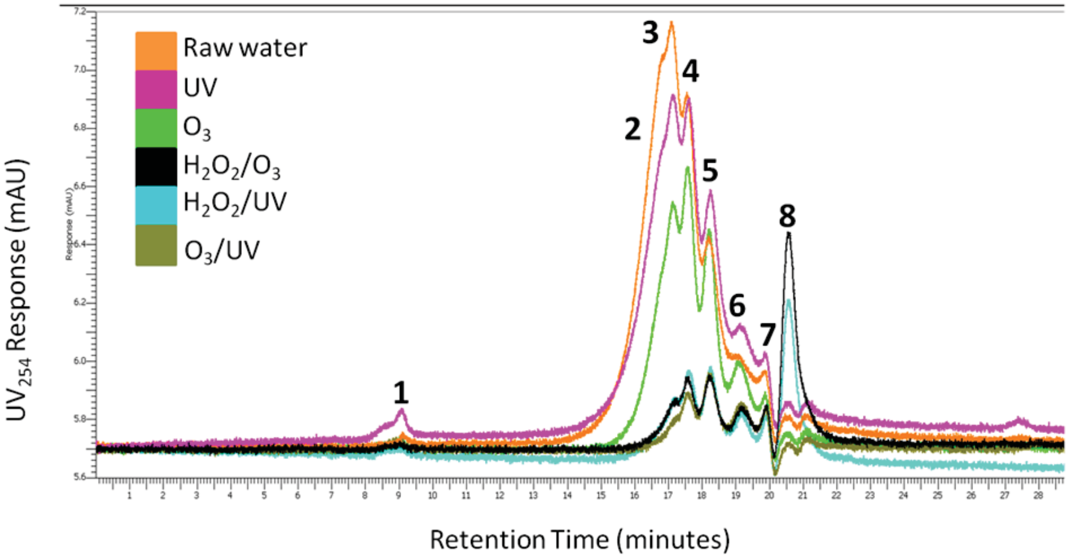

Figure C6 HPSEC Chromatograms of Raw and Oxidized Waters in summer 2009.

Appendix D – Chapter 8 Raw and Supplemental Data

Table D1 Bench-scale HPSEC Data

Raw water 1

Peak	RT	Area	% area	MW	Start MW	End MW
1	9.017	2186.2	1.473	55705.4	71180.8	41909.4
2	16.577	64989.5	43.799	2062.1	8056.6	1323.0
3	16.827	24195.4	16.306	1185.2	1323.0	1043.2
4	17.307	21942.1	14.788	911.3	1043.2	757.4
5	18.070	15216.4	10.255	649.5	757.4	524.7
6	19.066	11381.1	7.670	416.3	524.7	318.0
7	19.827	4654.7	3.137	288	318.0	244.1
8	20.391	826.5	0.557	214.7	241.3	191.6
9	20.990	2988.7	2.014	162.1	186.8	134.8

Raw Water 2

Peaks	RT	Area	% area	MW	Start MW	End MW
1	8.999	2153.2	1.443	56160.4	71648.6	4296.0
2	16.559	66115.6	44.319	2086.7	8056.6	1323.0
3	16.848	24250.5	16.258	1185.2	1323.0	1043.2
4	17.328	21913.5	14.689	911.4	1043.2	756.4
5	18.026	14992.8	10.050	649.4	756.4	524.7
6	18.937	11198.5	7.507	416.3	524.7	318.0
7	19.803	4521.0	3.031	288.5	318.0	244.1
8	20.446	890.2	0.597	213.8	239.4	190.5
9	20.969	3147.0	2.109	162.3	186.3	132.0

NF Permeate 1

Peaks	RT	Area	% area	MW	Start MW	End MW
7	19.924	3863.4	52.613	294.3	366.1	242.3
8	20.453	943.5	12.848	214.7	242.3	190.7
9	20.950	2536.3	34.539	163.0	186.4	132.8

NF Permeate 2

Peaks	RT	Area	% area	MW	Start MW	End MW
7	19.838	3726.4	46.902	291.5	356.3	242.2
8	20.398	1105.7	13.917	212.5	242.2	186.3
9	20.998	3112.9	39.181	162.8	186.3	133.1

H_2O_2/UV 1 Pretreatment

Peaks	RT	Area	% area	MW	Start MW	End MW
2	17.105	4347.0	13.616	1324.4	2113.5	1051.4
3	17.450	5441.5	17.045	901.9	1051.4	754.8
4	18.058	6630.7	20.770	633.8	754.8	479.7
5	19.020	4139.4	12.966	401.6	479.7	328.9
6	19.823	2932.9	9.187	293.9	328.9	257.8
7	20.440	2251.4	7.052	213.6	244.3	194.2
8	20.822	4072.6	12.757	174.9	194.2	149.2
9	21.729	2109.4	6.607	109.4	141.2	79.2

H_2O_2/UV 2 Pretreatment

Peaks	RT	Area	% area	MW	Start MW	End MW
2	17.097	5186.3	16.319	1368.5	2675.9	1034.6
3	17.449	4926.3	15.501	908.9	1034.6	782.5
4	18.118	6818.3	21.455	650.6	782.5	498.4
5	19.164	4279.9	13.467	407.8	498.4	330.1
6	19.796	2875.5	9.048	293.7	330.1	257.0
7	20.450	2391.4	7.525	213.3	243.7	194.3
8	20.822	4228.1	13.304	174.6	194.3	146.6
9	21.864	1074.5	3.381	119.3	141.6	100.3

H_2O_2/O_3 1 Pretreatment

Peaks	RT	Area	% area	Mw	Start Mw	End Mw
1	8.750	1000.3	1.39	60228.6	79548.9	42903.8
2	16.848	26925.5	36.032	1504.1	3059.0	1098.0
3	17.304	14684.0	19.650	962.7	1098.0	812.8
4	17.994	14240.8	19.057	674.1	812.8	498.9
5	18.983	8184.7	10.953	404.7	498.9	319.1
6	19.849	3772.5	5.048	289.2	319.1	250.5
7	20.620	1835.0	2.456	210.2	243.4	193.0
8	20.788	3697.7	4.948	176.2	193.0	145.7
9	22.476	385.8	0.516	72.1	78.7	66.4

H_2O_2/O_3 2 Pretreatment

Peaks	RT	Area	% area	Mw	Start Mw	End Mw
1	8.988	1569.5.3	2.083	56099.6	76108.9	39974.0
2	16.839	26188.2	34.760	1461.3	3059.0	1070.7
3	17.318	12952.0	17.191	952.2	1070.7	813.1
4	17.963	13349.2	17.719	680.1	813.1	514.8
5	19.031	8889.3	11.799	407.8	514.8	318.6
6	19.791	3933.8	5.221	289.2	318.6	250.5
7	20.628	1920.7	2.549	211.9	243.4	193.0
8	20.760	3859.1	5.122	175.9	193.0	145.7
9	21.618	677.9	0.554	112.5	145.3	79.6

O_3/UV 1 Pretreatment

Peaks	RT	Area	% area	Mw	Start Mw	End Mw
3	17.007	9608.7	19.116	1340.5	2212.3	1080.4
4	17.378	11007.8	21.899	933.0	1080.4	780.6
5	18.067	12627.5	25.121	653.2	780.6	497.2
6	19.028	9335.0	18.571	404.4	497.2	318.2
7	19.824	4170.7	8.297	287.6	318.2	247.8
8	20.577	1919.7	3.819	201.3	237.6	171.8
9	21.173	1596.4	3.176	149.6	171.8	122.2

O_3/UV 2 Pretreatment						
Peaks	**RT**	**Area**	**% area**	**Mw**	**Start Mw**	**End Mw**
3	16.892	8798.0	17.644	1327.1	2212.3	1080.4
4	17.379	10747.5	21.553	933.3	1080.4	781.9
5	18.060	12760.5	25.590	653.7	781.9	497.4
6	19.064	9504.6	19.061	402.3	497.4	316.7
7	19.790	4137.6	8.298	287.2	316.7	247.8
8	20.570	1999.9	4.011	198.5	239.7	166.7
9	21.110	1916.5	3.844	144.5	166.7	116.5

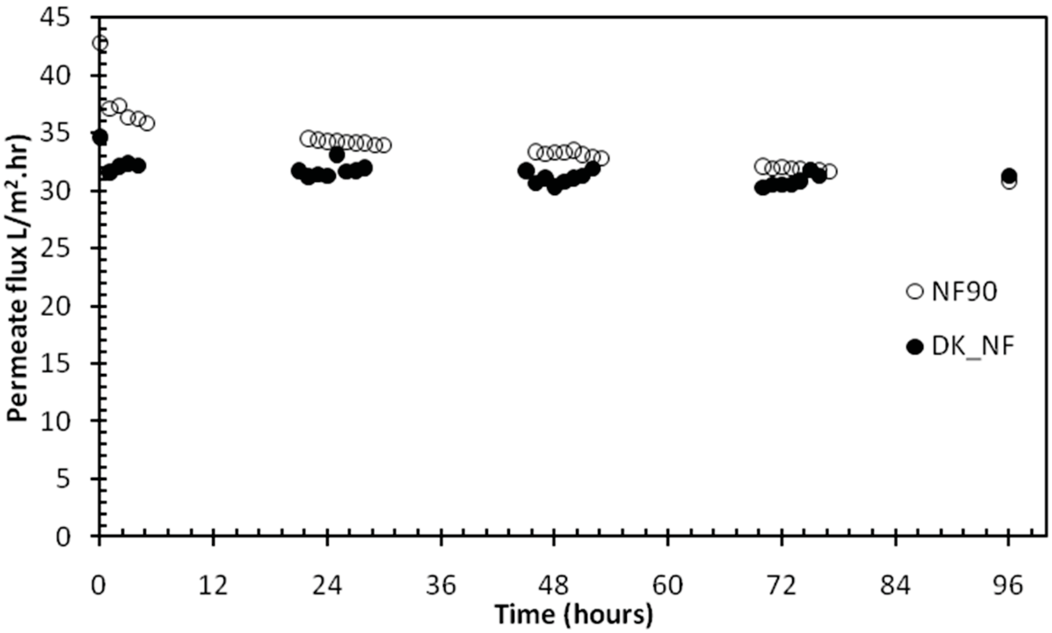

Figure D1 Comparison of NF Membrane Performance with the Source Water from Tatamagouche WTP.

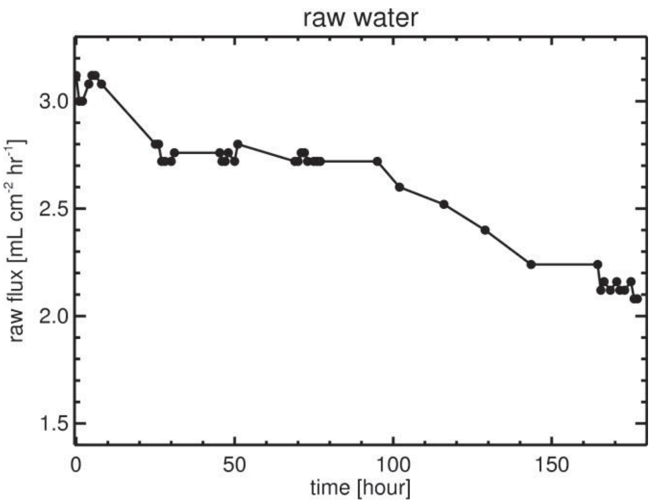

Figure D2 Measured Permeate Flux over Time for NF-90 Membrane with Raw Water. The Operating Condition was Maintained at TMP = 300 psi, T = 27 ± 2°C, flow rate (Q) = 2L/min, Cross Flow Velocity = 0.223 m/s.

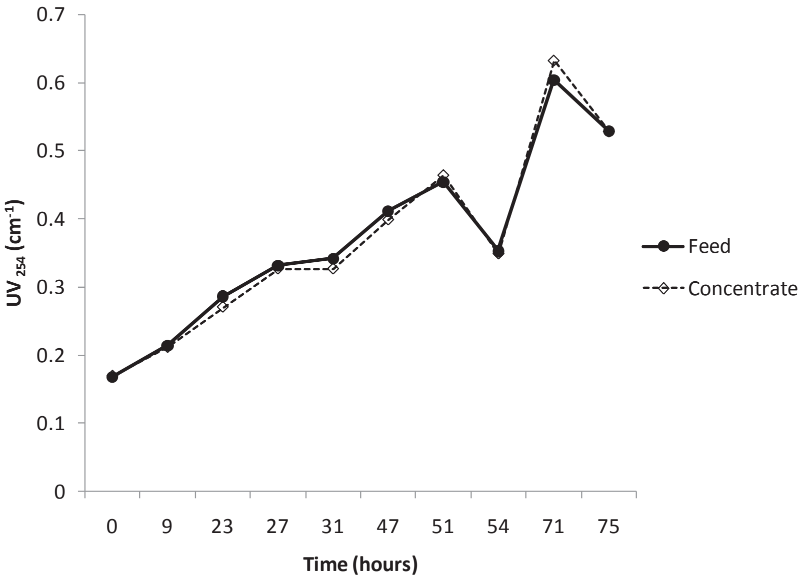

Figure D3 Measured UV_{254} Absorbance for Feed (solid) and Concentrate (dotted) Waters versus Time during NF-90 Membrane Fouling Experiment with Raw Water.

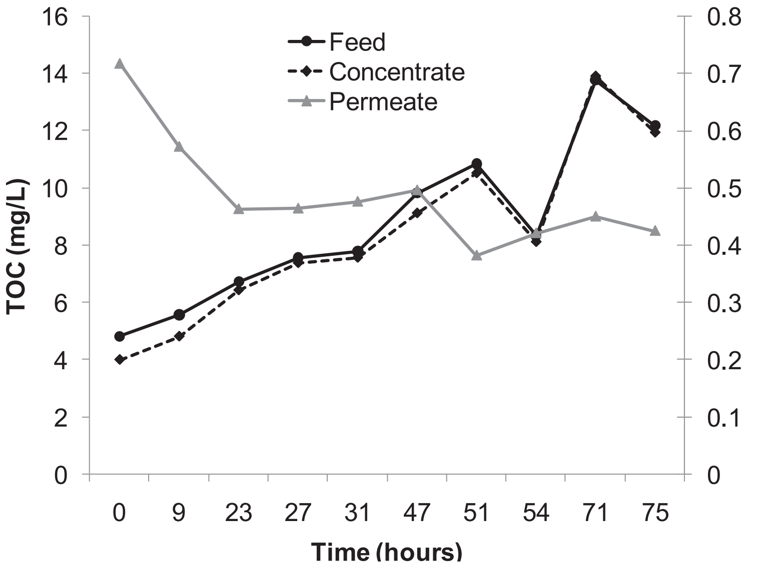

Figure D4 Measured TOC Concentrations for Feed (Solid Black) and Concentrate (Dotted Black) Waters versus Time during NF-90 Membrane Fouling Experiment. The Brown Line Represents Permeate TOC Concentration. Note that Different Scale (right) is used for Permeate Water.

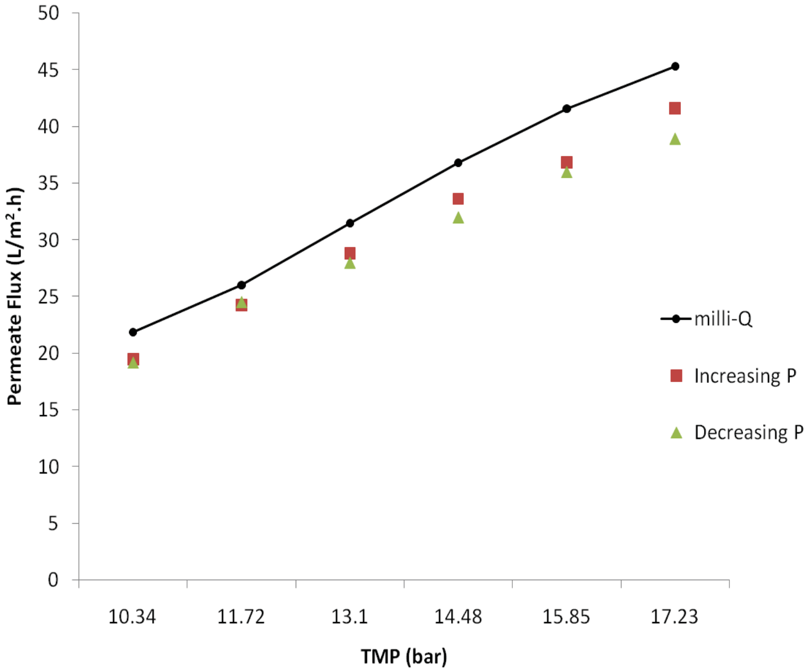

Figure D5 Permeate Fluxes as a Function of Pressure for the French River Raw Water during Critical Flux Experiment.

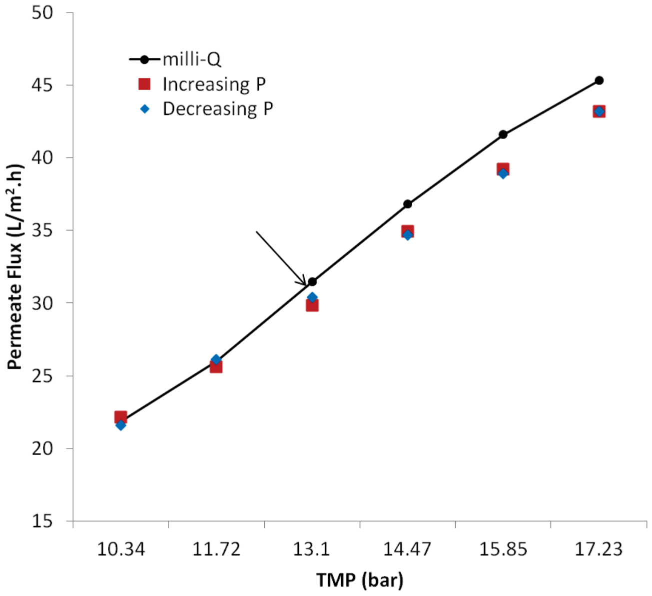

Figure D6 Permeate Fluxes as a Function of Pressure for O_3/UV Oxidized Water during Critical Flux Experiment.

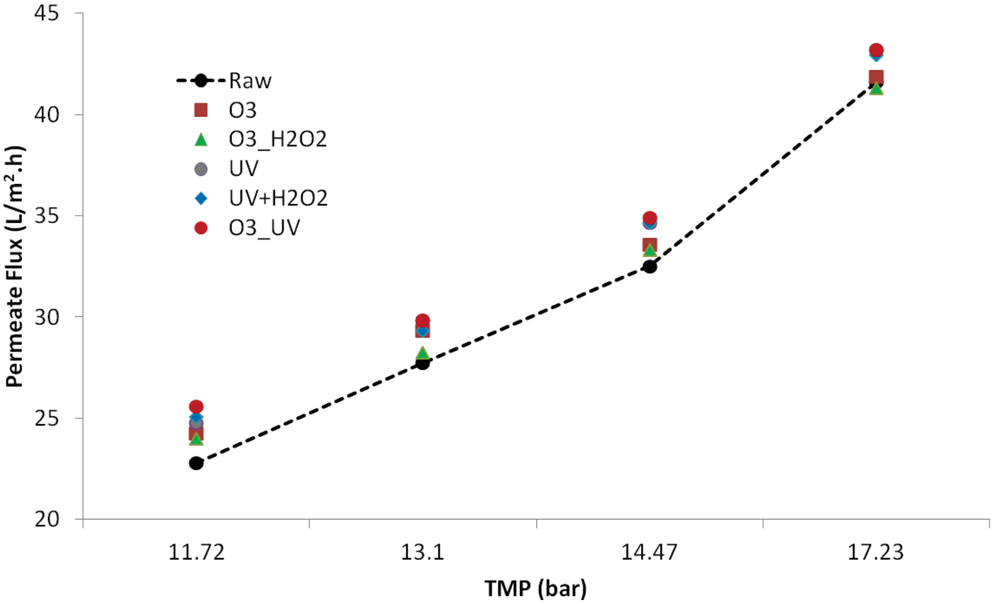

Figure D7 Comparison of Permeate Fluxes for Raw and Oxidized Waters during Critical Flux Experiments.

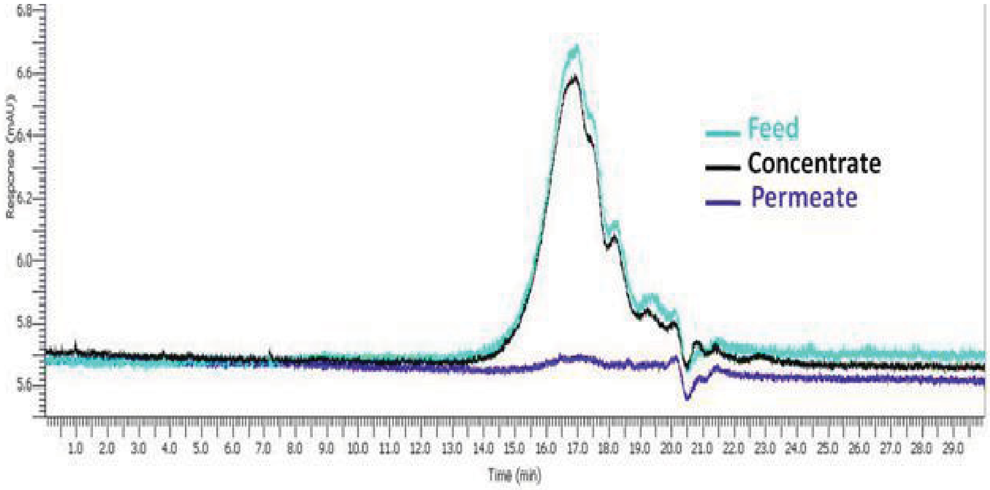

Figure D8 HPSEC Chromatograms of Feed, Concentrate and Permeate Waters Passing Through NF-90 Membrane.

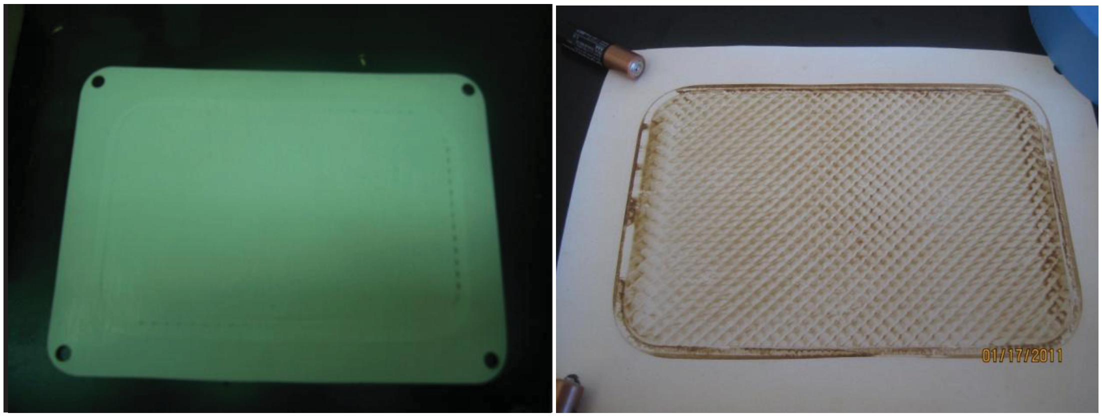

Figure D10 Virgin DK-NF Membrane after 24 hours Compaction with Milli-Q Water (left) and Fouled Membrane with Raw Water from the French River.

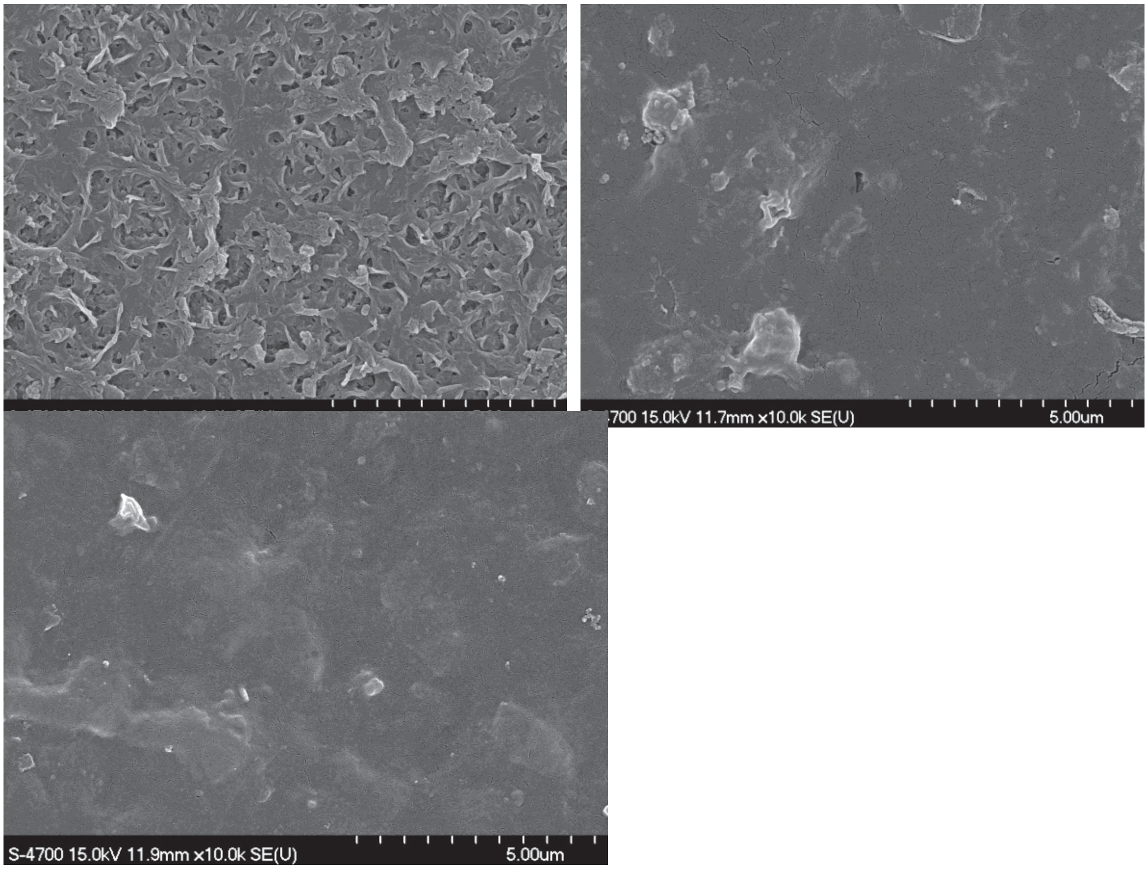

Figure D9 Scanning Electron Microscopy Picture of NF-90 Virgin (upper left) and Fouled Membrane Surface. Upper Right is Membrane Cut from Edge and Lower Left is from Centre Part of the Membrane.

Appendix E – Letter of Copyright Permission from Journal of Water Supply: Research and Technology-AQUA

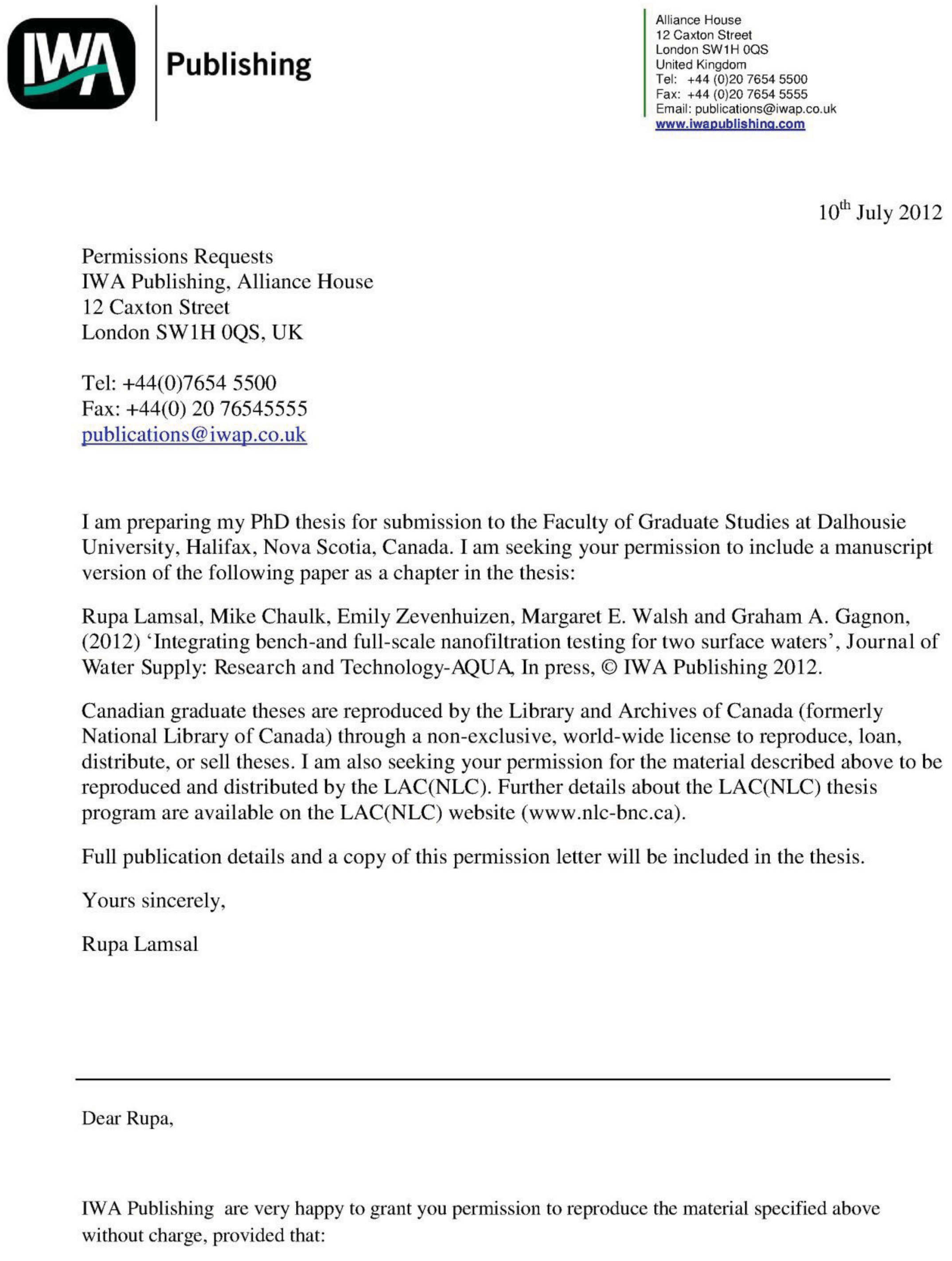

Publishing

Alliance House
12 Caxton Street
London SW1H 0QS
United Kingdom
Tel: +44 (0)20 7654 5500
Fax: +44 (0)20 7654 5555
Email: publications@iwap.co.uk
www.iwapublishing.com

10th July 2012

Permissions Requests
IWA Publishing, Alliance House
12 Caxton Street
London SW1H 0QS, UK

Tel: +44(0)7654 5500
Fax: +44(0) 20 76545555
publications@iwap.co.uk

I am preparing my PhD thesis for submission to the Faculty of Graduate Studies at Dalhousie University, Halifax, Nova Scotia, Canada. I am seeking your permission to include a manuscript version of the following paper as a chapter in the thesis:

Rupa Lamsal, Mike Chaulk, Emily Zevenhuizen, Margaret E. Walsh and Graham A. Gagnon, (2012) 'Integrating bench-and full-scale nanofiltration testing for two surface waters', Journal of Water Supply: Research and Technology-AQUA, In press, © IWA Publishing 2012.

Canadian graduate theses are reproduced by the Library and Archives of Canada (formerly National Library of Canada) through a non-exclusive, world-wide license to reproduce, loan, distribute, or sell theses. I am also seeking your permission for the material described above to be reproduced and distributed by the LAC(NLC). Further details about the LAC(NLC) thesis program are available on the LAC(NLC) website (www.nlc-bnc.ca).

Full publication details and a copy of this permission letter will be included in the thesis.

Yours sincerely,

Rupa Lamsal

Dear Rupa,

IWA Publishing are very happy to grant you permission to reproduce the material specified above without charge, provided that:

IWA Publishing

Alliance House
12 Caxton Street
London SW1H 0QS
United Kingdom
Tel: +44 (0)20 7654 5500
Fax: +44 (0)20 7654 5555
Email: publications@iwap.co.uk
www.iwapublishing.com

- the material to be used has appeared in our publication without credit or acknowledgement to another source;
- suitable acknowledgement to the source is given in accordance with standard editorial practice, e.g.,

Reproduced from (2012) 'Integrating bench-and full-scale nanofiltration testing for two surface waters', Journal of Water Supply: Research and Technology-AQUA, In press, 2012, with permission from the copyright holders, IWA Publishing".

- Reproduction of this material is confined to the purpose for which this permission is given.

I trust this permission will be satisfactory; if any point needs clarification or you have any further queries, please do not hesitate to contact us again.

Chloe Parker

Name: Chloe Parker

Title: Digital Publishing Assistant

Date: 10th July 2012

Appendix F – Letter of Copyright Permission from Elsevier for Water Research, Separation and Purification Technology and Desalination Journals.

Dear Rupa Lamsal

Thank you for your email.

As author of the requested article, you do not need to seek Elsevier's permission to include it in your thesis as it is part of the rights you retain as an Elsevier journal author.

If your thesis is being hosted online by your university, then the version you should include in your thesis should not be Elsevier's PDF version but the Accepted Author Manuscript ("AAM"), it is the author's version of the manuscript of an article that has been accepted for publication and which may include any author-incorporated changes suggested through the processes of submission processing, peer review, and editor-author communications. AAMs do not include other publisher value added contributions such as copy-editing, formatting, technical enhancements and (if relevant) pagination.

If you require an official grant, then Elsevier requires you to go through Rightslink service to obtain permission by following the instructions stated in our automated response:

Locate the publication containing your published article on http://www.sciencedirect.com/

*	Click on the article/chapter name to access the abstract

*	Click on “Permissions & Reprints”, which is directly under the DOI link and is above the article Abstract

*	The Rightslink request page will then be launched (turn off your pop-up blocker)

*	Select the way you would like to reuse the content

*	Create a Rightslink account if you haven’t already

*	Accept the terms and conditions and you’re done

Yours sincerely
Jennifer Jones
Rights Associate
Global Rights Department

Elsevier Ltd
PO Box 800
Oxford OX5 1GB
UK